SCERP Mission

The Southwest Center for Environmental Research and Policy (SCERP) was established by the U.S. Congress in October 1990 to "initiate a comprehensive analysis of possible solutions to the acute air, water quality, and hazardous waste problems that plague the United States-Mexico border region." SCERP is a consortium of five U.S. universities (Arizona State University, New Mexico State University, San Diego State University, University of Texas at El Paso, and University of Utah) and five Mexican universities (El Colegio de la Frontera Norte, Instituto Tecnológico de Ciudad Juárez, Instituto Tecnológico y de Estudios Superiores de Monterrey, Universidad Autónoma de Baja California, and Universidad Autónoma de Ciudad Juárez). SCERP carries out its mission through a cooperative agreement with the U.S. Environmental Protection Agency. A permanent administrative office is maintained by the consortium in San Diego.

Environmental Problems of the U.S.–Mexican Border Region

The border region lies 100 kilometers (60 miles) on each side of the U.S.–Mexican border and encompasses parts of four states in the United States (Texas, New Mexico, Arizona, and California) and six Mexican states, including Baja California, Sonora, Chihuahua, Coahuila, Nuevo León, and Tamaulipas. Approximately 13 million people live in the U.S. counties and Mexican municipalities on the border. The high density of people and increased industrialization since the passage of NAFTA have placed an even greater burden on the inadequate infrastructure and environmental resources of the region. Exacerbating the problem is the fact that many U.S. counties along the border are categorized as "economically distressed," and few communities possess the resources needed to address environmental concerns. Just some of the critical border environmental issues include:

- Rapid urbanization and lack of adequate infrastructure
- Air pollution from open burning, vehicle emissions, and industrial operations
- Contamination of surface and groundwater from open sewers and industrial waste
- Overuse of aquifers and surface steams
- Transportation and illegal dumping of hazardous wastes
- Destruction of natural resources

The SCERP Solution

SCERP uses a broad, integrated, multidisciplinary approach to address the issues of the border. SCERP's researchers collaborate with the U.S. Environmental Protection Agency (EPA) and Mexico's Secretaría de Medio Ambiente y Recursos Naturales (SEMARNAT), as well as local and state governments, business and industry, nongovernmental organizations, and communities of the border region. SCERP organizes research, outreach, and training programs devoted to improving environmental conditions and to building capacity in the border region for resolving critical environmental problems. SCERP is pioneering a model of binational cooperation that brings U.S. and Mexican researchers together and introduces new skills and perspectives in binational environmental problem solving.

CENTRO DE INVESTIGACION Y POLITICA AMBIENTAL DEL SUROESTE
SOUTHWEST CENTER FOR ENVIRONMENTAL RESEARCH & POLICY

The U.S.-Mexican Border Environment: Air Quality Issues along the U.S.-Mexican Border

SCERP

THE U.S.-MEXICAN border environment: Air Quality Issues along the U.S.-Mexican Border

Edited by
Alan Sweedler

SCERP Monograph Series, no. 6

Southwest Center for Environmental Research and Policy

THE U.S.-MEXICAN BORDER ENVIRONMENT

Air Quality Issues along the U.S.-Mexican Border

SCERP Monograph Series, no. 6

A series edited by Paul Ganster

Contributors

J.M. Cardona-Carrizalez	Instituto Tecnológico y de Estudios Superiores de Monterrey
K. Collins	San Diego State University
R. Currey	University of Texas at El Paso
S. Dattner	Texas Commision on Environmental Quality
J. Dworzanski	University of Utah
H. J. S. Fernando	Arizona State University
M. Fertig	San Diego State University
R. W. Gray	University of Texas at El Paso
J. Greenlee	New Mexico State University
S-M. Lee	Arizona State University
W. Li	University of Texas at El Paso
H. L. C. Meuzelaar	University of Utah
G. M. Mejia-Velázquez	Instituto Tecnológico y de Estudios Superiores de Monterrey
R. Okrasinski	New Mexico State University
N. J. Parks	University of Texas at El Paso
M. Quintero-Núñez	Universidad Autónoma de Baja California
M. Rodríguez-Gallegos	Instituto Tecnológico y de Estudios Superiores de Monterrey
J. Saenz	Texas Commision on Environmental Quality
S. Sheya	University of Utah
A. Sweedler	San Diego State University
D. D. Tejeda-Honstein	Instituto Tecnológico y de Estudios Superiores de Monterrey
C. D. Turner	University of Texas at El Paso
V. Valenzuela	Texas Commision on Environmental Quality
J. A. VanDerslice	State of Washington Department of Health
D. R. Van Schoik	Southwest Center For Environmental Research And Policy

The Southwest Center for Environmental Research and Policy (SCERP) is a consortium of U.S. and Mexican universities dedicated to addressing environmental issues of the U.S.-Mexican border region through applied research, outreach, and regional capacity-building.

SCERP Universities
Arizona State University
El Colegio de la Frontera Norte
Instituto Tecnológico de Ciudad Juárez
Instituto Tecnológico y de Estudios Superiores de Monterrey
New Mexico State University
San Diego State University
University of Texas at El Paso
University of Utah
Universidad Autónoma de Baja California
Universidad Autónoma de Ciudad Juárez

SCERP website: www.scerp.org

THE U.S.-MEXICAN BORDER ENVIRONMENT

Air Quality Issues along the U.S.-Mexican Border

Edited by Alan Sweedler

San Diego State University Press

Published by
San Diego State University Press
5500 Campanile Drive
San Diego, CA 92182-4402
http://www-rohan.sdsu.edu/dept/press

Cover photos by N.J. Parks

ISBN 092561338-X

9 780925 613387

Previously published volumes in the SCERP Monograph Series, *The U.S.-Mexican Border Environment*

No. 1 A road map to a sustainable 2020

No. 2 Water issues along the U.S.-Mexican Border

No. 3 Economy and environment for a sustainable border region

No. 4 U.S.-Mexican border communities in the NAFTA era

No. 5 Overcoming vulnerability: The Southwest Center for Environmental Research and Policy's research program (1990-2002) and future agenda

About this volume:

All times are local

All monetary figures are US$ unless otherwise specified

Contents

Foreword

SCERP began comprehensive studies of air quality issues in a number of the largest binational border communities in the early 1990s. These applied research efforts were designed as a first step to improve our understanding about the basic characteristics of the transborder air pollution present in these communities. Goals included developing better information on contaminant sources, types, transport, trajectories, and deposition, among other characteristics. They also included developing information on exposures, doses, sensitivities, and physiological effects—elements all related directly to human health effects. Since launching its air quality program more than a decade ago, SCERP has conducted 93 applied research projects related to air quality. The present volume contains the results of a number of these projects. Additional collections of research reports are in progress that will disseminate the results of other SCERP air projects more widely to border communities; to the research community; to state, local, and federal agencies; and to students.

Studies of the sort included in this volume present special challenges when conducted in the U.S.-Mexican border region. While the major U.S. border communities of California and Texas have had well-developed air monitoring networks functioning for many years, similar networks and data availability are relatively recent for the Mexican cities that share these binational airsheds. Thus, gaps in data for the entire border region are typical rather than exceptional. Mexico has moved rapidly in recent years to provide some of the data needed for air quality analysis and now has monitoring systems in place in major northern border cities to facilitate better understanding of the regional issues. A number of SCERP projects specifically geared toward doing so have also been helpful in addressing issues of insufficient data.

The involvement in SCERP projects of U.S. and Mexican researchers as well as advanced students and stakeholders from the region has contributed to the development of expertise and capacity for understanding and resolving transborder air pollution issues. SCERP air studies have provided important support for initiatives along the border to mitigate the negative effects of air contaminants. These include provision of data for the Paso del Norte Air Quality Task Force and basic studies that have been useful for efforts to address transnational air quality issues in the San Diego-Tijuana region and the Imperial Valley-Mexicali Valley region.

The editor of this volume on air quality, Alan Sweedler, is director for the Center for Energy Studies and chair of the Environmental Sciences Program at San Diego State University. He selected the articles in this volume from SCERP research efforts and other studies along the border. These are the results of studies that examined more than just a single pollutant, as poor air quality in the border is usually caused by a combination of several criteria pollutants.

The volume and series editors thank the authors and their research teams for their professionalism and attention to cross-boundary air issues. The guidance provided by Paul Rasmussen of the EPA Office of Air and Radiation is also much appreciated. The editors also recognize the work of SCERP's Amy Conner, who coordinated production of this volume, and also note the efforts of graphic artists Jenny Carlsson and Mayra Navarro for their work on the figures. This volume is dedicated to the many community-based organizations that work to educate citizens about health effects of air pollution.

Paul Ganster, San Diego State University
SCERP Monograph Series General Editor

Executive Summary

Air Quality in the United States-Mexican Border Region

D. R. Van Schoik

ABSTRACT

Air pollution is one of the most important environmental issues in the U.S.-Mexican binational region. It is ubiquitous but includes a variety of types, sources, and effects. It threatens economic development and human and environmental health. It originates from, flows to, and needs solutions from both sides of the border. And it is worsening in many cases for a variety of reasons.

The region surrounding the 1,952-mile long border has the fastest growing population in North America. Its growth rate is almost double the Mexican rate and the region includes the cities of the Lower Rio Grande Valley, which are growing at a blistering pace. The border population is expected to double from its current level of approximately 12 million to more than 24 million by 2025. Most of that growth, which will occur faster in Mexico than the United States, will be in the urban twin-city pairs along the border.

The 1992 passage of the North American Free Trade Agreement (NAFTA) and its current implementation exacerbates the already-fast growth rate. The border is the gateway—some would say "door-mat"—for the North American trade of agricultural products, tourism, raw materials, and the finished products of a large and still-growing manufacturing and assembly industry, known as the maquiladora industry, which is located mostly in the border region.

The number of car, small truck, and heavy-duty truck crossings to accommodate the industry and trade increases without commensurate infrastructure improvements or regulatory relief, causing congestion at the border ports of entry and intensifying air pollution in local areas.

The region remains impoverished compared to the rest of the United States. Unemployment is higher and wages are lower—and continue to decrease—relative to the whole of the United States. The lower salary rates are reflected in the tax base and coffers of the governments, and this translates into less means to monitor, understand, address, and even publicize the issues.

The region has some indigenous fossil fuels. Natural gas exists in Texas, Coahuila, Nuevo León, and Tamaulipas; Chihuahua and Coahuila have coal; and Texas has petroleum. Some renewable energy sources exist throughout the region, including solar, wind, and geothermal. The region's limited but rapidly increasing electrical generating facilities depend primarily on oil and coal (Carbón I and II) in Mexico and oil and gas in United States. In Baja California most of the current and planned power plants are powered by natural gas imported from the United States. The border region continues to import both fuels and electrical power.

Resumen Ejecutivo

Calidad del Aire en la Región Fronteriza México-Estados Unidos

Resumen

Entre los problemas de la región binacional México-Estados Unidos, la contaminación del aire se sitúa entre los de más alta prioridad. Es ubicua pero incluye una variedad de tipos, fuentes y efectos. Amenaza el desarrollo económico así como la salud humana y ambiental. Se origina, fluye y necesita soluciones desde ambos lados de la frontera. Y está empeorando en muchos casos debido a causas diversas.

La región que rodea la frontera con 1,952 millas de largo, tiene quizás la población con más rápido crecimiento en Norteamérica. Su tasa de crecimiento es casi el doble que la de México y la región incluye las ciudades situadas en la parte baja del Valle de Río Grande, las cuales crecen a un paso vertiginoso. Se espera que la población duplique su número actual de aproximadamente 12 millones a más de 24 millones para el año 2025. La mayoría de ese crecimiento, el cual ocurrirá más rápido en México que en los Estados Unidos, será en los pares urbanos de ciudades gemelas ubicadas en la frontera.

La aprobación en el año de 1992 del Tratado de Libre Comercio (TLC) y su actual implementación, acelera el ya rápido índice de crecimiento. La frontera es el medio de acceso–algunos dirán "la alfombra de bienvenida"–para el comercio norteamericano de productos agrícolas, turismo, materias primas, y los productos terminados de una grande y todavía creciente industria de manufactura y ensamble como lo es la industria maquiladora, la cual se sitúa en su mayor parte en la región fronteriza. El número de autos y camiones de carga ligera y pesada que deben cruzar para satisfacer las necesidades de la industria aumenta sin las mejoras proporcionales de infraestructura o regulatorias, causando congestión en los accesos fronterizos y la intensificación de contaminación aérea en áreas locales.

La región permanece empobrecida comparada con el resto de los Estados Unidos. El desempleo es más alto y los salarios más bajos–y continúan disminuyendo–en relación con la totalidad de los E.U. Los bajos salarios se reflejan en la base tributaria así como en los fondos de los gobiernos, y esto se traduce en menos recursos para monitorear, entender, atender, y hasta difundir los asuntos en cuestión.

AIRBASINS

The region has a number of officially recognized and informally designated common binational airbasins—geographic regions defined by airflows. An airbasin is usually determined by a mountainous circumference that limits airflow, making activities in any part of the basin interdependent on activities in others.

The binational airbasins are characterized by their topography, climate, and weather. Most are defined by mountain ranges, predominant but seasonally shifting winds, and potentially strong thermal inversions—locations where cooler air masses trap warmer air pockets after accumulating local sources of pollution until the temperature gradient equalizes. For example, residents of San Diego and Tijuana share an airbasin since a coastal mountain range somewhat limits movements of air in the area. Daily reciprocal coastal-offshore breezes mix the local air from as far north as Los Angeles and as far south as Ensenada, while predominately westerly winds eventually move the air to the east. The Imperial County-Mexicali airbasin is low (partly below sea level), hot (over 100 degrees Fahrenheit on summer days), and bounded by mountains to the east and west. The El Paso-Ciudad Juárez, or Paso del Norte, airbasin is defined by predominant westerly winds and a pass in the mountain range through which the winds are channeled. The same predominant winds cross the Big Bend region—a mix of mountains and plateaus—making it hard to determine where pollutants present there originate. Finally, the Lower Rio Grande Valley is flat, more tropical, and has coastal breeze influences from the Gulf of Mexico.

In the case of the U.S.-Mexican border region, there are several valleys transversed by the political border in which cities have developed on both sides (San Diego-Tijuana, El Paso-Ciudad Juárez, Calexico-Mexicali). Here the residents of both cities from the two countries share the same atmospheric space; thus, activities in one directly affect the other. Since these twin cities have developed under distinct governmental regulations, as well as under very different economic and social conditions, the sources of air pollution on each side are different. Just as the pollutants generated on one side affect the other, solutions need to be determined, understood, and implemented binationally. Examples of border airbasins are described in this volume geographically from west to east, including San Diego-Tijuana, Imperial County-Mexicali, the Paso del Norte area of El Paso-Ciudad Juárez, the Big Bend region, and the Lower Rio Grande Valley.

Types of Pollutants and Their Effects

The binational airbasins are plagued by dangerous levels of several air pollutants that originate on both sides of the border. Some are monitored to some degree under efforts to reach air quality goals. The United States Environmental Protection Agency (EPA) uses six "criteria pollutants" as indicators of air quality and has established for each of them a maximum concentration above which adverse effects on human health may occur. These threshold concentrations are called National Ambient Air Quality Standards. Each state also has standards that may meet or exceed the federal standard. Likewise, the Mexican Secretaría de Medio Ambiente y Recursos Naturales (SEMARNAT) has its own standards that in some cases match, but in others exceed, United States standards. The table below identifies air chemistry components of greatest concern to the various regions. The standards range from attainment of standards to moderate nonattainment, to strict restrictions on additional emissions due to severe nonattainment.

Table 1. Border Air Quality Goal Attainment Status

Airbasin	Ozone (O_3)	Carbon Monoxide (CO)	Particulate Matter (PM)	Sulfur Dioxide (SO_2)
San Diego-Tijuana	Serious	Transitional	Attainment	Attainment
Imperial Valley-Mexicali	Transitional	Transitional	Moderate	Attainment
Douglas-Agua Prieta	Attainment	Attainment	Moderate	Primary
El Paso - Ciudad Juárez	Serious	Moderate	Moderate	Attainment
Big Bend Park region	Attainment	Attainment	Attainment	Attainment
Lower Rio Grande Valley	Attainment	Attainment	Attainment	Attainment

When an area does not meet the air quality standard for one of the criteria pollutants, it may be subject to the formal rulemaking process that designates it as "nonattainment." The Clean Air Act further classifies ozone, carbon monoxide, and some particulate matter nonattainment areas based on the magnitude of an area's problem. Nonattainment classifications may be used to specify what air pollution reduction measures an area must adopt and when the area must reach attainment. The following is a discussion of the standards, designations, and classifications of these areas. More and current information may be found on the websites of the EPA at www.epa.gov, SEMARNAT at www.semarnat.gob.mx, and the Centro de Información sobre Contaminación de Aire/Center for Information on Air Pollution at www.epa.gov/ttn/catc/cica.

Ozone

Ozone (O_3) is a photochemical oxidant and the major component of smog. While O_3 in the upper atmosphere is beneficial to life by shielding the earth from harmful ultraviolet radiation from the sun, high concentrations of O_3 at ground level are a major health and environmental concern. O_3 is not emitted directly into the air but is formed through complex chemical reactions between precursor emissions of volatile organic compounds (VOC) and oxides of nitrogen (NO_x) in the presence of sunlight. These reactions are stimulated by sunlight and temperature so that peak O_3 levels occur typically during the warmer times of the year. Both VOCs and NO_x are emitted by transportation and industrial sources. VOCs are emitted from sources as diverse as automobiles, chemical industries, dry cleaners, paint shops, and other businesses using solvents.

The reactivity of O_3 causes health problems because it damages lung tissue, reduces lung function, and predisposes the lungs to sensitivity to other irritants. Scientific evidence indicates that ambient levels of O_3 not only affect people with impaired respiratory systems, such as asthmatics, but healthy adults and children as well. Exposure to O_3 for several hours at relatively low concentrations has been found to reduce lung function significantly and induce respiratory inflammation in normal, healthy people during exercise. This decrease in lung function is generally accompanied by symptoms including chest pain, coughing, sneezing, and pulmonary congestion.

Carbon Monoxide

Carbon monoxide (CO) is a colorless, odorless, and poisonous gas produced by incomplete burning of carbon in fuels. When CO enters the bloodstream, it reduces the delivery of oxygen to the body's organs and tissues. Health threats are most serious for those who suffer from cardiovascular disease, particularly those with angina or peripheral vascular disease. Exposure to elevated CO levels can cause impairment of visual perception, manual dexterity, learning ability, and performance of complex tasks. More than three-quarters of the CO emissions nationwide are from transportation sources; motor vehicles on highways contribute the most emissions. Thus, the focus of CO monitoring is on traffic-oriented sites in urban areas where the main source is motor vehicle exhaust. Other major CO sources are woodburning stoves, incinerators, and industrial activities. The National Ambient Air Quality Standard for carbon monoxide over an eight-hour average is 9ppm, or parts per million (also equal to 10 micrograms per cubic meter).

Nitrogen Dioxide

Nitrogen dioxide (NO_2) is a brownish, highly reactive gas present in all urban atmospheres. NO_2 can irritate the lungs, cause bronchitis and pneumonia, and lower resistance to respiratory infections. Nitrogen oxides are an important precursor both to O_3 and acid deposition, or acid rain (which causes acidification of lakes and streams and can damage trees, crops, and historic buildings and statues), and may affect both terrestrial and aquatic ecosystems. The major mechanism for the formation of NO_2 in the atmosphere is the oxidation of the primary air pollutant nitric oxide (NO). Both NO and NO_2 (known collectively as NO_x) play a major role, together with VOCs, in the atmospheric reactions that produce O_3. NO_x forms when fuel is burned at high temperatures. The two major emissions sources are transportation and stationary fuel combustion in electric utility and industrial boilers.

Sulfur Dioxide

High concentrations of sulfur dioxide (SO_2) affect breathing and may aggravate existing respiratory and cardiovascular disease. Sensitive populations include asthmatics, individuals with bronchitis or emphysema, children, and the elderly. SO_2 is also a primary contributor to acid rain. In addition, sulfur compounds are one of the causes of impaired visibility in many regions of the country. This is especially noticeable in national parks. Ambient SO_2 results largely from stationary sources such as coal and oil combustion sites, steel mills, refineries, pulp and paper mills, and non-ferrous smelters.

Particulate Matter

Particulate matter refers to dust, dirt, soot, smoke, and liquid droplets directly emitted into the air by sources like factories, power plants, cars, construction activity, fires, and natural windblown dust. Particles formed in the atmosphere by condensation or by the transformation of emitted gases such as SO_2 and VOCs are also considered particulate matter.

Based on studies of human populations exposed to high concentrations of particles (sometimes in the presence of SO_2) and laboratory studies of animals and humans, there are major concerns for human health. These include effects on breathing and respiratory symptoms, aggravation of existing respiratory and cardiovascular disease, alterations in the body's defense systems against foreign materials, damage to lung tissue, carcinogenesis, and premature death. The major subgroups of the population that appear to be most sensitive to the effects of particulate matter include asthmatics, the elderly, children, and individuals with chronic obstructive pulmonary or cardiovascular disease, or influenza. Particulate matter also damages materials and is a major cause of visibility impairment in the United States. The smallest particles pose the greatest health risk because they can be aspirated deep into the lungs with each breath and can evade the respiratory system's natural cleansing abilities. Because some are produced by combustion, they are carcinogenic and mutagenic and thus, they can cause substantial illnesses, acute respiratory diseases, and premature death.

Particulate matter is defined by aerodynamic diameter: PM_{10} are those particles less than 10 microns; PM_{coarse} are those particles between 10 microns and 7.5 microns; and $PM_{2.5}$ or PM_{fine} are those less than 2.5 microns.

Lead

Even low doses of lead damage the central nervous system. Recent studies have also shown that lead may be a factor in high blood pressure and in subsequent heart disease in middle-aged males. Lead gasoline additives, non-ferrous smelters, and battery plants are the most significant contributors to atmospheric lead emissions. In 1993, transportation sources contributed 33% of the annual emissions, down substantially from 81% in 1985. Total lead emissions from all sources dropped from 20,100 tons in 1985 to 4,900 tons in 1993. The decrease in lead emissions from highway vehicles accounts for essentially all of this decline.

Sources and Fates

The primary sources of air pollution in the region are dust, combustion of fuels, open burning, and vehicles and other mobile sources. The predominant economic activities in the region—agriculture, manufacturing, and residential development—create a mix of pollutants. Sources particular to these arid, border twin-cities include:

- Agricultural practices such as plowing, rotating, and weeding soils; airborne pesticide application, fallowing of fields, and burning of wastes
- Natural geologic sources such as sands and clays from unpaved roads, dried lakes, and streambeds
- Industrial activities such as mining, refining, wastewater treatment, and geothermal energy generation
- Food cooking, especially outdoors and over wood-burning fires

Local meteorological and geographic conditions determine much of the effect of pollutants. Strong winds tend to pick up and suspend large particles longer, moving them greater distances. Some pollutants, such as ozone, are created and destroyed daily, but may circulate in an area due to local wind patterns both on the ground and in the air. Still other pollutants combine or dissociate to make new compounds. Details about specific sources, transport, fates, and offspring are found in each chapter.

Binational Approaches to Address and Resolve Air Pollution

All efforts to address air quality issues in the border region begin with binational cooperation in monitoring and analyzing air. The 1990s saw new initiatives along the border and even entire databases developed out of the effort. The Centro de Información sobre Contaminación de Aire (CICA) is dedicated to air quality issues and data in the border region. The EPA has developed several technical tools, including source databases, dispersion models, and processors of meteorological data, some of which are available in Spanish specifically for analytical use in the border region.

Remedies revolve around informing the public, as well as planning and implementing optimal solutions. Outreach mechanisms include public service announcements and interpretation of local, real-time conditions by weather reports on news programs. For example, a website provides real-time information about ozone conditions and impacts in the Paso del Norte. Strategic planning and prioritization of implementation strategies are also being conducted. The EPA and SEMARNAT created a number of working groups as part of their binational Border XXI Program to address concerns in the region jointly. The Air Working Group, a Joint Task Force in the Paso del Norte, and later a NAFTA-recognized Joint Advisory Council in the Paso del Norte wrote a remediation plan that is slowly being funded and implemented. A Binational Air Quality Alliance in the San Diego-Tijuana region is also engaged in mid-term planning for solutions to local challenges. United States legislation has included the Border Smog Reduction Act of 1998 (HR 8), sponsored by then-Congressman Brian Bilbray, to mandate that Mexican vehicles regularly spending time in the United States meet California air emissions standards. Other coalitions are attempting to introduce sufficient alternative fuel infrastructure to power a fleet of vehicles. Oxygenated additives are used in some areas threatened by CO and O_3 hazards. These are just a few examples of the ongoing binational efforts to address the pressing concern of air pollution in the border region.

THE ROLE OF SOUTHWEST CENTER FOR ENVIRONMENTAL RESEARCH POLICY

SCERP has successfully completed numerous studies on air quality, alternative fuel, energy conversion, global climate change, and implementation strategies. In just the last five years, SCERP has conducted:

- Air Quality/Meteorology Projects on almost all air chemistry components for the Paso del Norte, San Diego-Tijuana, Mexicali-Calexico, Big Bend, Hidalgo-Reynosa, and Nuevo Laredo, New Mexico regions, the results of which are used to prioritize air cleanup implementation strategies
- A Binational Air Emissions Permit Trading study to harness market forces to clean emissions and save money in the entire border airbasin
- Major Carbon Sequestration efforts in Mexicali and Ojinaga by growing trees with partially treated wastewater
- Brick-Making Kiln studies and created designs to make brick-firing more efficient, cost-effective, cleaner, and safer for the operators
- Global Climate Change studies to investigate feedbacks from land use patterns, vegetation cover, soil, moisture, and desert temperatures; accelerated changes are used to alert local planners and resource managers

SCERP has also:

- Built and redesigned Domestic Heating Unit Efficiency prototypes to lower emissions and improve home heating efficiency

- Collected Car, Light Truck, and Diesel Truck Emissions and Activity data for regional mobile-emissions inventories and models
- Developed Air Quality Improvement Willingness to Pay models to assess drivers' abilities to change maintenance and driving patterns and to plan the most cost-effective policies
- Created Hybrid Wind-Generator engineering and hardware to provide renewable and reliable energy to communities off the traditional grid

SCERP also sponsored its third Border Institute, "Trade, Energy and the Environment: Challenges and Opportunities in the Border Region, Now and in 2020," to address the relationship of air quality to energy development and the long-term policy solutions to air quality issues. Those proceedings are included in another SCERP monograph.

Summary of Papers

In "Air Quality in the California-Baja California Border Region," authors A. Sweedler, M. Fertig, and K. Collins from San Diego State University and M. Quintero-Núñez from Universidad Autónoma de Baja California give a comprehensive description of the climate geomorphology, economy, transportation, and energy setting and the resultant air quality conditions in California's and Baja California's two airbasins—San Diego-Tijuana and Imperial Valley-Mexicali. Rapid population growth, expanded industrialization—including that of maquiladora plants—and extreme congestion at border crossings by cars and light- and heavy-duty trucks, exacerbate an already dire situation. While the region has significant solar, geothermal, and wind resources, it continues to import fuels and electricity. Monitoring of air quality at binational sites has improved dramatically in the last five years, contributing to a better understanding of airbasin dynamics. Future progress on the overall issue is possible, thanks to past efforts to monitor and model the airbasin.

An extensive study by SCERP to understand the types, source apportionment, and fates of particulates in the Paso del Norte is ongoing and will be the subject of a subsequent monograph.

However in this volume, "Air Quality in the Paso del Norte Airshed: Historical and Contemporary," by J. Parks, W. Li, C. D. Turner, R. W. Gray, R. Currey, S. Dattner, J. Saenz, V. Valenzuela, and J. A. VanDerslice of the University of Texas at El Paso, provides an overview of the Paso del Norte airshed region, which is comprised of Ciudad Juárez, Chihuahua; El Paso, Texas; and Doña Ana County, New Mexico. The authors identify stakeholders and provide a framework for industry, academia, non-governmental advocates, and government agencies at various levels to collaborate on air issues. They also provide a number of important websites for information.

S-M. Lee and H. J. S. Fernando at Arizona State University declare the need to accurately understand and model planetary boundary layer behavior to understand the fate of air pollution in their contribution to this volume, "Planetary Boundary-Layer Structure of the Paso del Norte Airshed: A Numerical Study." The paper describes the meteorologically determined fate of airborne contaminants. Heat, moisture, wind direction, and speed all affect trajectories from sources and fall-out rates of the components. The three-dimensional model-driven simulations from two different schemes in various seasons closely match actual sounding measurements. Among the conclusions is that there is a need for more data from carefully planned experimental designs. The value of such models is the ability to begin to ask air quality improvement questions including what if these sources are prohibited, scheduled, relocated, and/or minimized? The trajectory models provide a necessary understanding of fates, alludes to effects, and discerns populations at risk.

Another approach to air pollution issues is provided by R. Okrasinski and J. Greenlee of New Mexico State University in their report, "Correlation of Wind Flow and Visibility at Big Bend National Park." They ask where contaminants in a particular area originate and examine the air chemistry in the Big Bend region—which contains national and state parks, monuments, preserves, and refuges on both sides of the border and is plagued by poor visibility caused to some degree by fine particulates (0.4 to 0.7 microns). Specifically, they measure penetration of visible light using transmissometers to determine the deciview (visibility units) at various locations. Then, using diffusion models corrected with radiosonde station data, they match signatures with probable sources within a 600km radius to attribute the relative contribution from each. Dramatic seasonal variability creates the best conditions when predominant winds are from the north and west, and the worst conditions when from the east and south. The Mexican coal-burning plants known as Carbón I and II, long suspected of being major sources of air pollution in the Big Bend National Park, were absolved of primary responsibility while sources in eastern Texas are questioned. Such understanding is critical to binational solutions. This study demonstrates the importance of applied scientific research to understanding these complex problems.

Finally, “Characterization and Dynamics of Air Pollution in the Lower Rio Grande Valley,” by G. Mejia-Velazquez, S. Sheya, J. Dworzanski, M. Rodriguez-Gallegos, D. D. Tajeda-Honstein, J. M. Cardona-Carrizalez, and H. L. C. Meuzelaar of the University of Utah, takes a comprehensive look at critical pollutants, VOCs, particulates, and NO_X. They describe transient episodes of relatively high particulate concentrations to determine causes and an outlook for the future. Using receptor sensors (size distribution scales and particle counters), meteorological studies, principal component analysis, and a photochemical model, the researchers were able to identify several sources, including mobile sources, a PEMEX refinery, and a power plant (in descending order), as the primary causes. As population and trade increase, the contribution from traffic and industry is expected to push the region into nonattainment of standards.

Overall, the papers illustrate the diverse challenge to air quality within the border region alone, as well as the need to comprehensively understand the situation in order to tailor remedies to the specific, local situation. The papers also exemplify that the political will necessary to address the issue does exist and is effective when applied. Outreach to the local community to promote their understanding and involvement is a common theme in all reports. These studies also show the importance of the existence of a consortium of United States and Mexican universities within the border region that can facilitate a coordinated, multidisciplinary approach to a focused issue like air. At the same time, these studies show how this medium is so intertwined with others. Only through a binational, comprehensive, multimedia approach can the complexity of border environmental issues be addressed.

I

Air Quality in the California-Baja California Border Region

A. Sweedler, M. Fertig, K. Collins, and M. Quintero-Núñez

Abstract

This chapter offers a comprehensive description of the climate geomorphology, economy, transportation, and energy setting and the resultant air quality conditions in California's and Baja California's two airbasins—San Diego-Tijuana and Imperial Valley-Mexicali. Rapid population growth, expanded industrialization—including that of maquiladora plants—and extreme congestion at border crossings by cars and light- and heavy-duty trucks, exacerbate an already dire situation. While the region has significant solar, geothermal, and wind resources, it continues to import fuels and electricity. Monitoring of air quality at binational sites has improved dramatically in the last five years, contributing to a better understanding of airbasin dynamics. Future progress on the overall issue is possible, thanks to past efforts to monitor and model the airbasin. The authors also point out several short- and long-term, technical, and institutional recommended measures that would improve air quality in the region.

Calidad del Aire en la Región Fronteriza California-Baja California

A. Sweedler, M. Fertig, K. Collins, y M. Quintero-Núñez

Resumen

Este capítulo presenta una descripción comprensible de la geomorfología del clima, la economía, el transporte, la situación energética, y las condiciones resultantes en la calidad del aire para las dos cuencas atmosféricas de California y Baja California–San Diego-Tijuana y Valle Imperial-Mexicali. El rápido crecimiento poblacional, la expansión industrial—incluyendo la de las maquiladoras- y el congestionamiento extremo en los cruces fronterizos de autos y camiones de carga ligera y pesada, agravan la ya pésima situación. Aunque la región cuenta con recursos solares, geotérmicos y eólicos importantes, continúa importando combustibles y electricidad. El monitoreo de la calidad del aire en localidades binacionales ha mejorado dramáticamente en los últimos cinco años, contribuyendo a una mejor comprensión de las dinámicas de las cuencas atmosféricas. El avance futuro sobre el asunto general es posible, gracias a los esfuerzos anteriores para monitorear y modelar las cuencas. Los autores también señalan algunas recomendaciones técnicas e institucionales para el corto y largo plazo que podrían mejorar la calidad del aire en la región.

Introduction

The U.S.-Mexican border region consists of San Diego and Imperial counties in California and the Mexican *municipios* of Tijuana, Rosarito, Ensenada, Tecate, and Mexicali (Figure 1).

Figure 1. Map of California-Baja California Region

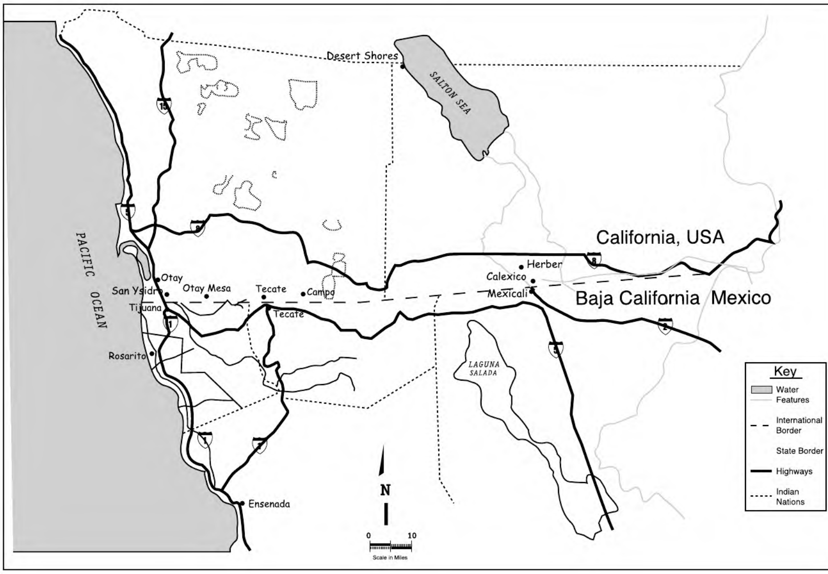

Source: California Environmental Protection Agency Border Environmental Program

The border runs 220km eastward from the San Diego-Tijuana region on the Pacific Ocean to the Colorado River, which forms the border between California, Arizona, and the Mexican states of Baja California and Sonora. Approximately 5 million people—nearly one half the population of the entire U.S.-Mexican border region—live in the California-Baja California region, which has grown significantly over the years. Figure 2 shows population growth in the region from 1930 to 2000. Table 1 gives population data by counties and *municipios* and projections to 2020. In the San Diego-Tijuana section of the border alone, the population is expected to be 5.7 million in 2020—an increase of 43% in just 20 years. This large population increase will have a major impact on air quality in the region.

An important characteristic of this rapidly growing population is its concentration in urban areas along the border, coupled with increased industrialization in the Mexican border cities. The combination of increased population, urbanization, and industrialization has put considerable pressure on the region's underlying ecosystems and is the principal source of the region's environmental problems, including its air pollution.

Figure 2. Population Growth in the California-Baja California Region, 1930–2000

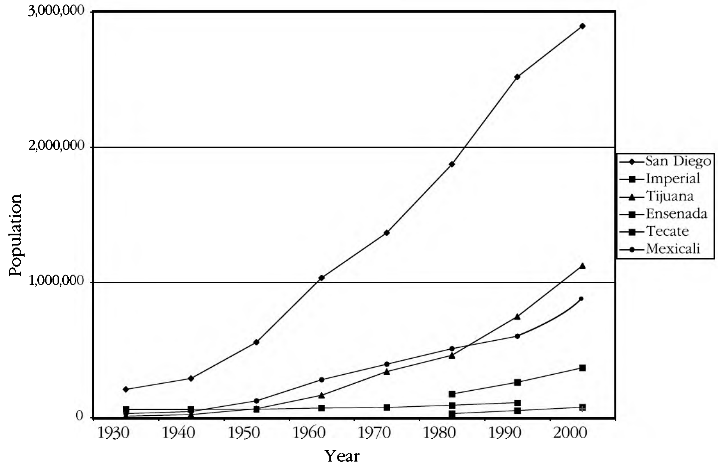

Source: Instituto Nacional de Estadística, Geografía e Informática (INEGI)

Table 1. Population Growth and Projections in the California-Baja California Border Region

Year	San Diego	Imperial	Tijiuana	Ensenada	Tecate	Mexicali	Rosarito
1930	209,659	60,903	11,000	not available	not available	29,985	not available
1940	289,348	59,740	22,000	not available	not available	44,399	not available
1950	556,808	62,975	65,000	not available	not available	124,362	not available
1960	1,033,011	72,105	166,000	not available	not available	281,333	not available
1970	1,367,200	74,400	341,000	not available	not available	396,324	not available
1980	1,873,300	92,500	462,000	175,000	31,000	510,664	not available
1990	2,520,500	110,400	747,381	261,000	52,000	601,938	not available
1995	2,690,255	141,500	1,032,415	314,000	62,000	695,805	not available
2000	2,896,900	182,653	1,125,200	369,573	77,444	not available	63,549
2010	3,360,700	303,037	1,491,300	not available	111,022	not available	not available
2020	3,791,400	491,778	1,946,300	not available	159,547	not available	not available

Source: INEGI and J. Peach

These are just some of the major issues related to air quality in California-Baja California border region:

- In 1999, San Diego was designated a nonattainment area for United States ambient air quality standards for ozone (O_3) and Imperial County for PM_{10} and ozone; San Diego and Imperial Counties also failed to meet California air quality standards for ozone and PM_{10}
- Tijuana and Mexicali do not meet Mexican air quality standards for particulate matter, ozone, and carbon monoxide
- Increased numbers of vehicles and increased transboundary traffic, especially heavy-duty trucks, have resulted in the dramatic increase of air pollution from mobile sources
- Mexico lacks sufficient information about emissions sources, especially mobile sources; lack of such data makes it difficult to obtain a reliable emissions inventory for the border region
- In Tijuana and Mexicali, there is uncertainty regarding the ability to maintain a sufficiently robust ambient air quality monitoring system
- There are currently no binational planning efforts to reduce emissions into the atmosphere
- No alternative sources of energy for the region have been developed, yet fossil-based fuels are the principal source of air pollution in the border region

San Diego-Tijuana Region

Population and Economy

When discussing regional air quality issues, it is important to remember that San Diego and Tijuana, in which 75% of the border region's inhabitants reside, are extremely dynamic cities and are growing and changing rapidly. As San Diego pulled out of the defense-industry-related recession of the early 1990s, job creation has brought new residents, new housing developments, more vehicles on the road, and other impacts on the regional air quality. At the same time, Tijuana is growing at a blistering pace, with its population doubling about every 10 years. Table 2 shows growth rates for San Diego and Tijuana from 1930 through 2000 with projections to 2020. In 1996 and 1997, population growth rates for San Diego increased more than 2% per year, while those of Tijuana remained the same as in the previous five years. Given the rapid population growth rates for both cities, regional air quality will likely decline unless significant efforts are made on both sides of the border to deal with the underlying causes of air pollution.

Table 2. Population Growth for San Diego and Tijuana, 1930-2020

Year	San Diego	Tijuana
1930	209,659	11,000
1940	289,348	22,000
1950	556,808	65,000
1960	1,033,011	166,000
1970	1,367,200	341,000
1980	1,873,300	462,000
1990	2,520,500	747,381
1995	2,690,255	1,032,415
2000	2,896,900	1,125,200
2010 (projected)	3,360,700	1,491,300
2020 (projected)	3,791,400	1,946,300

Source: INEGI

Another important characteristic of the border region is the sharp economic contrast between California and Baja California. San Diego is one of the wealthiest counties in the United States with a per capita income 3% above the national average. Although Tijuana and Mexicali are among the wealthiest regions in Mexico in terms of per capita income and standard of living, they are still far below that of San Diego.

San Diego's continued economic expansion pushed the gross regional product (GRP) beyond $90 billion before the end of the twentieth century. The GRP—the value of all goods and services produced in San Diego County—reached $110.2 billion in 1999 and $101.41 billion in 2000. San Diego not only fully recovered from the recession in the first half of the decade, but it far surpassed former record levels of production set in the 1980s. Since 1995, San Diego has established a new record in economic output for the region.

By contrast, the GRP for the municipality of Tijuana is only $3 billion. This translates to San Diego having a per capita GRP nearly 12 times greater than that of Tijuana. Minimum wage in San Diego is approximately eight times higher than that of Baja California. These basic facts of economic asymmetry affect all aspects of life in the transborder region, including resources available to combat air pollution.

San Diego's former reliance on defense spending allowed the region to be somewhat immune from other state and national economic trends. The transition in the 1990s away from this sole reliance upon defense dollars into more commercial and international endeavors has made San Diego's economy much more entwined with the rest of California and the United States, as well as with Mexico and international markets.

San Diego's economy can be broken down into several main sectors: defense, high technology, telecommunication, biotechnology, international trade, and tourism. None of these sectors are considered to be intense energy consumers or large sources of air pollution as are heavy, and even some light, manufacturers. Mobile sources of gaseous pollutants (oxides of nitrogen [NO_X], carbon monoxide [CO], and volatile organic compounds) are considered the primary cause of ozone formation in San Diego.

Tijuana's economy is structured quite differently than that of San Diego. One of the most important differences is the growing importance of the manufacturing sector, especially the large number maquiladoras (multinationally owned manufacturing plants), which are large consumers of power, gaseous fuels, and water. As of July 2002, there were 641 maquiladoras in Tijuana with a work force of about 148,706 people. The maquiladora sector is an important part of the local economy and accounted for about 48% of all jobs created in Tijuana from 1980 to 1990.

Energy Sector

Since the use of energy is one of the major sources of air pollution in the binational region, a brief description of this important sector is relevant to develop programs and policies to improve air quality.

The outstanding characteristic of energy use in the border region is the almost total dependence on energy resources from outside the area. With the notable exception of the geothermal fields located south of Mexicali, virtually all of the energy consumed in the region originates from distant sources. These "imported" energy resources are in the form of natural gas, uranium, electricity, and petroleum products, including gasoline, diesel, jet fuel, liquefied petroleum gas, and fuel oil. In 1994, approximately $3 billion per year left the San Diego economy to pay for this energy. All of Baja California's transportation, industrial, and residential fuels must be transported long distances from refineries located in southern Mexico. Moreover, the electric power grid in Baja California is not connected to the main Mexican power system and the state has no natural gas pipeline system, with the exception of a small distribution system in Mexicali.

The salient features of the energy sector in the binational region are the lack of indigenous or nearby energy resources for both San Diego and Baja California, the relatively high cost of electricity in San Diego, the isolation of the Baja California power grid from the rest of Mexico, the absence of a natural gas pipeline system in Baja California, and the growing demand for energy resulting from the increasing industrialization and population in northern Tijuana and San Diego. These facts also provide a rationale for developing increased cooperation in the energy field between California and Baja California.

Total installed capacity in Baja California is 1.4 gigawatts, compared to 2.5 gigawatts in San Diego. San Diego does not meet its own electric demand by in-region generation and must import nearly 60% of its electricity from other areas of North America. Baja California is also unable to meet demand by in-region power generation and must import electricity from San Diego. Per capita electric consumption in San Diego is much greater than in Baja California. Residents on the United States side of the border use 3.5 times as much electricity per capita than do people living in Baja California. Per capita consumption of electricity in Baja California is expected to increase rapidly as industrialization and urbanization continue to expand. To meet these future energy needs, new energy sources will be required. If the region's heavy dependence on fossil fuels continues, there is a high probability that air quality will be negatively impacted.

The fuels used for electricity generation in Baja California were oil (44%), geothermal (44%), and diesel (12%). Most of this power was generated in two large plants, one near Rosarito that used oil and the other at Cerro Prieto near Mexicali that used geothermal heat. Several smaller plants in Tijuana, Mexicali, and Ensenada use diesel. Increasingly, natural gas is being made available and used as a fuel.

Air Quality in the San Diego-Tijuana Region

Ambient Air Quality Monitoring Stations

Ambient air quality is monitored in the border region by a series of monitoring stations on both sides of the border. The monitoring stations on the United States side are operated and maintained by the state or local air pollution control agency. In San Diego County, the San Diego County Air Pollution Control District operates and maintains the monitoring stations, while in Imperial County, monitoring is the responsibility of the Imperial County Air Pollution Control District. Data from these monitoring stations are quality-assured and quality-controlled (QA/QC) by the responsible agency and the United States Environmental Protection Agency (EPA). The actual data are stored on the EPA's mainframe computer system located in Research Triangle Park, North Carolina, in the Aerometric Information Retrieval System database (AIRS).

Until recently, little or no data were available for Mexican cities along the border. Within the last few years, however, a system of monitoring stations has been installed as a result of a cooperative effort by the EPA and Secretaría de Medio Ambiente y Recursos Naturales (SEMARNAT). Many of these monitors have now been in operation for several years and the data are now becoming available. The monitors on the Mexican side of the border are, in most cases, identical to those on the United States side, and all the data are processed through the AIRS system, ensuring appropriate QA/QC. It is thus possible to compare data from the United States and Mexico with a high degree of confidence. Only monitors located within approximately 100km of the U.S.-Mexican border and whose data are accepted by AIRS are included in this discussion. State agencies have reviewed the data submitted to AIRS, including the data presented here, to assure data quality. The location and type of pollutants measured by the monitors in San Diego and Tijuana are shown in Figure 3 and Table 3.

Figure 3. Location of Monitoring Stations in San Diego and Tijuana

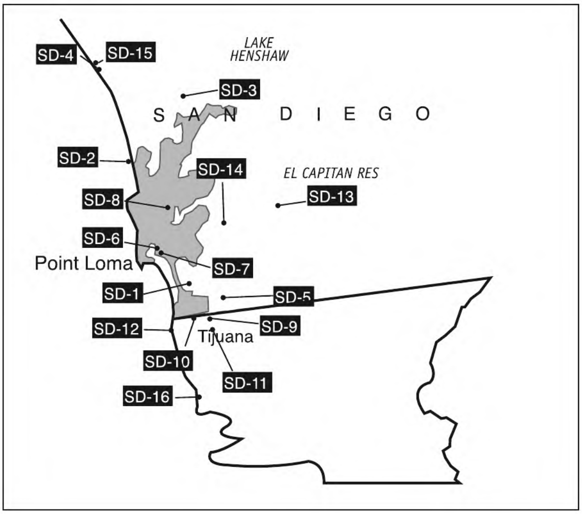

Source: EPA, Office of Air and Radiation, Center on Air Pollution (CICA)

Table 3. Types of Pollutants Measured at Monitoring Stations in San Diego and Tijuana

Monitor Designation	Location	CO	SO_2	NO_2	O_3
SD-1	San Diego	•	•	•	•
SD-5	San Diego	•	•	•	•
SD-7	San Diego	•	•	•	•
SD-9	Tijuana		•		•
SD-11	Tijuana	•	•	•	•
SD-16	Tijuana	•	•	•	•

Source: EPA, Office of Air and Radiation, Center on Air Pollution (CICA)

The pollutants measured by the monitoring stations in the border zone include the following criteria pollutants:

- Particulate Matter 10 microns (μm) or less in diameter (PM_{10})

- Lead (Pb)
- Sulfur Oxides (SO_X), measured as SO_2
- Nitrogen Oxides (NO_X), measured as NO_2
- Ozone (O_3)
- Carbon Monoxide (CO)

Data are also provided for a large number of noncriteria pollutants (including air toxics).

Mexico and the United States have similar ambient air quality standards for designated criteria pollutants (Table 4). In addition to the United States standards, San Diego and Imperial Counties must also meet the more stringent California standards for ambient air quality established by the California Air Resources Board (CARB).

Table 4. Mexico and United States Ambient Air Quality Standards for Designated Criteria Pollutants

	Mexico		U.S.	
Pollutant	Units	Average	Units	Average
O_3	0.11 ppm	1 hour	0.12 ppm	1 hour
SO_2	0.13 ppm	24 hours	0.14 ppm	24 hours
	0.03 ppm	annual	.03 ppm	annual
NO_2	0.21 ppm	1 hour	0.25 ppm	1 hours
			0.053 ppm	annual
CO	11 ppm	8 hours	9 ppm	8 hours
			35 ppm	1 hour
TSP	260 $\mu g/m^3$	24 hours	n/a	n/a
	75 $\mu g/m^3$	annual		
PM_{10}	150 $\mu g/m^3$	24 hours	150 $\mu g/m^3$	24 hours
	50 $\mu g/m^3$	annual	50 $\mu g/m^3$	annual
Lead	1.5 $\mu g/m^3$	3 months	1.5 $\mu g/m^3$	3 months

Ambient Air Quality

San Diego

In 1998, San Diego was designated a nonattainment area for ozone and PM_{10} and a nonattainment transitional area for carbon monoxide by CARB. San Diego was also designated a nonattainment area by the EPA for failing to meet federal standards for ozone. Ozone is the principal air pollution problem in San Diego, and although ozone levels have been dropping over the years, neither federal nor state criteria for attainment have been achieved.

Figures 4 and 5 reveal the number of days ozone levels exceeded federal and state clean air standards, respectively, in San Diego from 1980 to 1999. The graphs are further broken down to show the number of days exceeding the standards that were attributed to transported pollution and those due to local sources. The monitoring station in Alpine, 30 miles east of San Diego, consistently records the most exceedences of both the federal and state ozone standards. Measurements taken at Alpine reflect smog levels for all lower-mountain slope areas of the county, from Palomar Mountain to the Mexican border, at elevations between 1,500 feet and 3,000 feet. Ozone levels for the Alpine site are reflected in Table 5, which shows that in San Diego County, nine days exceeded the federal one-hour ozone level, eight of which were measured in Alpine, and 33 days exceeded the eight-hour ozone levels, 31 of which were measured in Alpine.

Figure 4. Number of Days Exceeding Federal Clean Air Standard (One-Hour) for Ozone in San Diego, 1980–1999

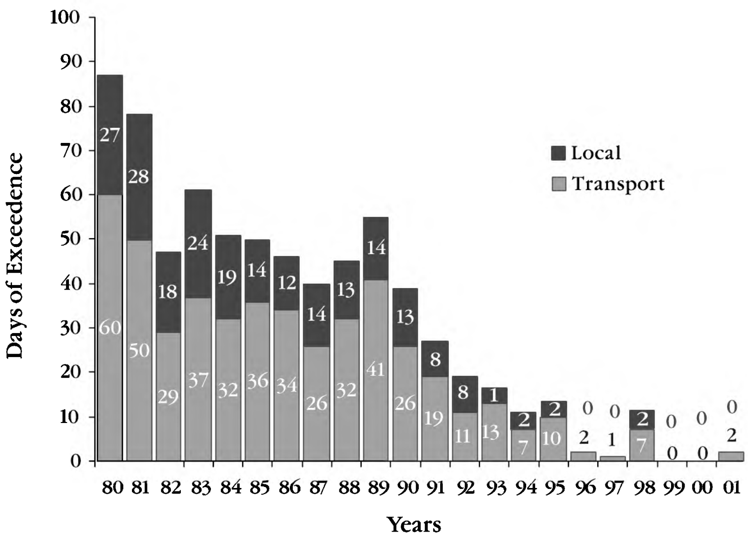

Source: San Diego Air Pollution Control District

Figure 5. Number of Days Exceeding State Clean Air Standard (One-Hour) For Ozone in San Diego, 1980–1999

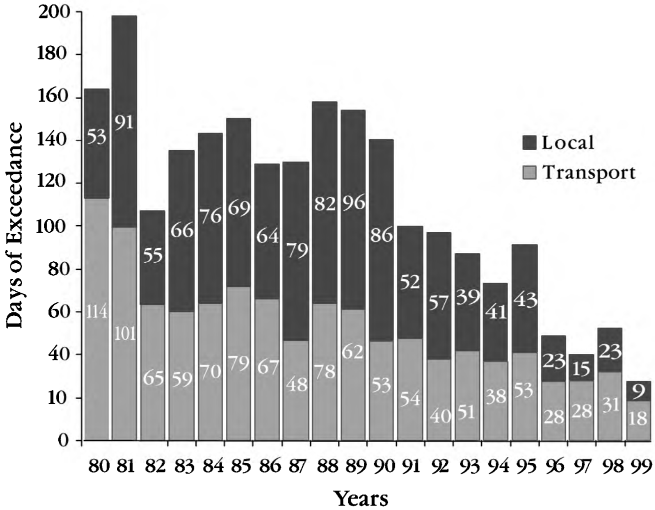

Source: San Diego Air Pollution Control District

Table 5. Highest Four Daily Maximum Hourly Ozone Measurements (Parts per Million) and Number of Days (*) above the Hourly Standards at Alpine

	1997	PPM	1998	PPM	1999
Highest	July 4	0.136	July 16	0.164	February 28
2nd Highest	July 5	0.120	July 27	0.135	March 1
3rd Highest	August 3	0.117	August 4	0.135	March 29
4th Highest	August 2	0.115	July 26	0.131	March 30

*Days > State Standard in 1997, 1998, and 1999 respectively: 29, 47, 1
*Days > National Standard in 1997, 1998, and 1999 respectively: 1, 8, 0
Source: California Air Resources Board

Due to prevailing wind patterns, ozone and precursor emissions are transported to San Diego from the South Coast Airbasin—which includes the metropolitan areas of Los Angeles, Orange, San Bernardino, and Riverside Counties—during relatively mild "Santa Ana" weather conditions. Winds blowing toward the southwest transport the South Coast's polluted air out over the ocean, and the sea breeze brings it onshore into San Diego County. When the transported smog is at ground level, the highest ozone concentrations are measured at coastal and near-coastal monitoring sites. When the blown-in smog cloud is elevated, coastal sites may be passed over, and the transported ozone is measured further inland and on the mountain slopes.

San Diego has not had a Stage I smog alert since 1991 and there have been no Stage II alerts since 1979. A Stage I alert occurs when smog levels reach 20pphm (parts per hundred million) and a Stage II alert is called when smog levels reach 35pphm. California adopted a health advisory level in 1991 after medical research showed that ozone posed a health threat at this lower concentration, especially for children, the elderly, people with heart or lung disease, and to people doing strenuous exercise. A health advisory is issued when smog levels reach 15pphm, and the community is advised to reduce vigorous outdoor activity. No health advisories were issued in the county during 1996 or 1997; one was issued in July 1998.

In 1997, San Diego met state and federal air quality standards for carbon monoxide, nitrogen dioxide, sulfur dioxide, and lead. Although the current federal PM_{10} standard was met, the state standard was exceeded for inhalable particulates.

The improved air quality in San Diego County relative to the early 1990s is partially the result of the introduction of reformulated fuels, enhanced air pollution control equipment on mobile sources, and better control of point sources. At the same time, decreased economic activity and population growth rates in San Diego due to the recession of the early 1990s also had a beneficial effect on the region's air quality.

Emissions Inventory

The latest estimated annual average emissions inventory for San Diego is from 2001 (Table 6). Mobile sources account for 89% of estimated CO emissions, 91% of NO_x, 57% of organics, 83% of SO_x, and 9% of PM_{10}. The main sources of PM_{10} include farming, unpaved-road dust, and construction. Since ozone is the principal air pollution problem in San Diego, it is clear that mobile sources (cars, truck, buses, ships, and planes) are the main source of pollutants responsible for ozone formation in the region. Thus, any attempt to reduce ozone levels must address ways to reduce emissions from mobile sources, especially for the more than 2 million private vehicles in San Diego.

Table 6a. Estimated Annual Average Emissions for the San Diego Airbasin, 2001

SRC-Type	Subcategory	TOG	VOC	CO	NO_X	SO_X	PM	PM_{10}
Stationary	Electric utilities	1.05	0.47	15.38	5.75	0.07	1.30	1.30
Stationary	Cogeneration	2.41	1.68	2.08	2.59	0.01	0.35	0.25
Stationary	Oil and Gas Production (Combustion)	0	0	0	0	0	0	0
Stationary	Petroleum Refining (Combustion)	0	0	0	0	0	0	0
Stationary	Manufacturing and Industrial	1.10	0.79	1.79	4.60	0.22	0.32	0.30
Stationary	Food and Agricultural Processing	0.92	0.77	15.15	0.01	0.17	0.32	0.32
Stationary	Service and Commercial	1.71	0.46	1.72	2.23	1.41	0.30	0.29
Stationary	Other (Fuel Combustion)	1.63	0.19	0.89	0.68	0.04	0.13	0.13
Stationary	Sewage Treatment	0.20	0.04	0.10	0.07	0.01	0.02	0.02
Stationary	Landfills	243.05	2.78	0.05	0.11	0.04	0.12	0.07
Stationary	Incinerators	0	0	0	0	0	0	0
Stationary	Soil Remediation	0.01	0.01	0	0	0	0	0
Stationary	Other (Waste Disposal)	0.09	0.01	0	0.01	0	0	0
Stationary	Laundering	3.54	0.06	0	0	0	0	0
Stationary	Degreasing	2.55	1.77	0	0	0	0	0
Stationary	Coatings and Related Process Solvents	27.09	24.92	0	0	0	0	0
Stationary	Printing	3.86	3.86	0	0	0	0	0
Stationary	Adhesives and Sealants	3.93	3.47	0	0	0	0	0
Stationary	Other (Cleaning and Surface Coatings)	0.29	0.24	0	0	0	0	0
Stationary	Oil and Gas Production	0	0	0	0	0	0	0
Stationary	Petroleum Refining	0	0	0	0	0	0	0
Stationary	Petroleum Marketing	64.82	6.03	0	0	0	0	0
Stationary	Other (Petroleum Production and Marketing)	0	0	0	0	0	0	0
Stationary	Chemical	4.15	3.43	0	0	0	0.01	0.01
Stationary	Food and Agriculture	0.11	0.11	0	0	0	0.04	0.03
Stationary	Mineral Processes	0.15	0.15	0.12	0.12	0.01	6.94	3.38
Stationary	Metal Processes	0	0	0	0	0	0.02	0.02
Stationary	Wood and Paper	0	0	0	0	0	0	0
Stationary	Glass and Related Products	0	0	0	0	0	0	0
Stationary	Electronics	0	0	0	0	0	0	0
Stationary	Other (Industrial Processes)	0.83	0.53	0.34	0.14	0	4.20	1.63

Table 6b. Estimated Annual Average Emissions for the San Diego Airbasin, 2001

SRC-Type	Subcategory	TOG	VOC	CO	NO_X	SO_X	PM	PM_{10}
Area-wide	Consumer Products	27.26	22.77	0	0	0	0	0
Area-wide	Architectural Coatings and Related Process Solvents	10.80	10.55	0	0	0	0	0
Area-wide	Pesticides/Fertilizers	1.28	1.27	0	0	0	0	0
Area-wide	Asphalt Paving/Roofing	1.32	1.32	0	0	0	0.01	0.01
Area-wide	Refrigerants	0	0	0	0	0	0	0
Area-wide	Other (Solvent Evaporation)	0	0	0	0	0	0	0
Area-wide	Residential Fuel Combustion	7.89	3.47	59.36	3.09	0.31	8.50	7.96
Area-wide	Farming Operations	20.6	1.65	0	0	0	0.87	0.40
Area-wide	Construction and Demolition	0	0	0	0	0	71.16	34.82
Area-wide	Paved Road Dust	0	0	0	0	0	72.83	33.30
Area-wide	Unpaved Road Dust	0	0	0	0	0	37.97	22.57
Area-wide	Fugitive Windblown Dust	0	0	0	0	0	0.63	0.34
Area-wide	Fires	0.07	0.05	0.60	0.01	0	0.09	0.09
Area-wide	Waste Burning and Disposal	1.29	0.73	8.53	0	0	1.18	1.16
Area-wide	Utility Equipment	0	0	0	0	0	0	0
Area-wide	Cooking	2.5	1.74	0	0	0	3.76	2.63
Area-wide	Other (Miscellaneous Processes)	0	0	0	0	0	0	0

Table 6c. Estimated Annual Average Emissions for the San Diego Airbasin, 2001

Mobile	Light Duty Passenger (LDA)	58.54	53.90	510.24	47.74	0.31	1.81	1.78
Mobile	Light and Medium Duty Trucks	0	0	0	0	0	0	0
Mobile	Light Duty Trucks-1 (LDT1)	11.35	10.45	127.89	11.62	0.05	0.29	0.28
Mobile	Light Duty Trucks-2 (LDT2)	12.83	11.64	139.90	20.76	0.11	1.08	1.06
Mobile	Medium Duty Trucks (MDV)	7.98	7.32	90.27	9.59	0.05	0.32	0.32
Mobile	Heavy Duty Gas Trucks (All)	0	0	0	0	0	0	0
Mobile	Light Heavy Duty Gas Trucks - 1 (LHDV1)	5.07	4.68	33.18	2.24	0.01	0.03	0.03
Mobile	Light Heavy Duty Gas Trucks - 2 (LHDV2)	0.43	0.39	3.48	0.43	0	0.01	0.01
Mobile	Medium Heavy Duty Gas Trucks (MHDV)	2.23	2.08	18.19	1.68	0	0.01	0.01
Mobile	Heavy Heavy Duty Gas Trucks (HHDV)	0.83	0.77	13.18	0.79	0	0	0
Mobile	Heavy Duty Diesel Trucks (All)	0	0	0	0	0	0	0
Mobile	Light Heavy Duty Diesel Trucks - 1 (LHDV1)	0.05	0.04	0.11	0.63	0	0.01	0.01
Mobile	Light Heavy Duty Diesel Trucks - 2 (LHDV2)	0.07	0.06	0.18	0.87	0.01	0.02	0.02
Mobile	Medium Heavy Duty Diesel Trucks (MHDV)	0.29	0.26	1.67	9.40	0.10	0.28	0.28
Mobile	Heavy Heavy Duty Diesel Trucks (HHDV)	1.74	1.53	6.72	31.18	0.32	0.83	0.83
Mobile	Motorcycles (Mcy)	1.75	1.66	12.52	0.30	0	0.02	0.01
Mobile	Heavy Duty Diesel Urban Buses (UB)	0.14	0.12	0.53	2.47	0.03	0.05	0.05
Mobile	Heavy Duty Gas Urban Buses (UB)	0.08	0.07	1.00	0.08	0	0	0
Mobile	School Buses (SB)	0.06	0.06	0.79	0.37	0	0.01	0.01
Mobile	Motor Homes (MB)	0.25	0.21	5.76	0.91	0	0.01	0.01
Mobile	Other (On-Road Motor Vehicles)	0	0	0	0	0	0	0
Mobile	Aircraft	3.66	3.27	18.23	7.00	0.18	1.73	1.69
Mobile	Trains	0.08	0.07	0.21	1.98	0.02	0.05	0.05
Mobile	Ships and Commercial Boats	1.01	0.89	4.41	11.66	4.73	1.41	1.39
Mobile	Recreational Boats	10.70	9.86	70.09	2.74	0.06	0.59	0.53
Mobile	Off-Road Recreational Vehicles	1.74	1.6	16.39	0.34	0.02	0.04	0.04
Mobile	Off-Road Equipment	11.73	10.26	111.38	37.14	4.37	2.52	2.49
Mobile	Farm Equipment	0.74	0.66	4.47	4.81	0.63	0.31	0.31
Mobile	Fuel Storage and Handling	7.84	7.84	0	0	0	0	0
Mobile	Other (Other Mobile Sources)	0	0	0	0	0	0	0

Table 6d. Estimated Annual Average Emissions for the San Diego Airbasin, 2001

SRC-Type	Subcategory	TOG	VOC	CO	NO_x	SO_x	PM	PM_{10}
Natural	Geogenic Sources	0	0	0	0	0	0	0
Natural	Wildfires	2.73	1.56	44.93	2.10	0	9.19	8.84
Natural	Windblown Dust	0	0	0	0	0	0	0
Natural	Other (Natural Sources)	0	0	0	0	0	0	0
Total		580.42	226.57	1341.83	228.24	13.29	231.69	131.08

Source: California Air Resources Board

Tijuana

Ambient air quality has been continually measured in Tijuana and Rosarito only since 1996, so there is a much shorter historical record of air quality data for these areas when compared to San Diego. Nevertheless, there are currently five monitoring stations operating and data from these stations yield sufficient information to draw conclusions about air quality in Tijuana and surrounding areas.

Figures 6 and 7 show examples of daily criteria pollutant cycles data for NO_x and ozone taken on one or two days, one during the summer and the other during the winter. A typical pattern for nitrogen oxide is an increase in the morning hours, most likely due to commuter and commercial traffic, followed by generation of photochemical ozone during the afternoon period. The evening buildup of NO_x is once again due to commuter traffic. Similar daily cycles are also seen from the other monitoring stations.

Figure 6. Daily Criteria Pollutant Cycles Data for NO_X and Ozone Taken in Summer 1997

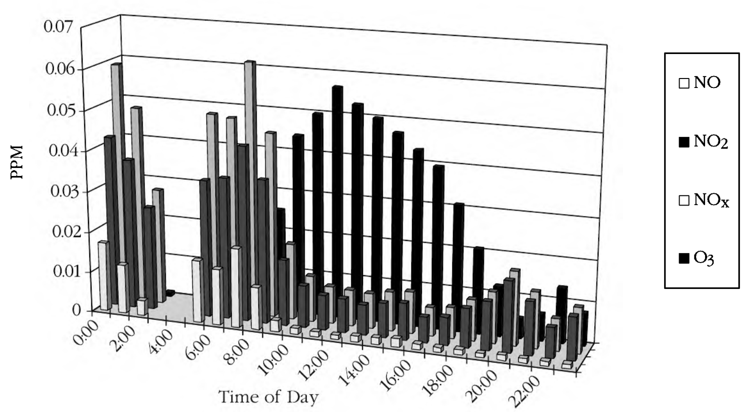

Over the 23 months for which data were taken at four of the ambient monitoring stations in Tijuana and Rosarito, 10 exceedences were recorded, primarily at the two sites nearest heavy traffic and industrial activity. The highest levels occurred during the warmer months, as would be expected.

Figure 8 is a comparison of ozone levels between San Diego and Tijuana. High levels of ozone are consistently recorded at the monitoring station in Alpine and at the La Mesa site, located in downtown Tijuana. These data suggest that the concentration of ozone in the atmosphere is similar for both San Diego and Tijuana. For CO and NO_2, although ambient atmospheric concentrations are somewhat higher in Tijuana than in San Diego, both are within limits set by Mexico and the United States, based on measurements taken in 1996.

Figure 7. Daily Criteria Pollutant Cycles Data for NOx and Ozone Taken in Winter 1997

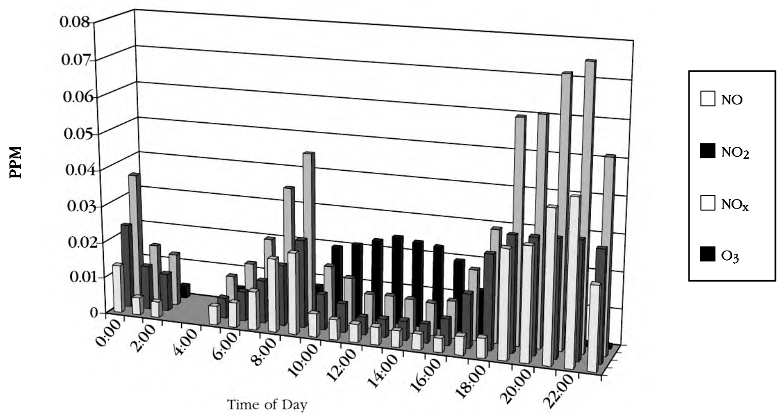

Figure 8. Comparison of Ozone Levels between Various Stations in San Diego and Tijuana

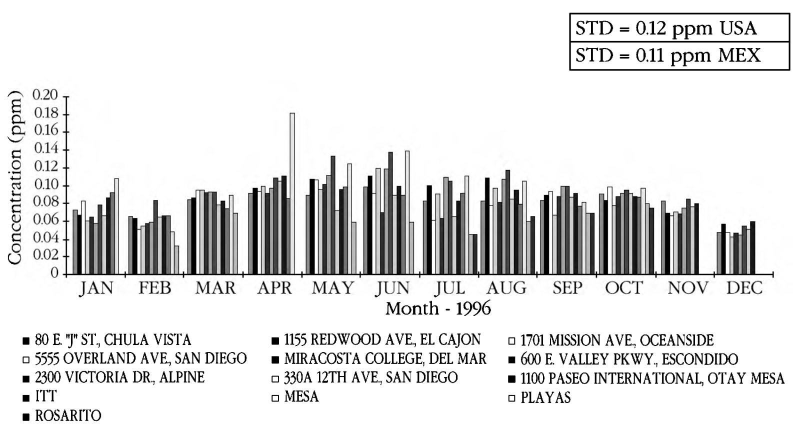

Source: Alan Sweedler Presentation at 1998 SCERP Technical Conference in El Paso, Texas

Figure 9. Ambient Concentration of PM_{10} for Stations in Tijuana

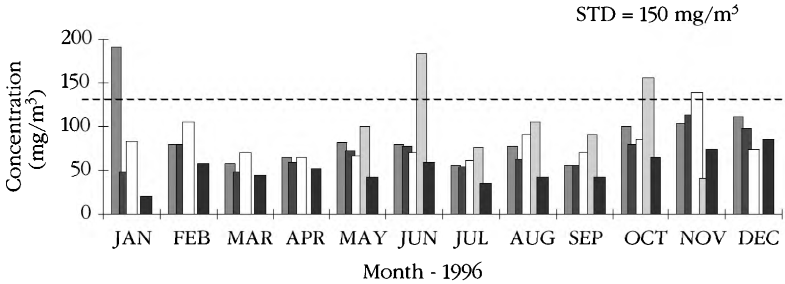

Source: Alan Sweedler Presentation at 1998 SCERP Technical Conference in El Paso, Texas

Figure 9 gives the ambient concentration of PM_{10} for Tijuana. With just a few exceptions, levels are within limits set by the Mexican government. For the San Diego-Tijuana region, the principal criteria pollutant of concern is ozone. Reducing ozone levels in the binational airshed will require programs and policies to reduce emissions from mobile sources.

Heavy-Duty Trucks

The number of diesel burning, heavy-duty trucks crossing the border and circulating in the San Diego-Tijuana region has increased significantly during the past few years. In 1993, nearly 900,000 trucks crossed through California's three commercial ports of entry. By 1996, the number of trucks crossing the California-Mexico border had increased to more than 1.5 million per year.

A survey of the number and types of trucks crossing at the Otay Mesa border crossing was conducted in 1997 to characterize the truck fleet and to determine how long trucks had to wait before crossing the border. The results of the study showed that:

- More than 95% of Mexican registered trucks were manufactured in the United States
- 78% of these trucks used diesel
- 22% used gasoline

- 85% of diesel-burning trucks bought their fuel in Mexico
- 54% of gasoline burning trucks bought their fuel in Mexico
- 76% of trips were within San Diego County

As trade continues to grow between the United States and Mexico, more trucks will cross the border and circulate on United States and Mexican roads and highways. To determine the impact on air pollution associated with the truck fleet, emissions testing of heavy-duty trucks will be necessary so that accurate emission factors can be obtained. Without these emission factors and associated driving patterns, it will not be possible to obtain reliable information on the contribution Mexican trucks make to the emissions inventory of the region.

Imperial County-Mexicali Valley Region

Geographical Region and Population Distribution of Imperial County

Imperial County is located in the southeast corner of California with Riverside County to the north, San Diego County to the west, and the state of Arizona to the east. Mexico forms its southern border. Imperial County is the ninth largest county in California, covering more than 11,906 square kilometers.

Approximately one-half of the land is undeveloped and under federal ownership and jurisdiction. Presently, one-fifth of the more than 1.2 million hectares (3 million acres) of the county is irrigated for agricultural purposes, most notably the central area known as Imperial Valley. The developed area, where the county's incorporated cities, unincorporated communities, and supporting facilities are situated, comprises less than 1% of the land. Approximately 7% of the county is the Salton Sea, a man-made sea created when the Colorado River changed its course and followed the irrigation canal, flooding the lowest part of the valley.

The city of El Centro, the largest of the three major cities in the Imperial Valley, is the county seat and principal trading center of the county. It is accessible via Interstate 8, running east and west near the Mexican border and State Highways 86 and 111, which run north-south to the Mexican border.

The population of Imperial County is more than 142,000. Table 7 provides the county's population broken down by cities and unincorporated areas. Some 35% of all jobs are in government services, 29% are in wholesale and retail trade sectors, and 5% are in manufacturing. Imperial Valley is characterized by a much smaller population density than Mexicali, but there are a number of rapidly growing communities, including Imperial, Brawley, Holtville, the border town of Calexico, and the county government center of El Centro.

Table 7. Population of Imperial County Cities, 1990–1998

City	1990	1998	(% Change)
Brawley	19,208	22,953	19.5%
Calexico	18,916	26,562	40.4%
Calipatria	2,742	7,461	172.1%
El Centro	31,877	37,363	17.2%
Holtville	4,893	5,697	16.4%
Imperial	4,175	7,044	68.7%
Westmorland	1,401	1,786	27.5%
Unincorporated	27,722	35,185	26.9%
Total	110,934	144,051	29.9%

Source: U.S. Bureau of the Census

Mexicali

The State of Baja California is divided into two regions: the Colorado Valley and the Pacific Coast. In the Colorado Valley region lies the City and Valley of Mexicali. Its territorial extension represents 21% of the state and 0.7% of the country (i.e., 13,700km^2) and it has an approximate population of 750,000. The coastal boundary of the municipality is located on the Sea of Cortez with an approximate length of 210 kilometers. Within its jurisdiction, 10 islands cover approximately 11,000 hectares. From north to south, these islands are Gore, Montague, Encantada, San Luis, Angel de la Guarda, Pond, Partida, Rosa, Salsipuedes, and San Lorenzo.

The municipality consists of three zones; coastal, valley, and urban. San Felipe, the most important delegation, is situated in the

Gulf of California coastal zone. Puebla, Ciudad Morelos, Guadalupe Victoria, and Estación Coahuila are situated in the valley zone. The urban zone consists of Mexicali and the surrounding area of González Ortega, Cerro Prieto, and Progreso.

Important climatic characteristics of the region are the very long summers and short winters. The weather is dry and the average precipitation is only slightly higher than 7.6mm per year. Mexicali is located slightly to the north of the ridge of the Colorado River delta and has an average altitude of 11m above sea level. Toward the south, the terrain descends to the Sea of Cortez. To the north, the descent is in the direction of the Salton Sea, approximately 85m below sea level.

Although the Mexicali Valley is an urban area, it is divided into 14 municipal delegations: Algodones, Benito Juárez, Progreso, González Ortega, Hechicera, Ciudad Morelos, Batáquez, Cerro Prieto, Venustiano Carranza, Colonias Nuevas, San Felipe, Hermosillo, Estación Delta, and Guadalupe Victoria. In these delegations, there are 268 small populations of agricultural groups, called *ejidos*, dispersed throughout the fertile Mexicali Valley agricultural area. Together with Tijuana, Tecate, Mexicali, and the California Counties of San Diego, Imperial, the California-Baja California border region contains almost one-half of the entire U.S.-Mexican border population.

Geomorphology of Border Region

The extremes in climate are matched by extremes in the terrain. The delta of the Colorado River partly fills a triangular depression about 300km long and 160km wide known as the Salton Trough. It is separated from the Pacific Ocean to the southwest by the 3,000m high Peninsular Ranges, to the northeast by the 1,500m high Mojave Desert, by the Chuckwalla and Chocolate Mountains, and to the south by the Gulf of California. The 2,250km Colorado River, which drains an area of 625,000km^2, enters the Trough at Yuma about midway along the eastern boundary of the Salton Trough and flows south to the Gulf of Mexico. The delta is divided in two by a purely political boundary, separating the Mexicali Valley to the south from the Imperial Valley to the north. Much of the Imperial Valley is below sea level and occupied by a closed basin, formerly called the Salton Sink, the bottom of which lies at 83m below sea level.

Nowhere else in North America are the uncertainties of the struggle between man and nature more manifest than in the low desert of the Colorado River delta in the Salton Trough of Alta and Baja California. This is due to the burgeoning population of the two Californias making an ever-increasing demand upon the limited resources of a fragile desert environment. Until the initiation of massive irrigation schemes in the 1920s it was also one of the most desolate regions in North America. At the turn of the twentieth century, the population of the region was only 10,000. Today, the population exceeds 750,000. In the interim, irrigation has transformed the arid landscape. Seen from the air, the land resembles that of a checkerboard with green irrigated lands and browns, grays, and yellows of the salt bush, creosote scrub, salinas, sand dunes, and tidal flats of the delta region. Differences in the availability of water and irrigation practices make the international border between Alta and Baja California visible to the naked eye.

Climate Trends and Prevailing Wind Patterns

The weather in the Mexicali and Imperial Valleys is typically hot and dry with very large temperature extremes during summer and winter. Annual mean temperatures of 21°C to 23°C are observed during the year, but in the summer, from June to September, the mean temperature is above 30°C. In July, the hottest month of the year, the average temperature ranges between 32°C and 34°C and the maximum mean temperature is 41°C to 43°C. In January, the coldest month of the year, the monthly mean temperature is 11°C to 14°C. In both valleys, temperature extremes have been have recorded as high as 54.3°C and as low as –7.0°C. Evapotranspiration can be in excess of 3m per year.

Influenced by the winter frontal systems, the annual precipitation is greatest in the months of December and January, with an average precipitation of 11.1mm and 9.8mm respectively. June is the driest month with an average of 0.2mm of annual precipitation, followed by the month of May with 0.6mm annual precipitation. In July and August, a second rainy season occurs, caused by the occasional arrival of humid but weak tropical perturbations. In general, the precipitation is very low, with an average annual rainfall of 72.6mm. Imperial Valley has a higher annual average rainfall (about 100mm) than Mexicali.

The sequence of monthly relative humidity presents a pattern similar to the precipitation. The annual average relative humidity is 45.7% in December and January, while May and June experience between 33% and 35.5% average relative humidity. In general, Mexicali is more humid in the summer than the Imperial Valley.

The wind patterns in both valleys are characterized by a flow of maritime wind modified from the Pacific Northwest (from the beginning of autumn until mid-spring). In June and August and until mid-September, both valleys are dominated by very hot dry air, which has a low pressure due to intense solar radiation. This air mass contrasts notably with a humid, tropical, cooler air mass from the Sea of Cortez, which is characterized by a high-pressure system. This results in the prevailing winds going from south and southeast to north during the summer season and produces an uncomfortable combination of high temperatures and high humidity. An important difference between both valleys is that during winter the wind direction in the Imperial Valley changes so that it comes from the west and southwest, whereas in the summer the wind direction and the speed are very similar in both valleys.

Demographics of the Imperial-Mexicali Region

The Imperial and Mexicali Valleys are characterized by rapid population growth as seen in Tables 8 and 9. The combined regional population in 1995 was 837,305. It is also interesting that although growth rates for Mexicali exceeded those of Imperial Valley for most of the period from 1940 to 1980, from 1980 to 2000 Imperial Valley's growth was greater than that of Mexicali. An important characteristic of this rapidly growing population is its concentration in urban areas coupled with increased industrialization (mostly due to the maquiladora industry) in Mexicali and, to a smaller degree, in the Imperial Valley. One element of the rapidly expanding Mexican population is the capacity of the northern border of Mexico to attract people from the rest of the country.

Table 8. Annual Population Growth Rates for Imperial County and Mexicali, 1930–2000

Decade	Imperial County (Annual % Change)	Mexicali (Annual % Change)
1930-1940	-0.20%	4.0%
1940-1950	0.50%	10.8%
1950-1960	1.50%	8.5%
1960-1970	0.20%	3.6%
1970-1980	2.20%	2.5%
1980-1990	1.80%	1.7%
1990-2000	2.80%	2.4%

Sources: U.S. Bureau of the Census; California Department of Finance; INEGI

Table 9. Population of Imperial County and Mexicali, 1930–2000

Year	Imperial County	Mexicali
1930	60,903	29,985
1940	59,740	44,399
1950	62,975	124,362
1960	72,105	281,333
1970	74,492	396,324
1980	92,110	510,664
1990	109,303	601,938
2000	145,300	764,902

Sources: U.S. Bureau of the Census; California Department of Finance; INEGI

Economic Activities and Trends in the Region

Mexicali

The municipality of Mexicali extends 13,696km^2, covering 21% of the state's land surface. The city was founded in 1903 and has since distinguished itself by receiving and integrating people from all over Mexico and the world.

The most important economic activity in Mexicali is agriculture and its related industry and services. The Valley of Mexicali consists of 180,000 irrigated hectares (444,789 acres) with the rural area characterized by quality soil, especially for cotton and wheat. The most important agro-industrial factories for the transformation of these products are found in the valley.

In the Mexicali Valley, there are two main areas—Ejido Nuevo León and Guadalupe Victoria. The large geothermal fields of Cerro Prieto are located in the former and attracts industry wanting to take advantage of the power available. The second area has the best developed services and industrial infrastructure in the region and is where the largest quantity of vegetables are grown for export.

In Mexicali, the economically active population is estimated to be more than 96% and the unemployment rate is about 4%, one of the lowest in Mexico. The economic activities that characterize Mexicali have been determined by the accelerated dynamics of the urbanization process and its proximity to the border. Industries such as plastic and metal furniture production, the manufacturing of chemical products, and the maquiladora industry have grown in recent years.

In terms of employment, the leading sectors are manufacturing, commerce, services, and agriculture. The average salary in Mexicali in the maquiladora industry was 34 pesos per day ($3.65 dollars per day) as of June 9, 1999.

Imperial County

The opening of the new port of entry in Imperial County has intensified economic development activity in the area and has been the catalyst to increase the county's participation in the international and regional trade area. There were 2.9 million legal admissions at the two ports of entry between Imperial County and Mexicali, according to a March 1998 survey conducted by San Diego Dialogue and Centro de Estudios Económicos del Sector Empresarial de Mexicali. Nearly 80% of these admissions were at the existing port of entry and 20% were at the new port of entry. Approximately 75% of these admissions were passengers in vehicles and 25% were pedestrians.

Imperial County and the Valley of Imperial Development Alliance (VIDA) have developed regional collaboration to widen the economic development planning area to include the Coachella Valley and the Mexicali Valley in Mexico, as well as Yuma, Arizona.

Energy Sector

Since the production, distribution, and use of energy are main sources of air pollution, a brief description of the energy sector in the Imperial-Mexicali region follows. The most important characteristic of the energy sector in the California-Baja California border region is the total dependence on outside sources of energy, with the notable exception of the geothermal fields located south of Mexicali at Cerro Prieto (Ejidos Nuevo León and Pescaderos) and south (Heber, East Mesa) and north (Salton Sea) of Imperial Valley. Imperial County has several microhydroelectric dams located along the All American Canal. Apart from the geothermal and microhydroelectric power, most energy resources are imported into the region in the form of natural gas, electricity, and products derived from oil, such as gasoline, diesel, turbosine, liquefied petroleum gas (LPG), and fuel oil.

The Baja California power system is operated by the Comisión Federal de Electricidad (CFE), the nationally-owned electric utility. This transmission grid, which serves Baja California, is physically isolated from the rest of Mexico. It is, however, linked to California's electric grid, where exchange of energy takes place when needed. Baja California's primary fuel for electricity generation is fuel oil (44%). Diesel fuels account for another 12% of total electricity fuel generation. The rest of the generation is based on geothermal resources. There is a 230KV transmission inter-tie between the Imperial Valley substation in the United States and La Rosita substation in Mexico.

Cerro Prieto is the largest geothermal plant in Latin America, with an installed capacity of 620MW, and plans were to add an additional 100MW. In addition to the large plant at Cerro Prieto, several smaller gas turbines with an installed capacity of 62MW operate in Mexicali.

Currently, the City of Mexicali is connected to a natural gas pipeline, which crosses the border into Calexico near the new port of entry. The 29km pipeline runs along the eastern section of the city and supplies 33 companies. The distribution of natural gas is carried out by a private company called ECOGAS: Distribuidora de Gas Natural de Mexicali, S.R.L. de C.V. ECOGAS is owned by a consortium of three companies, including the Mexican enterprise Proxima Gas, and Sempra International and Pacific Enterprises International, which are both American companies.

Liquid petroleum products (gasoline, diesel, fuel oil) are transported to Mexicali via a 12-inch pipeline that cuts across the mountains from Rosarito on the west coast, where cargo ships unload the fuel brought from the state of Oaxaca in the south of Mexico. The main storage facility is located by the Centinela Mountain, west of the City of Mexicali.

Imperial Valley

The Imperial Irrigation District (IID) provides residential, commercial, and industrial electrical service for the Imperial Valley region. The IID service area covers 16,760km^2—all of Imperial County and parts of Riverside and San Diego Counties. The primary fuel used to generate power is natural gas, which provides 95% of the fuel used by IID electric generation in the Imperial Valley. The rest is geothermal and microhydroelectric. The total installed capacity in Imperial County is 781MW, of which 493MW are IID-owned and 288 are generated by other energy sources.

Southern California Gas Company supplies natural gas to the Imperial Valley, which is odorized and compressed at the major natural gas transmission processing center at Desert Center, California. The bulk of natural gas delivered locally originates in Texas and is shipped via the Southwest Transmission Pipeline. As already noted, IID uses natural gas to generate 95% of its electricity, making power generation a main user of natural gas use in the Imperial Valley.

Liquid petroleum products come to and pass through the valley via the 12-inch Southern Pacific Pipeline. This line, generally within the Southern Pacific Railroad right of way, follows the northwest-to-southeast trend of the valley.

Transportation Infrastructure

The North American Free Trade Agreement (NAFTA) has made the Mexicali and Imperial Valleys a major transportation corridor. The tangible signs of NAFTA's impact on the area include the widening of State Highway 86 from two lanes to four lanes from the Mexico Port of Entry to Interstate 10 in Indio. In 1996, a new port of entry opened east of Calexico to facilitate the increased commercial traffic. For the California-Baja California border, the number of truck crossings has more than doubled from 1993 to 1998, from 886,000 to 1.8 million per year, respectively. An additional port of entry, which opened east of the Mexicali-Calexico border crossing, began operations in December 1996. It is the main commercial trade point in the region, similar to the Otay Mesa crossing near San Diego and Tijuana.

Mexicali

The City of Mexicali plays an important role in the economic development of the northwest region of Mexico. It is located on Federal Highway 2, the principal road connecting this part of Mexico to the United States. The highway also serves as the main route between Mexicali, Tecate, and Tijuana.

The City of Mexicali is classified as an urban center with a high number of vehicles per capita—more than one vehicle per every three inhabitants. In 1997, there were 209,006 registered automobiles in a population of 612,208. It is suspected that there are 60,000 unregistered automobiles with United States license plates. The public transport service in the City of Mexicali covers 85% of the urban zone. It provides 700 buses for 45 routes that cover 85% to 90% of the public transport users and 981 taxis for 21 routes that service the remaining 10% to 15% of the public transport users.

Mexicali has two international airports, one located 20km from the city (General Rodolfo Sánchez Taboada) and the other located in San Felipe near the Sea of Cortez. Mexicali has the only railroad station in the State of Baja California, and freight service is available to the rest of the country, as well as to California and the rest of the United States. However, there is no longer any passenger rail service in the region.

Imperial County

The new port of entry has great potential for commercial and industrial development. Imperial County is working to remedy the lack of a major road connection to the interstate highway system. According to county officials, there has been a major increase in the flow of trucking traffic into the county since the opening of the Calexico east port of entry. Most of the traffic goes through the new port and travels through county roads and Calexico city streets. It has been the county's goal to pursue state and federal resources for continued construction of Highway 7, which begins at the Calexico east port of entry and ends at Highway 98. The proposed construction would extend Highway 7 to Interstate 8 and will cost approximately $43 million.

County officials hope business and industry will locate near the new commercial port of entry and complement the thriving maquiladora industry in Mexicali. Some of these industries supply raw material and components, warehousing and distribution, transportation services, and brokerage services.

Air Quality Issues in the Imperial County-Mexicali Valley Region

Air quality is a serious problem in this border region, as many residents are exposed to levels of pollution that threaten human health. Of the criteria pollutants presently monitored here, total suspended particles (TSP) represent the most serious problem of atmospheric pollution. The principal source of particulates is dust produced by wind blowing on unpaved streets, uninhabited fields, and abandoned agricultural fields near urban areas. These conditions contribute to Mexicali's having the third-highest concentration of dust clouds in Mexico, behind Mexico City and Torreón in the State of Coahuila.

Activities and characteristics of the Imperial and Mexicali Valleys that contribute to the high levels of particulates found in the atmosphere include:

- Fine clay soil and sand dunes
- Desert vegetation or cleared fields
- Fallowed fields
- Unpaved roads in metropolitan areas south of Mexicali

- Aerial application of pesticides
- Atmospheric deposition by geothermal facilities
- Mining
- Pollen from seed crop agriculture

Also, foam at municipal wastewater facilities releases pathogens into the air.

Suspended dust and vehicle emissions were found to be the principal sources of the transport of particles smaller than 10µm (PM_{10}) in the Mexicali and Imperial Valleys, according to a 1997 study. Food processing and burning of crop residuals also contribute, especially during the winter months. Industrial emissions from fixed sources do not appear to contribute significantly to PM_{10} emissions in the Mexicali region.

Other sources of atmospheric pollution in the municipality of Mexicali include intensive use of pesticides, combustion products from brick-making operations, malfunctioning of the sewage water treatment plant (especially during the summer), evaporation from the highly polluted New River that runs through the city, and emissions from the combustion of heavy fuel oil. It is expected that the latter will be reduced with the expansion of the natural gas distribution system in Mexicali.

Emissions to the Atmosphere

An emissions inventory is the first and most important element for the development of effective mitigation strategies to reduce air pollution in the binational region. Emissions inventories have been carried out for both the Imperial and Mexicali Valleys and are summarized in Table 10. These data should be understood as only a rough guide when comparing emissions from both sides of the border because the inventory years are different and the methodology used was not the same for Imperial Valley and Mexicali. Moreover, the emissions inventory for Mexicali is considered only preliminary.

Table 10. Comparison of Emission Inventory for the Imperial-Mexicali Valleys (Ton/Year)

	PM_{10}	SO_2	CO	NO_x	HC
MEXICALI* (1997)	76,780	3,803	247,849	19,025	44,991
IMPERIAL** (1995)	54,750	255	58,400	13,870	26,645

*SEMARNAT Delegación B.C., 1999, "Primer Informe de la Calidad del Aire de la Ciudad de Mexicali 1997"
**California Air Resources Board 1997b

Sources of Emissions: Point, Mobile, and Area

The sectors responsible for emission of all criteria pollutants in the Mexicali and Imperial Valleys are given in Table 11. These data reflect the different sectors and show somewhat the nature of each of the valleys. In Mexicali, the large contribution from the transport sector (74%) is reflected in the high level of CO emissions from the large number of inadequately maintained vehicles. Most vehicles in the region do not have emissions controls.

Table 11. Emissions Inventory by Sector for Imperial and Mexicali Valleys (Percent)

Sector	Imperial*	Mexicali**
Industry	4.6	3
Transport	8.2	74
Area***	8.7	10
Soils and Vegetation	78.5	13

*California Air resources Board, 1997b
**SEMARNAT Delegación B.C., 1999, "Primer Informe de la Calidad del Aire de la Ciudad de Mexicali 1997"
***Includes the emissions from commerce, services, and unpaved streets

Ambient Air Quality Monitoring in the Imperial-Mexicali Valley Region

Mexicali

The ambient air quality monitoring network of the City of Mexicali started operations in January 1997 under a cooperative agreement between the U.S. EPA, the California Air Resources Board (CARB), and SEMARNAT, within the framework of Border XXI agreements. There are six monitoring stations, four of which are automatic. These measure ozone, nitrogen dioxide, sulfur dioxide, carbon monoxide, and some meteorological parameters such as temperature, humidity, and wind speed and direction. PM_{10} is sampled manually at these stations. The remaining two stations sample only PM_{10}. The stations are located at Centro de Bachillerato Técnico Industrial y de Servicios (CEBTIS21), Instituto de Ingeniería de la Universidad Autónoma de Baja California (UABC), Instituto Tecnológico de Mexicali (ITM), Colegio de Bachilleres de Baja California (COBACH), Centro de Salud en la Colonia Progreso, and Colegio Nacional de Estudios Profesionales (CONALEP) (Table 12).

The information from the monitoring stations is automatically transmitted to CARB via modem and validated in the Data Analysis Office at Instituto Nacional de Ecología (INE).

Table 12. Ambient Air Monitoring Stations and Pollutants Measured in Mexicali

No.	Zone	Station	O_3	CO	SO_2	NO_2	PM_{10}
1	North	CBATIS21	•	•	•	•	•
2	South	UABC	•	•	•	•	•
3	Southwest	ITM	•	•	•	•	•
4	West	COBACH	•	•	•	•	•
5	West	Centro de Salud					•
6	Southeast	CONALEP					•

Imperial Valley

There are eight monitoring stations located throughout Imperial Valley as shown in Table 13. Four are automatic and measure ozone, nitrogen dioxide, sulfur dioxide, carbon monoxide, and some meteorological parameters like temperature, humidity, and wind speed and direction. PM_{10} is sampled manually. The locations and pollutants measured are given in Table 13.

Table 13. Ambient Air Monitoring Stations and Pollutants Measured in Imperial Valley

No.	Zone	Station	O_3	CO	SO_2	NO_2	PM_{10}
1	North	Niland					•
2	West	Westmorland					•
3	West	Brawley					•
4	Southwest	El Centro	•	•	•	•	•
5	South	Calexico-Grant	•	•	•	•	•
6	South	Calexico-Ethel	•	•	•	•	•
7	South	Calexico-Port of Entry	•	•	•	•	•
8	Southeast	Winterhaven					•

Analysis of Ambient Air Data

Representative data from two monitors are presented here for discussion. These stations are located at the Instituto de Ingeniería of the Universidad Autónoma de Baja California (UABC) and the Instituto Tecnológico de Mexicali (ITM) sites. These sites are reasonably representative because of their proximity to heavy traffic flow.

The ITM monitor is located in a residential area with industrial and commercial activities related to maquiladoras and service industries nearby. Most of the pollutants monitored at this site result from urban traffic with a small contribution from some industrial sites. The UABC monitor is located on the main campus where the main source of emissions is from heavy traffic in the area.

Typical daily readings for gaseous pollutants are shown in Figures 10 and 11 for summer and winter days respectively. These data indicate a typical daily cycle of ozone production resulting from the combination of oxides of nitrogen, volatile organic compounds, and sunlight—the classic ingredients of smog. The evening buildup of oxides of nitrogen is related to increased traffic as residents return home from work in cars and buses. None of the pollutants exceeded the legal standards on those days analyzed.

Figure 10. Summer Gaseous Pollutants at ITM Station 1997

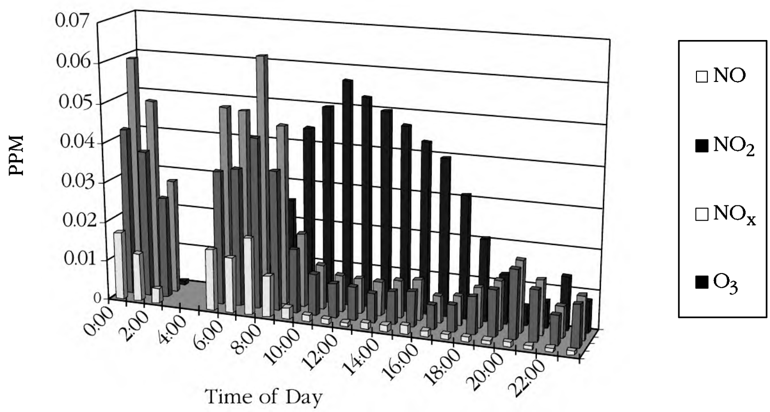

Source: Alan Sweedler Presentation at 1998 SCERP Technical Conference in El Paso, Texas

Figure 11. Winter Gaseous Pollutants at UABC 1997

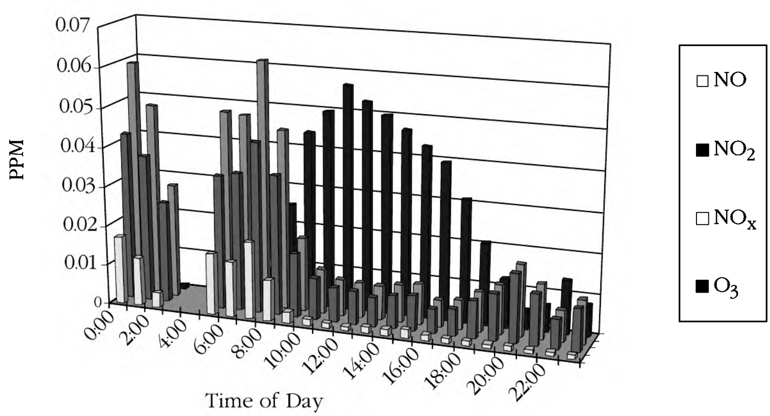

Source: Alan Sweedler Presentation at 1998 SCERP Technical Conference in El Paso, Texas

Trends and Exceedences in Criteria Pollutants

Mexicali

Gases

Carbon monoxide registered exceedences 11 months during 1999, reaching a maximum of 40% of the days in November. Ozone was also in excess of Mexican standards—its monthly frequency of exceedences was 19% of the month of May. For the other months of the year, the number of days in exceedence was less than 14%. Nitrogen dioxide and sulfur dioxide did not register any exceedences during the year.

A major problem in both valleys is PM_{10} particulates. Exceedences were recorded for 83% of the days in May, with a high number of exceedences for the rest of the year as well.

Total Suspended Particles

In Mexicali, TSPs represent the biggest atmospheric pollution problem. This is seen in Figure 12, where the standard is exceeded at those places where there are unpaved streets in the periphery and agricultural fields nearby. This is the case for the monitors located at the Colonia Progreso (located on the way to Tijuana), El Cobach, Baja California at Colonia Orizaba, and CONALEP at Ejido Puebla.

Figure 12. Total Suspended Particles Monthly Average Monitored at the Stations in Mexicali in 1997 (Standard = 260 $\mu g/m^3$ for 24 hours)

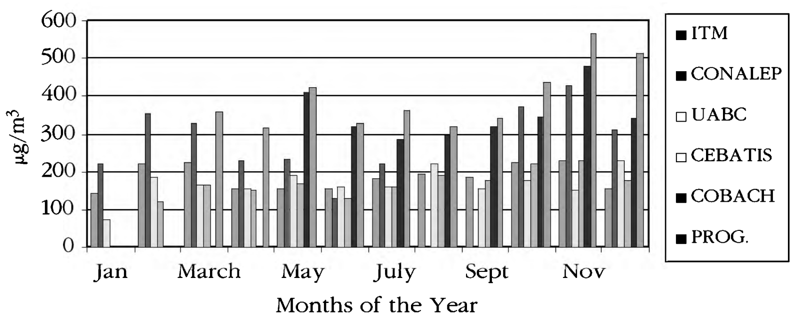

Imperial Valley

Gases

The air quality data obtained at the monitors at Calexico and El Centro indicated exceedences of nitrogen dioxide during all months of the year except March, June, July, and August. Exceedences of carbon monoxide were detected during the five months of winter (January, February, October, November, and December) at the Calexico High School monitor. Very few exceedences of the ozone standard were found, especially in the summer months of May and June. No exceedences of sulfur dioxide were found.

Particulates

The average concentration of PM_{10} in 24 hours at Imperial Valley in 1997 is shown in Figure 13. There were exceedences during three consecutive months in 1997 (October, November, and December) at the three monitors in Calexico, with one exception—Niland, in the month of October.

Figure 13. Monitoring of Maximum Average Concentration of PM_{10} at all Stations in Imperial Valley in 1997

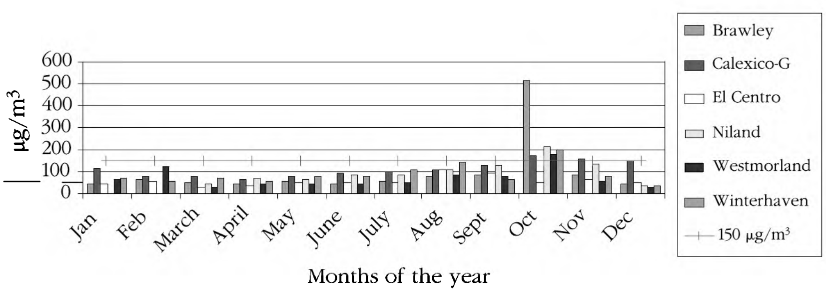

Pollution Abatement in the Border Region

Binational Efforts at Pollution Abatement

In May 1996, the Imperial-Mexicali Environmental Alliance formed to create cooperation between the two jurisdictions to obtain local, state, and federal assistance for environmental issues in both countries. The Alliance has been successful in the remediation of local transborder environmental issues, specifically the cleanup of the New River and the Salton Sea. Air quality has not been its area of interest so far.

The environmental impact of burning residual agricultural crops will be evaluated by the Mexican government and is on the Border XXI Program's Air Working Group agenda (Romero 1999). Since both cities share the same airshed, air pollution in one valley crosses the international border into the other, and the shared problems need to be addressed by both governments.

Another point of interest in the bilateral agenda is to discuss the abatement of CO, the principal pollutant in the city, especially at the ports of entry to both valleys due to border crossings (Ortiz 1999).

A campaign launched by a local Mexicali newspaper on environmental pollution titled "Let's Save Mexicali" started a series of contacts between the mayors of Calexico and Mexicali for an initial analysis of the problem (Márquez 1999). This served to motivate Mexicali's local congressmen to execute a series of measures to tackle the problem as a "principal priority." Their efforts focused on automobile emissions, watering of city streets, fiscal estimates for paving of streets, substitution of fuels for official vehicles, public outreach and education, and binational cooperation and coordination to protect the environment. As a result, the creation of a Bilateral Ecological Committee was proposed to solve pollution problems in both valleys (Romero 1998).

The "Border Smog Reduction Act" was proposed by then-California Congressman Brian Bilbray and approved by the United States Senate and President. It went into effect on April 27, 1999 (Romero 1998, 1999). This law prevents Mexican vehicles from crossing into California unless they meet the United States vehicle emissions requirements. Inspections of vehicles will begin and those vehicles found not in compliance with United States standards will be returned to Mexico. This law was applied to American citizens living in Mexico, foreigners residing in San Diego, and Mexican citizens who hold visas to work or attend school in the United States.

Main Policy Issues of Concern

Important environmental policy issues concern both valleys, including:

- Burning of residual crops, especially when it occurs on the agricultural fields close to the border. The mayors of both cities have been interested in regulating these events and have taken this issue to the federal authorities, but have not met with success.
- Establishing a bilateral commission to face the shared problem of transboundary pollution in both valleys. This type of organization may increase the alert for air quality problems and induce policies to improve it in the region.
- Developing an emissions inventory. Preliminary results are available for Mexicali and an emissions inventory has been in place in Imperial Valley for many years.
- Implementation of a pollution standard index in Mexicali (Indice Mexicano de Contaminación Ambiental—IMECA). Local IMECA in Mexicali have been monitoring several polluting events during the winter thermal inversions, which have put the Mexicali population at risk because there are no contingency measures.
- Continuity in the collection of air quality data in the region. A particular concern in Mexicali is who will take over at the monitoring stations in the city once the EPA's commitment has ended.

The most important entities in the Imperial Valley that deal with air quality issues are the Imperial County Air Pollution Control District (ICAPCD), the State of California Air Resources Board, and the EPA. The IPAPCD was established in 1971 and has county-wide jurisdiction. Imperial County is located within the Southeast Desert Airbasin.

In Mexicali, the entities that deal with air quality issues are Instituto de Ecología (INE) within SEMARNAT, Dirección de Ecología de Baja California, Dirección de Ecología de Mexicali, and Procuraduría Federal de Protección al Ambiente (PROFEPA).

Measures to Improve Air Quality in the Region: Technical and Institutional

Technical Needs

- Implement a pollution standard index report in Mexicali and Tijuana to understand and monitor pollution in real time.
- Establish a vehicular verification program to check the mechanical status and reduce the degree of pollution by the automobiles on the Mexican side. The program should be implemented by 2001 by the Dirección de Ecología del Estado (González 1999).
- Reduce automobile emissions at the ports of entry by constructing commuter lanes for frequently crossing vehicles and carpools.
- Increase the number of paved streets in Mexicali to reduce the production of dust and resulting respiratory diseases affecting residents.
- Characterize the mixture layer to define the zone of laminar flux of the atmosphere, which is important to evaluate the thermal inversion.

Institutional Needs

- Organize a bilateral commission to address the shared problem of transboundary pollution in both valleys. This organization should also be responsible for asserting policies to improve its quality in the region. In Mexicali, acute respiratory infections caused by thermal inversions, dust, pollen, and smog are quite common.
- Establish preventive measures.
- Characterize the emission factors of the various sources of pollutants and the thermal inversions in Mexicali.
- Continue studies on air dispersion models to characterize the transport of pollutants in both valleys.

Short- and Long-Term Recommendations

Short Term

- Develop programs for the study and improvement of the

quality of air (monitoring, emissions inventory, and modeling).
- Review and recommend strategies for the abatement of air pollution focused on transportation, industry, and natural sources.
- Reconvert and/or substitute official and public transport to natural gas or LPG, which will set an example in the community.
- Characterize the environmental vectors that contribute to air pollution to make prevention campaigns against allergic and respiratory diseases caused by air pollution more successful.
- Promote a change in the conventional refrigerant derived from the Chloro Fluorocarbons used in home and auto airconditioning systems for one that is more environmentally friendly.
- Standardize the burning of residual agricultural crops in the Mexicali Valley.
- Water the streets that are unpaved to diminish one source of particulate matter produced by automobiles or wind. Increase the number of paved streets in the city and recommend low-speed driving on unpaved roads.
- Restrict the burning of used tires and fire rockets during winter, which is the critical period when pollution increases to undesirable levels.
- Introduce a more efficient urban transportation system, eliminating old buses and introducing new buses with a more efficient transportation schedule.
- Introduce "Express Routes" based on transit engineering studies of the city (Galindo 1994).

Long Term
- Stimulate the participation of the community in finding solutions to air quality problems.
- Study the potential of economic incentives to reduce the air pollution.
- Think in terms of integrating environmental ecological taxes within reforms that may be passed by Congress, as that type of income will allow the municipalities to increase their budgets and attack pollution problems. All this has to be based on a

general consensus within the community.

- Stimulate the recycling of used tires for use as an alternative fuel in cement plants or energy utilities, as load material in the construction of roads, and as a source of raw material for steel and other chemical compounds. As well, communities should be encouraged to store used tires in a proper place to avoid a fire.
- Establish sanitary waste confinement sites to avoid the accumulation of used tires and plastic material, which when burned, produce large amounts of smoke. The ideal would be to have a waste classification system before it is confined.
- Establish a vehicular verification program to check the mechanical status of the transportation sector on the Mexican side and train people on emissions diagnostic technologies; all these should be accompanied by a campaign to convince the community about the advantages of these measures.
- Convince brickmakers to use a different type of fuel, such as natural gas or LPG. The actual fuel used (used tires, wood, and plastic) to heat the bricks contributes to the air pollution in the Mexicali Valley, especially in the evenings when most of the burning occurs. In Ciudad Juárez, a functional program exists to support the brickmakers that uses alternative fuels and provides a school for training in the proper use of LPG or natural gas (Ketter 1998).

Conclusions

Automobile emissions are a major contributor of air pollution in both valleys and more than half of the automobiles from Mexicali will not pass the California emissions test. It would be important to develop a geographical information systems (GIS) map that would include emissions and other relevant data for the international air-shed between Mexicali and the Imperial Valley. Once completed, this tool would provide scientists, politicians, and other interested parties with a method to determine the causes and consequences of the pollution in the area.

References

California Air Resources Board. 1998. Personal Communication.

Delgado, J. 1999. "Piden Solución a Quemas." *La Crónica* (22 January): 4A.

Distribuidora de Gas Natural de Mexicali Newsletter. 1998. Mexicali, Baja California: Distribuidora de Gas Natural de Mexicali, ECOGAS.

Dirección de Ingresos. 1998. Departamento de Finanzas del Estado de Baja California.

Ecología y Desarrollo. 1993. "Evaluación de la Calidad del Aire por Partículas Suspendidas Totales en Ensenada, Baja California." Ensenada, Baja California, Dic.

Ganster, P. 1999. *Tijuana, Basic Information*. San Diego: Institute for Regional Studies of the Californias, San Diego State University.

García, C. O. R. 1998. Laboratorio de Meteorología del Instituto de Ingeniería, UABC.

González, C. A. 1999. Personal Communication with author. Ensenada, Baja California (May).

González, O. L. 1997. Personal Communication with author. (4 December).

Greater San Diego Chamber of Commerce, Economic Research Bureau. 1999. "San Diego's General Economy." www.sdchamber.org.

Hermosillo, C. V. 1999. *Presentación del Primer Informe Preliminar de Calidad del Aire de Mexicali*. Mexicali: Canacintra.

Instituto Nacional de Ecología. 1999. "Primer Informe de Calidad del Aire de la Ciudad de Mexicali 1997." Mexicali, Baja California: SEMARNAT.

Kazimi, C., F. Cuamea, J. Alvarez, A. Sweedler, and Matt Fertig. 1999. "Emissions from Heavy-Duty Trucks at the San Diego-Tijuana Border Crossing." *Journal of Borderland Studies* 14 (1).

Ketter, R. G. 1998. "Paso del Norte Air Quality Task Force: A Case Study." El Paso, Texas: Environmental Defense Fund/Ford Foundation.

Magdaleno, V. 1999. "Solucionará Frontera XXI Exportación de Humo." *La Crónica* (18 January): 1.

Márquez, M. 1999. “Promete Victor Plantear Problema en Caléxico.” *La Crónica* (12 January): 1.

McNaughton, E. 1998. “La Calidad de Vida en Valle Imperial.” Paper presented at the UC-MEXAS binational workshop Water, Energy, and Quality of Life in the Imperial and Mexicali Valleys (9-11 November) UABC, Mexicali, Baja California.

Ortiz, L. A.1999. “Preocupan los Índices IMECA en Mexicali, Baja California.” *El Financiero.* (21 January): 54.

Páramo, V.H. 1999. Personal Communication. Mexicali, Baja California (March).

Peach, J. and J. Williams. 2000. “Population and Economic Dynamics on the U.S.-Mexican Border: Past, Present, and Future.” Pp. 31-72 in *The U.S.-Mexican Border Environment: A roadmap to a sustainable 2020,* Paul Ganster, ed. San Diego: San Diego State University Press

Planning Committee for the Development for the Municipality of Mexicali. 1999. Plan de Desarrollo Municipal de Mexicali 1998-2001. Mexicali, Baja California.

Quintero-Núñez, M.1995. “The Baja California Gas Market.” Paper presented at the U.S.-Mexico Energy Round Table, 20 October, La Jolla, California.

Rey, S., P. Ganster, G. del Castillo, J. Alvarez, K. Shellhammer, N. Clement, and A. Sweedler. 1998. “The San Diego-Tijuana Region.” Pp. 105–164 in *Integrating Cities and Regions: North America Faces Globalization*, James W. Wilkie and Clint F. Smith eds., Mexico: Universidad de Guadalajara, UCLA Program on Mexico, and Centro Internacional Lucas Alemán para el Crecimiento Económico A.C.

Romero, C. 1998. “Proponen Crear Comité Binacional de Ecología.” *La Crónica* (30 November): 1.

Romero, C. 1999. “Regresarán desde mañana EEUU autos contaminantes.” *La Crónica* (26 April): 1.

San Diego Association of Governments. 2002. *Regional Energy Plan*. San Diego: SANDAG.

Twin Plant News. 2000. (September) 16:2.

II

Planetary Boundary Layer Structure of the Paso del Norte Airshed: A Numerical Study

S-M. Lee and H. J. S. Fernando

ABSTRACT

The mesoscale meteorological model MM5 was employed to simulate the synoptically influenced local winds in the Paso del Norte Airshed (PdN) in support of air-quality studies conducted in the summer of 1996 and the winter of 1998 under the auspices of the Southwest Center for Environmental Research and Policy (SCERP). These experiments were designed to understand physico-chemical characteristics, transformations, and transports of major atmospheric pollutants in the area, in particular, aerosols and ozone. The PdN airshed is known to violate National Ambient Air Quality Standards for several regulated air pollutants. Model predictions of the synoptically influenced local mountain/valley circulation showed a good agreement with the observations. Details of the three-dimensional structure and the temporal evolution of the atmospheric boundary layer were also well-captured by the model. The correlation coefficients between model predictions and observations at approximately 250m-agl (meters above ground level) were as high as 0.92 for temperature and 0.80 and 0.61, respectively, for u- and v-wind components. The correlation coefficients, in general, depended on the variable and the height.

The performance of three turbulence closure schemes was evaluated vis-à-vis the observations. These closures include the Blackader non-local mixing scheme, Hong-Pan non-local closure scheme and the Gayno-Seaman 1.5-order scheme. Predictions based on the three schemes were found to be almost the same, except that some noticeable differences could be seen during the daytime of clear days, compared to days with relatively strong synoptic forcing. The computational efficiency of the Hong-Pan scheme was found to be 27% to 29% higher than the other two schemes.

The present study corroborates the notion that mesoscale meteorological models can provide useful basic information on flow structure for the better understanding of air quality problems.

Estructura de la Capa Planetaria Divisoria de la Cuenca Atmosférica Paso del Norte: Un Estudio Numérico

S-M. Lee y H. J .S. Fernando

RESUMEN

El modelo meteorológico de mesoescala MM5 fue empleado para simular los vientos locales sinópticos en la Cuenca Atmosférica Paso del Norte (PdN, por sus siglas en inglés) en apoyo a los estudios de calidad del aire realizados en el verano de 1996 y el invierno de 1998 con el patrocinio del Centro de Investigación y Política Ambiental del Suroeste (CIPAS). Estos experimentos fueron diseñados para entender las características fisicoquímicas, transformaciones, y transportes de los principales agentes contaminantes atmosféricos en el área, en particular, aerosoles y ozono. Es sabido que la PdN viola los Estándares Nacionales de Calidad del Aire de los Estados Unidos para varios agentes contaminantes regulados. Las predicciones del modelo de circulación sinóptica para la zona local montaña/valle, mostraron una buena concordancia con las observaciones. Los detalles de la estructura tridimensional y la evolución temporal de la capa atmosférica divisoria también fueron bien identificados por el modelo. Los coeficientes de correlación entre las predicciones del modelo y las observaciones a aproximadamente 250m-sns (metros sobre nivel suelo) fueron tan altos como 0.92 para la temperatura así como 0.80 y 0.61, respectivamente, para los componentes u y v del viento. Los coeficientes de correlación, en general, dependieron del tipo de variable y la altura.

El desempeño de los tres esquemas de cierre de turbulencia fue evaluado uno a uno contra las observaciones. Estos análisis incluyeron el esquema de mezcla no-local Blackader, el de cierre no-local Hong-Pan y el esquema de grado 1.5 Gayno-Seaman. Las predicciones basadas en los tres esquemas fueron casi las mismas, exceptuando que algunas diferencias notables pudieron apreciarse durante el dia de los días claros, en comparación con los días de esfuerzo sinóptico fuerte. La eficiencia computacional del esquema Hong-Pan fue de 27% a 29% más alta que la de los otros dos esquemas.

El presente estudio corrobora la idea de que los modelos meteorológicos de mesoescala pueden proporcionar información básica útil sobre la estructura del flujo para el mejor entendimiento de los problemas de calidad del aire.

INTRODUCTION

Meteorological fields are known to be of first-order importance in air-quality modeling. In particular, variables related to the planetary boundary layer, or PBL—the lowest layer of the troposphere that extends upward from the Earth's surface to between 100 meters (m) to 3,000m—have a strong influence on the fate of airborne contaminants. Accurate simulation of PBL structure requires parameterization of sub-grid scale physical processes, especially those responsible for realizing turbulent fluxes for heat, moisture, and momentum. First-order closure, the so-called K-theory, has been widely used in atmospheric numerical models because of its low computational cost and its ability to produce reasonable results under typical atmospheric conditions (Hong and Pan 1996). The K-theory, however, has glaring deficiencies that need to be remedied if these models are to be useful in predictions (e.g. Wyngaard and Brost 1984; Holtslag and Moeng 1991; Stull 1993). To overcome such deficiencies, higher-order closure approaches that include a prognostic equation for the turbulent kinetic energy (TKE) have been developed and implemented in meteorological models (Benoit et al. 1989, Pan et al. 1994, Janjic 1990, Janjic 1994, Ballard et al. 1991, Yamada 1983, Yamada and Bunker 1988). Non-local exchange schemes are an alternative to the above schemes in which the vertical diffusion is determined by the structure of the entire mixed layer (Blackadar 1979, Zhang and Anthes 1982, Stull 1988, Stull 1993) rather than the local properties and gradients. Non-local and higher order schemes, nonetheless, are computationally intense and not suitable for operational models. As a result, computationally efficient non-local diffusion schemes, the so-called non-local-K approaches, have been proposed (Hong and Pan 1996; Troen and Mahrt 1986). These approaches have their own advantages and disadvantages, and can have sensitivities to certain conditions. Therefore, it is instructive to evaluate the efficacy and performance of commonly used parameterizations in high-resolution mesoscale models, especially those routinely used in air quality studies.

This paper deals with the application of the MM5 mesoscale meteorological model to predict the circulation and PBL structure of the Paso del Norte (PdN) airbasin, in support of the PdN Air Research Program, which is administered by the Southwest Center for Environmental Research and Policy (SCERP). The focus of this program is to understand and mitigate air quality problems in the PdN area, as well as extend the knowledge generated to other Airbasins located in complex terrain.

The PdN area is a part of the basin-range geography of the southwestern United States and northern Mexico. Located along the U.S.-Mexican border, it contains three cities: El Paso, Texas; Ciudad Juárez, Chihuahua; and Sunland Park, New Mexico. The narrow north-south trending Franklin Mountain range in El Paso and southwest-running Juárez Mountains in Ciudad Juárez surround the basin, with the Rio Grande flowing between these high mountains.

The Sacramento Mountains, the Plains of San Agustin, and the foothills of the Sierra Madre also characterize the complex terrain of this area. With a population exceeding 2 million, more than 500,000 registered vehicles (including 40,000 vehicles crossing the border daily), and intense quarry and industrial operations, PdN has become one of the most polluted of the U.S.-Mexican border airsheds. Mixing, transport, and transformation of pollutants are key to understanding their distribution in this area.

The study reported herein aimed to predict the transport and turbulent mixing of contaminants in PdN. The observational field cases of interest are described, a brief description of the model and parameterization schemes employed are given, and the design of numerical experiments, including grid sizes and parameter options used for MM5, are described. Simulation results and their comparison with observations are also described. Special attention has been given to the surface-level circulation as well as the vertical structure and evolution of PBL—all of which play important roles in pollution build-up. Suitability of various parameterization schemes for simulating the PdN airshed and performances of the parameterization used are also discussed.

Cases of Simulations

Two field experimental cases conducted under the PdN air program were chosen for the simulations. The first is a summer experiment from August 12, 1996, to August 14, 1996, which coincided with an ozone episode. This period was characterized by atmospheric conditions conducive to pollution build up—clear skies, weak surface winds, and a deep mixed layer. The predominant synoptic feature during, prior to, and following the event was the expansion, intensification, and eastward slow progression of an upper level high-pressure feature. In addition to routine measurements—twice daily soundings and hourly surface observations—three radar wind profilers with radio acoustic sounding systems (RASS) provided hourly-averaged vertical profiles of wind speed, wind direction, and temperature. Vertical profiles of wind speed and direction were also measured at one SODAR site (Roberts et al. 1997).

The second was a winter "scoping" study from December 1, 1998 through December 3, 1998, when the skies were relatively cloudy and the development of PBL was not as striking as in the summer case. This field study investigated aerosol characteristics and transport, as well as atmospheric chemistry in the PdN airshed. Intense aerosol sampling was conducted, and the samples were analyzed using scanning electron microscopy (SEM) and PIXE instruments. Several days of meteorological data were collected at the measurement sites and added to data available from surface meteorological stations operated by the Texas Commission on Environmental Quality (TCEQ).

Model Description

MM5 is a non-hydrostatic primitive equation model based on terrain-following σ-coordinates. The vertical σ-coordinate of the non-hydrostatic version of MM5 is defined using the reference pressure, viz.

$$\sigma = \frac{p_0 - p_t}{p_s - p_t} \qquad (1)$$

where p_s and p_t are the surface and top pressures, respectively, of the reference states, which are independent of time. The reference state is an idealized temperature profile in hydrostatic equilibrium where the surface reference pressure depends entirely on the terrain height (Dudhia et al. 1996). Therefore, the lowest level of the vertical coordinate exactly follows the topographical surface. Arakawa B-grid staggering is used in horizontal planes. Two modes of four-dimensional data assimilation exist, depending on whether the data to be simulated are gridded or consist of individual observations. These gridded data, compiled to be congruous with the model grid, are often useful on larger scales, whereas individual observations, asynoptic data, or special platforms, such as profilers or aircraft observations, are used to nudge the model in smaller scales.

As stated, three turbulence closure schemes were used, which included a 1.5 order turbulence model (Gayno-Seaman scheme) and two non-local mixing schemes (Blackadar and Hong-Pan schemes).

Hong-Pan Scheme (or the MRF scheme)

This is a type of non-local mixing scheme that implements counter gradient terms in the traditional K-theory instead of using the fraction of mass exchange coefficient between a given level and the surface layer (Hong and Pan 1996; Troen and Mahrt 1986). Turbulence diffusion equations for prognostic variables can be expressed by

$$\frac{\delta C}{\delta t} = \frac{\delta}{\delta z}\left[K_c \left(\frac{\delta C}{\delta z} - \gamma_c\right)\right] \text{--(2)}$$

where, C can be any prognostic variable (u, v, Θ, q), K_c is the eddy diffusivity coefficient and γ_c is a correction to the local gradient that incorporates the contribution of large-scale eddies to the total flux. For mixed layer diffusion, the counter gradient term for Θ and q are given by

$$\gamma_c = b\,\frac{\overline{(w'c')}}{w_s} \text{---(3)}$$

where $\overline{(w'c')}$ is the surface flux (for either Θ or q), b is a coefficient of proportionality, and w_s is the mixed layer velocity scale. The diffusion scheme of the traditional local K-theory is used for the free atmosphere. Here the vertical diffusivity coefficient K is a function of local gradient Richardson number and vertical wind shear.

Gayno-Seaman Scheme

This scheme is based on the Mellor-Yamada (1974) hierarchy of turbulence models and consists of a prognostic equation for the TKE (equation 4) and a diagnostic equation for the dissipation timescale (equation 5).

$$\frac{dE}{dt} = -w'v'_H\,\frac{\delta v_H}{\delta z} + \frac{g}{\theta_v}\,w'\theta'_H - \frac{\delta}{\delta z}\,w'E - \frac{E}{\tau_0} \text{------------------------(4)}$$

$$\tau_0 = \frac{c_0\,l}{(E+F_L l^2 N^2)^{1/2}} \text{--(5)}$$

where, the overbars signify Reynolds averages, E is the TKE, w' the vertical velocity fluctuation, z the height, v'_H the horizontal wind vector fluctuation, τ_0 the dissipation timescale, l the Blackadar (1962) length scale, $c_0 = 5.524$ and $F_L = 7.098$. This scheme uses liquid-water potential temperature as a conserved variable, allowing the PBL to operate more accurately under saturated conditions (Ballard et al. 1991, Shafran et al. 2000).

Blackadar Scheme

This is a non-local mixing scheme that quantifies the vertical eddy fluxes of heat, moisture, and momentum using a hybrid non-local first-order closure. For nocturnal periods, wherein the atmospheric stratification is usually stable or at most, marginally unstable, a first-order closure is used. Here, the eddy transfer coefficient K is a function of the Richardson number. For the free convection regime, the vertical convective transfer of heat, moisture, and momentum is not determined by local gradients but by the thermal structure of the whole mixed layer and the surface heat flux. Accordingly, the vertical exchanges are realized between the lowest layer and each level of the mixed layer, instead of between adjacent layers as assumed in the K-theory. The mixing intensity is defined as the fraction of mass exchanged per unit of time between the surface layer and other PBL layers. It is directly related to the heat flux at the top of the surface layer and the vertically integrated potential temperature difference between the surface layer and the top of the mixed layer (Zhang and Anthes 1982, Blackadar 1979).

The Design of the Numerical Experiment

In the simulations, three nested domains were used to simulate meteorological fields in the PdN region. The outermost domain, Domain 1, covers a high mountain area located in the eastern part of Arizona and the southern part of New Mexico, Texas, and northern Mexico. Domain 2 includes the Sacramento Mountains and the Plains of San Agustin. The innermost domain, Domain 3, covers the cities of El Paso and Ciudad Juárez. The horizontal grid resolution of each domain was, respectively, 16km, 4km, and 1km for the winter case and 18km, 6km, and 2km for the summer case. National Centers for Environmental Prediction (NCEP) Eta model analysis output was used as the initialization field and available observations were nudged to enhance the quality of the initial value and lateral boundary values. No data assimilation was performed during the course of the simulation. Details of simulation options and relevant information are given in Table 1.

Table 1. Design of Numerical Experiments

	Summer case	Winter case
Period of simulation	0000 UTC August 12, 1998-0000 UTC August 15, 1998	0000 UTC November 30, 1998-0000 UTC December 3, 1998
Horizontal resolution of each grid	18km → 6km → 2km	16km → 4km → 1km
Initial value	NCEP Eta analysis output	
Cumulus parameterization	Kain-Fritch scheme for outermost domain and none for inner domains	
Microphysics scheme	Simple ice scheme	
Soil model	Five layer soil model	

Overview of Simulation Results

In general, the diurnal variation of the mountain-valley breeze was reasonably resolved by MM5 for both the summer and winter cases. Because of cloudy weather conditions during the winter case, the synoptic forcing and topographically driven thermodynamic forcing were dominant features. Therefore, daytime valley winds were not so noticeable in the simulations. The horizontal distribution of simulated wind fields at approximately 10m above ground level is shown in Figures 1a and 1b, which correspond to nighttime down-slope winds and daytime up-slope winds, respectively. In Figure 1a, a homogeneous northwesterly wind field was predicted in the basin located to the west of the Rio Grande Valley. This is due to the fact that the momentum of northwesterly wind at 850-hPa level was directly transported to the surface levels of the basin, thus weakening the influence of topographic forcing. Therefore, the topographic forcing in this valley was not as dominant as in the vicinity of steep mountains and valleys. Due to the southerly wind in the upper atmosphere, a southerly wind component was dominant in Figure 1b, except near the mountains and valleys where topographic winds were prevalent.

Figure 1a. The Distribution of Horizontal Wind at Approximately 10m Above Ground Level at 0500 November 30, 1998*

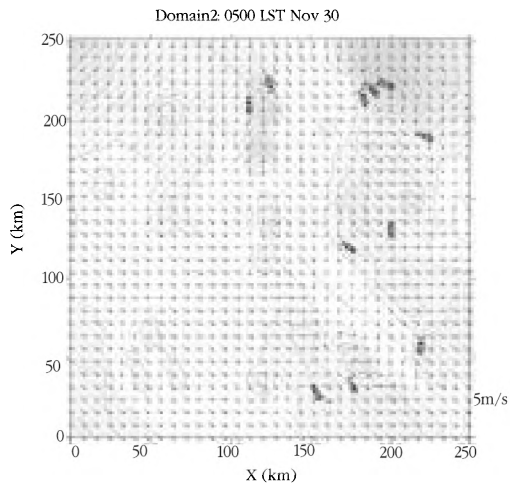

*Shading represents terrain heights

Figure 1b. The Distribution of Horizontal Wind at Approximately 10m Above Ground Level at 1400 December 1, 1998*

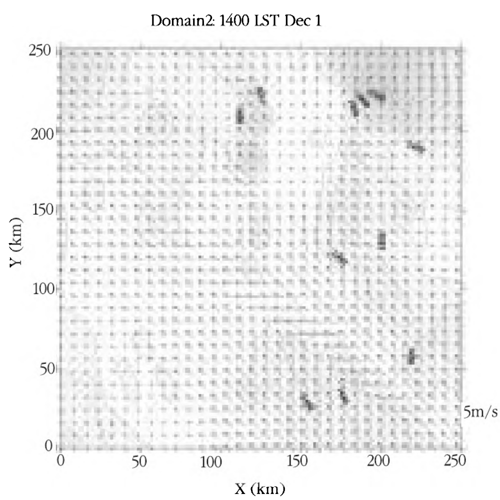

*Shading represents terrain heights

The temporal evolution of predicted near-surface variables was compared with that of the observations taken at C12, one of TCEQ's air monitoring sites located in downtown El Paso (Figure 2). Predicted surface temperatures showed good agreement with the observations, although slight differences in the minimum temperature could be discerned on the second day and at the end of simulation (first graph). Prevalent westerly wind was predicted both at the beginning and the end of the simulation, whereas easterly winds were predicted during the middle of the simulation period. The predicted wind direction and their shifts showed a reasonable agreement with observations, although wind speeds appear to be under-predicted in general. The predicted wind speeds, nonetheless, followed the observed patterns of speeding-up and slowing-down although the model did not capture the detailed high-frequency fluctuations of observed winds.

A comparison of the measured and calculated vertical profiles is presented in Figure 3. The sounding data were taken at the National Weather Service's (NWS) Santa Teresa upper air sounding station. The magnitude and height of the low-level jet observed around 300m-agl was well-predicted. Directional wind shear between easterly surface wind and southerly upper level wind was also well-predicted.

Figure 2. Comparison Between Observed Measurement of Temperature, Wind Speed, and Direction, and MM5 Predictions

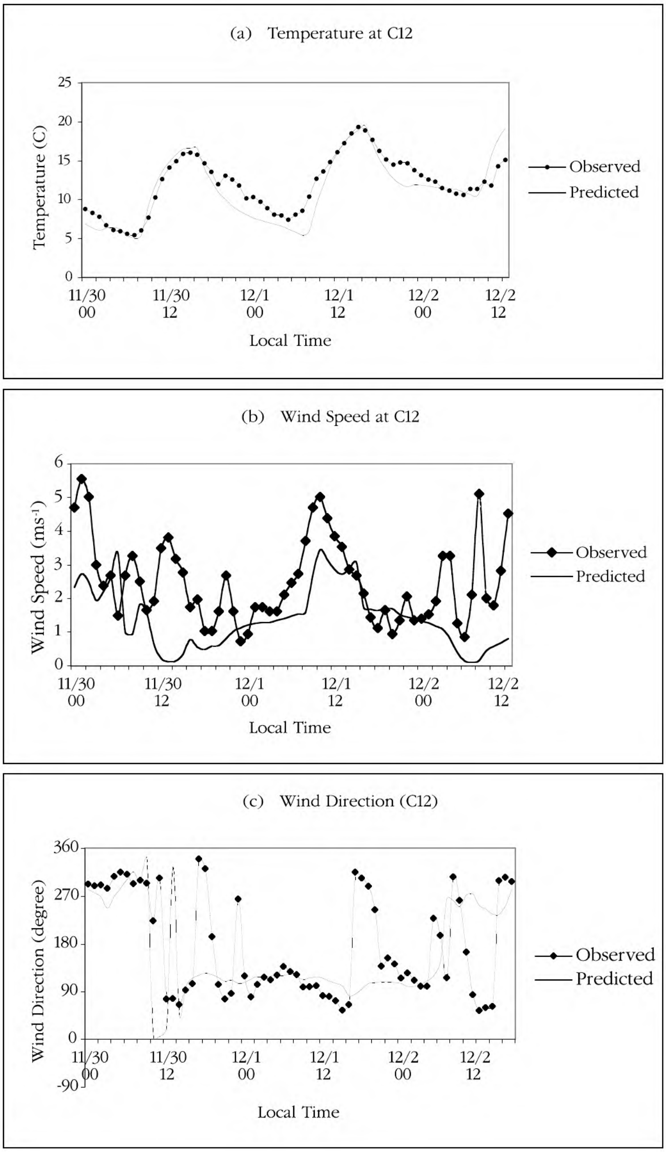

(The measurements were taken in downtown El Paso.)

Figure 3. Comparisons of Vertical Profiles Taken at the Santa Teresa NWS Station and Those Computed By MM5 For 1200 December 1, 1998

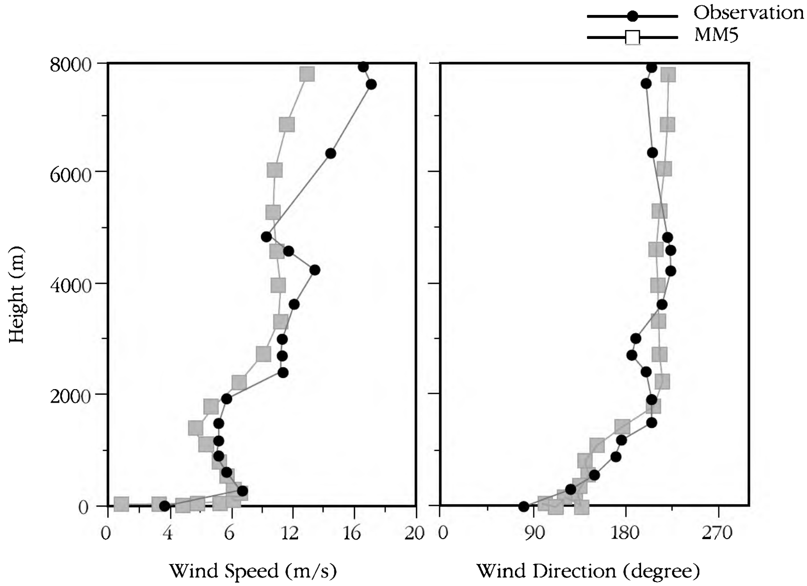

The Influence of the PBL Parameterization

Vertical Structure

The efficacy of different PBL parameterizations was tested for both summer and winter cases. Hong-Pan and Gayno-Seaman schemes were used for the winter simulations, and the differences in predictions between them were not significant, except near the ground. Cloudy weather that existed during this period apparently caused both the thermodynamics of the entire atmosphere and the local forcing within the PBL dominant. In the absence of strong synoptic forcing, the predicted convergence and divergence patterns of near-surface winds at topographic features intensified due to the use of higher-order scheme when compared to predictions based on the non-local mixing scheme. The near-surface vertical profiles of meteorological fields predicted by the higher-order scheme showed somewhat better agreement with the measurements (Figure 4). The heights of the daytime mixed layer computed using the two schemes compared well with each other, perhaps due to cloudy conditions that existed during the simulation period. In general, the higher-order scheme exhibited more sensitivity to topographic effects than the non-local mixing scheme.

Figure 4. Comparisons of Vertical Profiles Computed by Different Turbulence Closure Schemes with the Measurements Taken at the Santa Teresa NWS Station at 0500 December 1, 1998

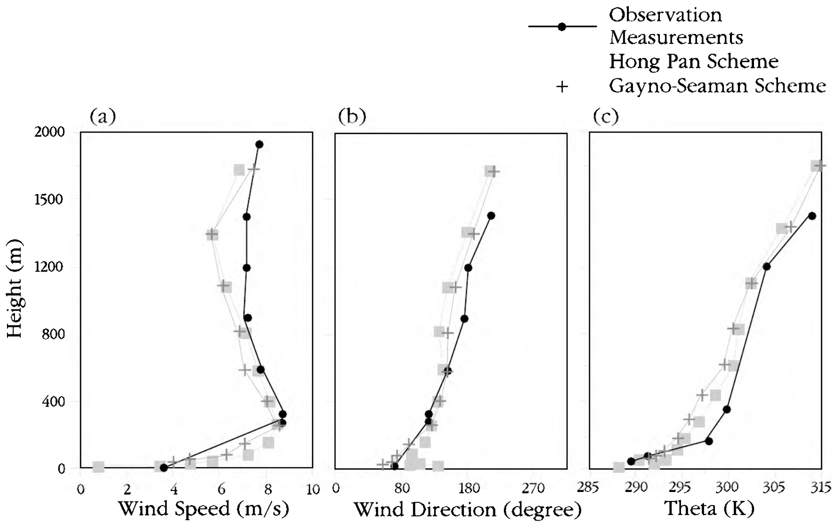

The summertime case was simulated using all three schemes of closure. Simulations with the higher-order scheme captured the features of daytime valley winds more robustly. The higher-order scheme also advanced the timing of transition from katabatic to anabatic winds. Figure 5 shows the vertical profiles of wind speed, wind direction, and the virtual potential temperature within the PBL. In general, both schemes showed reasonable agreements with the measurements. However, only the higher-order scheme captured the vertical variation of wind direction. Southeasterly flow near the surface gradually changed to southwesterly around 1,000m and finally became easterly synoptic flow in the upper atmosphere.

Figure 5. Same Measurements as Taken for Figure 4, but at 0600 August 14, 1996

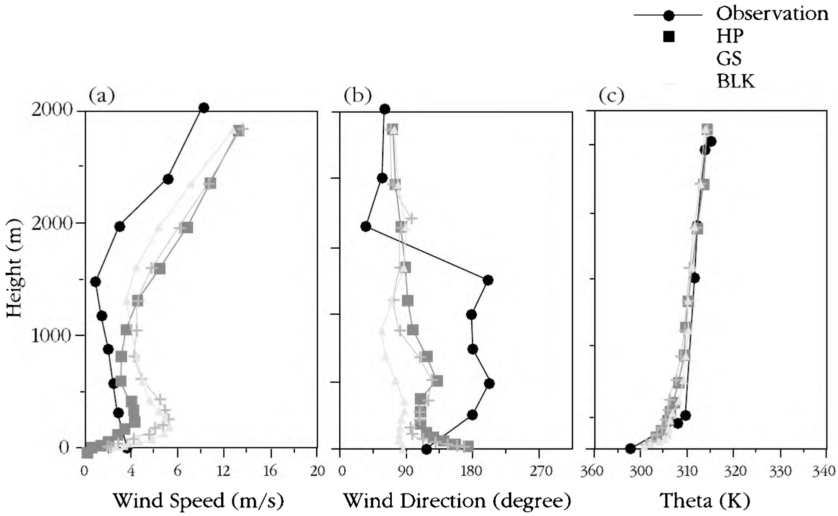

Correlation Between Observations and Predictions

Scatter diagrams of observations versus predictions, based on three different methods of turbulence parameterization, are shown in Figure 6. Correlation coefficients corresponding to each case in Figure 6 are listed in Table 2. The measurements plotted in Figure 6 are hourly averaged values taken by a RASS and radar wind profiler for 66 hours. The first six hours of simulation were excluded in this comparison. All three schemes show high correlations for the case of the scalar variable (temperature) when compared to those of the vector variables. It is hard to judge which scheme performs better by solely inspecting Table 2 or Figure 6. Contrary to the intuitive expectation, there were no significant differences between correlation coefficients for relatively lower (250m-agl) and upper (800m-agl) levels, and somewhat better v-component correlation was observed at the lower level. For temperature, the number of upper-level observations available was not sufficiently large to obtain reliable statistics, and hence it is not appropriate to compare the correlation coefficients obtained at the two levels.

Figure 6. Correlation Between Observations and Predictions Made by Three Different Methods of Turbulent Parameterization

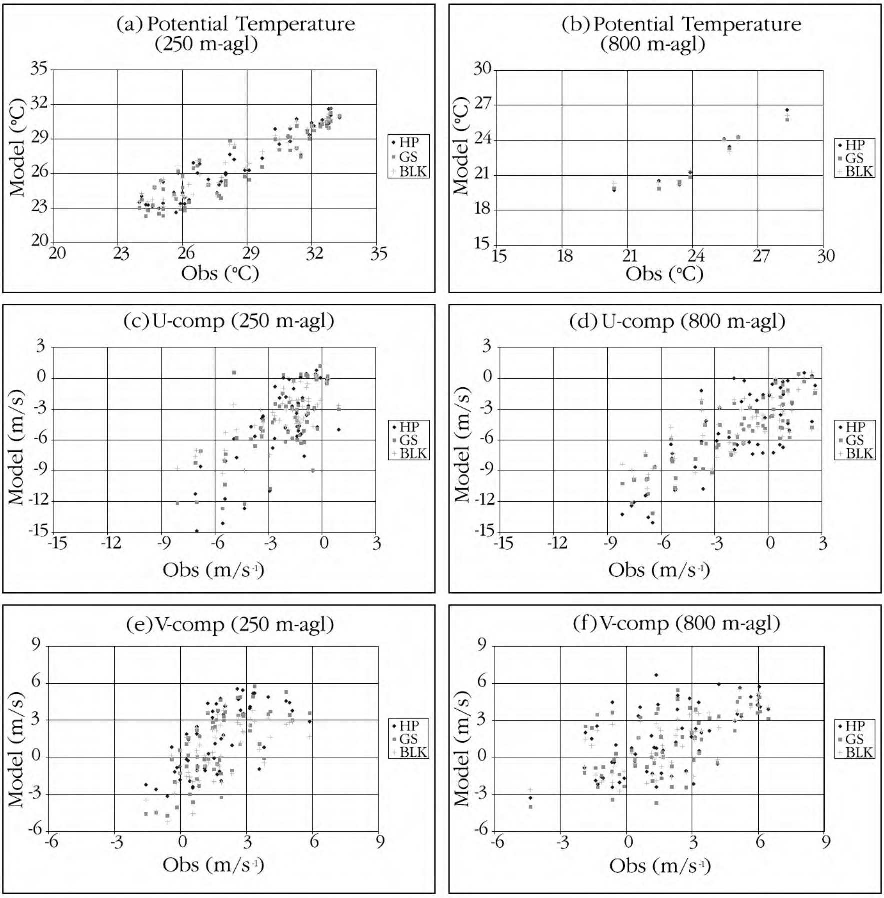

Observations were taken at the Delta-Haskel Wastewater Plant. Temperature was measured by RASS and wind components were collected by Radar profiler. Observations were corresponding to 250m/agl in left panels and 800m/agl in right panels.

Table 2. Correlation Coefficients Between Observations and Predictions at Approximately 250m-agl and 810m-agl

Variables		MRF	GS	BLK
Temperature	Lower level	0.92	0.92	0.86
	Upper level	0.83	0.89	0.68
u-component	Lower level	0.75	0.75	0.80
	Upper level	0.77	0.76	0.80
v-component	Lower level	0.52	0.55	0.61
	Upper level	0.43	0.41	0.59

Mixed Layer Height

The sounding data necessary for computing the mixed layer height is routinely taken at 0600 in the summer, or 0500 in the winter and 1800 or 1700 in the winter by the National Weather Service. Obviously such data are too sparse for mapping the detailed evolution of the PBL, which is one of the most important aspects of understanding and predicting air quality. Alternatively, the mixed layer height derived from a mesoscale model can be used for air quality studies as it is done in conventional air quality models such as Models-3, an approach that brings together many different models into one. Thus, it is instructive to compare the predictions of MM5 with available measurements and evaluate its suitability for predicting PBL height in complex terrain. Figure 7 shows the predicted mixed layer height during the day and the thickness of the stable boundary layer at night based on computed profiles of vertical virtual potential temperature profiles. The estimations were made only when the convective or inversion layer height was clearly discernible from the profiles. On clear summer days, the mixed layer was well developed, rising to heights as high as 4,000m. The Blackadar and Gayno-Seaman schemes predicted the highest and lowest mixed layer depths, respectively, for the daytime growth period. However, all three schemes predicted almost the same maximum mixed layer height and the time of its appearance.

Figure 7. Height of the Mixed Layer Derived from the Model Outputs Based on Different Methods of Turbulent Parameterization Schemes

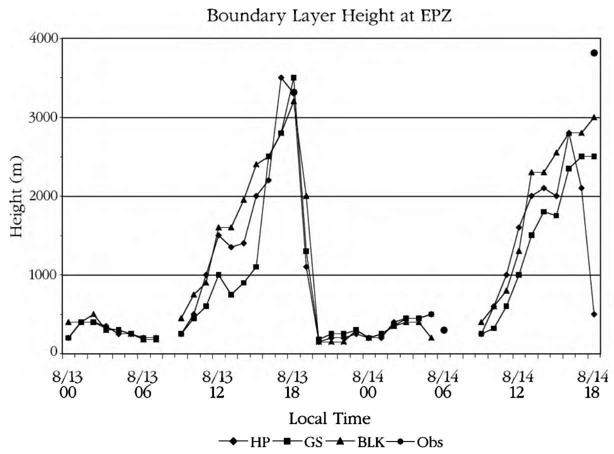

(Circles represent mixed layer height and the height of the surface boundary layer determined from the observed profile of virtual potential temperature.)

Also shown in Figure 7 are three observations of the mixed layer height based on NWS radiosonde ascends. An approximate one-hour time lag can be noted between the observations and predictions for August 13, 1996. The magnitude of the simulated mixed layer height, however, was comparable with the observations. Note that although in the computational domain the ground has begun to cool and the nocturnal stable layer has started developing by 1800, in the natural case the surface heating appears to still be effective in maintaining a mixed layer height of several kilometers. On the other hand, the model underestimated the mixed layer height on the following day although the simulated and observed patterns of surface heating/cooling matched each other. The lag of predicted and observed mixed layer heights in the evenings, however, should be viewed with circumspection. The observed height was evaluated using the temperature profiles of NWS radiosondes, which may have picked up the remnants of the inversion above the mixed layer that existed a few tens of minutes prior during active convection. As the convection is cut off, the turbulence in the mixed layer rapidly decays, yet the signature of the inversion can persist as a residual layer. Since the radiosonde launch and initiation of cooling were so close, the ground-based inversion may not have had time to develop sufficiently to create a signature in the profile; thus, the profile may indicate only the residual inversion. It may well be that the model parameterizations allow the development of the ground-based inversion too rapidly.

As is evident in Figure 7, the time evolution of the boundary layer is sensitive to the turbulence parameterization used. This sensitivity appears to be more pronounced during the day than at night. This is partly due to the fact that the Blackadar and Hong-Pan schemes employ different non-local closures for the unstable regime but use the same local K-theory (but with differing details) for stable conditions. Interestingly, for the same stable period, no significant difference was observed between the higher-order scheme and the local K-theory.

In all, the mixed layer simulations were in reasonable agreement with observations and demonstrate the feasibility of using the MM5 model output to estimate the mixed layer height. This inference gives credence to the current practice of using MM5 predictions as an essential meteorological input for air quality models such as Models-3. In addition, the present study corroborates the notion that mesoscale meteorological models can provide useful basic information on flow structure for the better understanding of air quality problems.

Summary and Conclusions

In this study, meteorological fields of the Paso del Norte airshed were simulated using a non-hydrostatic mesoscale model, MM5, implemented with high-resolution. Two field experimental periods, August 1996 (summer case) and December 1998 (winter case), were chosen as test cases. In the winter case, the synoptic forcing was prominent whereas both local thermodynamic forcing (which leads to local thermal circulation) and synoptic forcing (dominated by partly stagnant high-pressure conditions) characterized the summer experimental period. In both cases, synoptically influenced local mountain/valley circulation was well predicted and the model outputs showed good agreement with observations. The model also captured both the three-dimensional structure and the temporal evolution of the atmosphere reasonably well. Correlation coefficients between model predictions and observations at approximately 250m-agl were as high as 0.92 for the temperature and 0.80 and 0.61, respectively, for the u- and v-components of the winds.

The efficacy of three frequently used PBL parameterizations was investigated to ascertain their suitability for complex-terrain simulations. These included a non-local mixing (Blackader) scheme, an alternative non-local mixing scheme (non-local K-theory of Hong & Pan) and a higher-order (Gayno-Seaman) closure scheme. Comparisons of predictions with available measurements indicated that differences of predictions corresponding to these schemes are most pronounced during the day and negligible at night.

It was found that the Blackadar non-local scheme tends to manifest intense mixing during the period of the PBL growth when compared with the other two schemes. Correlation coefficients between observations and predictions, however, indicate that the performances of all three schemes can be considered almost identical. In addition, the maximum height of the daytime mixed layer and the thickness of the nocturnal stable boundary layer predicted by the three schemes were nearly the same. With regard to computational demands, the Hong-Pan non-local K-closure was 27% more efficient than the Gayno-Seaman scheme and 29% more effective than the Blackadar scheme. CPU times for calculations with the Gayno-Seaman and Blackadar schemes were almost the same.

The value of such models is the ability to begin to ask air quality improvement questions such as what if these sources are prohibited, scheduled, relocated, and minimized? The trajectory models provide necessary understanding of fates, alludes to effects, and discerns populations at risk.

ACKNOWLEDGMENTS

Urban air quality studies at Arizona State University are funded by the Southwest Center for Environmental Research and Policy (SCERP), the National Science Foundation, the Department of

Energy Environmental Meteorological Program, and the Army Research Office. The computations reported herein were primarily funded by SCERP through its Paso del Norte Air Program. We wish to thank Professor David Pijawka, Professor Adel Sarofim, and Dr. Michael Brown for their support, without whom this work could not have been realized.

REFERENCES

Ballard, S. P., B. W. Golding, and R. N. B. Smith. 1991. "Mesoscale Model Experimental Forecasts of the Haar of Northeast Scotland." *Monthly Weather Review* 119: 2107-2123.

Benoit, R., J. Cote, and J. Mailhot. 1989. "Inclusion of a TKE Boundary Layer Parameterization in the Canadian Regional Finite-Element Model." *Monthly Weather Review* 117: 1726-1750.

Blackadar, A. K. 1962 "The Vertical Distribution of Wind and Turbulent Exchange in a Neutral Atmosphere." *Journal of Geophysical Research* 67: 3095-3102.

Blackadar, A. K. 1979. "High Resolution Models of the Planetary Boundary Layer." Pp. 50-85 in *Advances in Environmental Science and Engineering*, Vol. 1, J. Pfafflin and E. Ziegler, eds. Langhorn, Penn.: Gordon and Breach.

Dudhia, J. 1996. "A Multi-Layer Soil Temperature Model for MM5." Preprints of the proceedings of The sixth PSU/NCAR Mesoscale Model Users' Workshop, (22-24 July) Boulder, Colorado.

Holtslag, A. A. M., and C-H. Moeng. 1991. "Eddy Diffusivity and Countergradient Transport in the Convective Atmospheric Boundary Layer." *Journal of Atmospheric Science* 48: 1690-1698.

Hong, S. Y., and H. L. Pan. 1996. "Nonlocal Boundary Layer Vertical Diffusion in a Medium-Range Forecast Model." *Monthly Weather Review* 124: 2322-2339.

Janjic, Z. I. 1990. "The Step-Mountain Coordinate: Physical Package." *Monthly Weather Review* 118: 1429-1443.

Janjic, Z. I. 1994. "The Step-Mountain Eta Coordinate Model: Further Developments of the Convection, Viscous Sublayer, and Turbulence Closure Schemes." *Monthly Weather Review* 122: 927-945.

Mellor, G. L. and T. Yamada. 1974. "A Hierarchy of Turbulence Closure Models for Planetary Boundary Layers." *Journal of Atmospheric Science* 31: 1791-1806.

Pan, Z., S. Benjamin, J. M Brown, and T. Smirnova. 1994. "Comparative Experiments with MAPS on Different Parameterization Schemes for Surface Moisture Flux and Boundary Layer Processes." *Monthly Weather Review* 122: 449-470.

Roberts, P., C. MacDonald, H. Main, T. Dye, D. Coe, and T. Haste. 1997. *Analysis of Meteorological and Air Quality Data for the 1996 Paso del Norte Ozone Study*. Final report prepared for the U.S. Environmental Protection Agency, Region 6, Dallas, Texas. STI-997330-1754-FR.

Shafran, P. C., N. L. Seaman, and G. A. Gayno. 2000. "Evaluation of Numerical Predictions of Boundary Layer Structure During the Lake Michigan Ozone Study." *Journal Of Applied Meteorology* 39: 412-426.

Stull, R. B. 1988. *An Introduction to Boundary Layer Meteorology.* Dordrecht, Netherlands: Kluwer Academic Publishers.

Stull, R. B. 1993. "Review of Non-Local Mixing in Turbulent Atmospheres: Transilient Turbulence Theory." *Boundary-Layer Meteorology* 62: 21-96.

Troen, I., and L. Mahrt. 1986. "A Simple Model of the Atmospheric Boundary Layer: Sensitivity to Surface Evaporation." *Boundary-Layer Meteorology* 41, 102-112.

Wyngaard, J. C., and R. A. Brost. 1984. "Top-Down and Bottom-Up Diffusion of a Scalar in the Convective Boundary Layer." *Journal of Atmospheric Science* 41: 102-112.

Yamada, T. 1983. "Simulations of Nocturnal Drainage Flows by A Q2l Turbulence Closure Model." *Journal of Atmospheric Science* 40: 91-106.

Yamada, T., and S. Bunker. 1988. "Development of a Nested Grid, Second Moment Turbulence Closure Model and Application to the 1982 ASCOT Brush Creek Data Simulation." *Journal of Applied Meteorology* 27: 562-578.

Zhang, D., and R. A. Anthes. 1982. "A High-Resolution Model of the Planetary Boundary Layer – Sensitivity Tests and Comparisons with SESAME-79 Data." *Journal of Applied Meteorology* 21: 1594-1609.

III

Air Quality in the Paso del Norte Airshed: Historical and Contemporary

N. J. Parks, W. Li, C. D. Turner, R. W. Gray, R. Currey, S. Dattner, J. Saenz, V. Valenzuela, and J. A. VanDerslice

ABSTRACT

This chapter provides an overview of the Paso del Norte airshed region, which is comprised of Ciudad Juárez, Chihuahua; El Paso, Texas; and Doña Ana County, New Mexico. Stakeholders are identified and a framework for industry, academia, non-governmental advocates, and government agencies at various levels to collaborate on air issues is provided.

Visible air pollution has historically been a focal point for interaction among various constituencies concerned about health effects, economic and social attractiveness, and regulation in the Paso del Norte Airshed (PdNA). The authors have collaborated primarily on the evaluation of visibility degradation by air pollutants and its relationship to priority pollutant levels prescribed by the United States Environmental Protection Agency (EPA) for air contaminants (Parks 1998). This is of special interest because the sizes (0.4μm to 0.8μm) of particulate matter (PM) in the ambient aerosol that scatter light in the visible range are retained in the lungs after inhalation. These visible air pollutant particles are believed to be most hazardous if

they originate from urban sources. They typically vary in concentration with invisible air pollutant gases from urban sources in the PdNA because prominent temperature inversions trap the various urban air pollutants.

Calidad del Aire en la Cuenca Atmosférica Paso del Norte: Histórica y Contemporánea

N. J. Parks, W. Li, C. D. Turner, R. W. Gray, R. Currey, S. Dattner, J. Saenz, V. Valenzuela, y J. A. VanDerslice

Resumen

Este capítulo proporciona una visión general para la región de la cuenca atmosférica del Paso del Norte, la cual comprende a Ciudad Juárez, Chihuahua; El Paso, Texas; y el Condado Doña Ana, Nuevo México. Los sectores involucrados son identificados y se proporciona un marco para la colaboración en asuntos relacionados con el aire para la industria, academia, organizaciones no gubernamentales y agencias de gobierno en varios niveles.

La contaminación atmosférica visible ha sido históricamente un punto central para la interacción entre varias comunidades preocupadas sobre los efectos en la salud, la atracción económica y social y la regulación en la cuenca atmosférica del Paso del Norte. Los autores han colaborado principalmente en la evaluación de la degradación de la visibilidad causada por contaminantes del aire y su relación con los niveles de contaminantes criterio prescritos por la Agencia de Protección Ambiental de los Estados Unidos (EPA, por sus siglas en inglés) para contaminantes del aire. Esto es de especial interés porque los tamaños (0.4 µm a 0.8 µm) de materia particulada (PM, por sus siglas en inglés) en el aerosol ambiental que dispersan luz en el rango visible, son retenidos en los pulmones después de su inhalación. Se cree que estas partículas visibles contaminantes del

aire, son las de mayor riesgo si provienen de fuentes urbanas. Varían típicamente en concentración con gases invisibles contaminantes del aire que provienen de fuentes urbanas en la Cuenca Atmosférica Paso del Norte (PdNA, por sus siglas en inglés) debido a las grandes inversiones térmicas que atrapan los diversos contaminantes del aire urbano.

AIR QUALITY ISSUES: PAST AND PRESENT

Several historical and currently important issues are conveniently introduced in the Charles Binion photograph (El Paso Public Library archives) in Figure 1. This illustration of historical sites, geography, meteorology, industrial pollution abatement, and urban demographics was used by Willis Webb on the cover of his seminal monograph, *Mesometeorology* in El Paso (Webb 1971).

Figure 1. Easterly View of "The Pass" Between the Franklin Mountains to the North and the Sierra de Juárez Mountains to the South

(The international border marker is the white diamond in the middle foreground with New Mexico in the lower left corner, Texas across the river, and Chihuahua, Mexico, beyond the marker and to the right of the river. The stack is 828 feet high with the plume injected above inversions [typically]. Downtown El Paso and Ciudad Juárez appear in the distance.)

Beyond the smoke stacks of the ASARCO, Inc., smelter, downtown El Paso, and Ciudad Juárez (about 3km), a monument stands representing Capitán-General Don Juan de Oñate, who led a Spanish colonial expedition across the river in 1598. He named this location "El Paso del Río del Norte," which was later shortened to "Paso del Norte." Some 370 years later, in about 1968, the local research community that resided in the PdNA began to work on air quality issues, stimulated by their observations of poor air quality and the then-recent appearance of the American Association for the Advancement of Science report from its Air Conservation Committee (AAAS 1965).

A review of the salient background literature and symposia proceedings is intended to be representative rather than exhaustive. All work is referred to in at least one of the references herein. An important report was the previously cited monograph on mesometeorology, which Webb (1971) defined as meteorology on an intermediate scale—about the size of the metropolitan area in the PdNA. Webb was privy to the results of more than 3,900 rocket radiosonde shots from White Sands Missile Range, just north of El Paso. These shots collected wind data, ozone (O_3) concentrations, and ambient air samples in liquid neon traps at 25,000 feet (8,000m) elevation. Webb observed that, despite the PdNA being one of the most meteorologically studied areas at high altitude, explanations of complex ground level meteorological phenomena controlling air pollution was inadequate (1971). This situation was little improved until August 1996 when the Paso del Norte Ozone Study (Roberts 1996) was performed and re-visited in 1997 because few ozone exceedences were observed in 1996. August 1997 also proved to be relatively free of high ozone levels. This underscored the difficulties of matching an intense meteorological study period to an overlapping period of high levels of pollutants of interest. Pollutants of interest include ozone precursors and intermediates in the chemical cycles characteristic in ambient atmospheric aerosols that form ozone.

The second major symposia and proceedings publications were organized by Professors Applegate and Bath from the University of Texas at El Paso. This was *Air Pollution Along the United States-Mexico Border* (1974). This first binational symposium on air pollution was held on the University of Texas at El Paso (UTEP) campus in

September 1973. It was sponsored by two international health agencies, United States and Mexican environmental agencies, various universities, state health and environmental agencies, and municipal health and environment departments. Vehicular pollution, open burning, industrial sources, regulation, and future monitoring needs were central themes.

Health Issues of Concern

At a 1973 symposium, L. P. Jones, of UTEP's biology department (Jones 1973) noted, "Medical studies have clearly related contaminated air to a broad variety of respiratory problems in man such as asthma, bronchitis, lung cancer, and emphysema. In El Paso-Ciudad Juárez, we have the pollution, and we have the patients with respiratory disorders. I think the time has come for a study to analyze the effects of air on the people of this community." The lag time between this clarion call for health effects studies and the appearance of the first one in 1999 by VanDerslice and co-workers (Hart 1999) on pediatric asthma was 26 years. With the added information about air pollution health effects in other western areas (Heflin 1994; Schwartz 1999), health effects studies are even more important today. At present, no studies on even the mortality rate correlation with air quality have been performed for the PdNA. This report will argue for the appropriate support from public agencies such that the lag time between a 1999 call for health effects studies and actual performance of one falls in a "near term" time frame (i.e., one year to five years rather than 26).

The 1980s were a time when attention focused on numbers of vehicles, waiting time at the international bridges, vehicle emissions, general air pollution, and health effects for people in and around the international bridges. A collaboration of El Paso city and county officials and academics led to the summarizing publication of much of the 1980s air quality effort in the PdNA. The book, *Vehicular Traffic and Air Pollution in El Paso-Ciudad Juárez* by R. Gray, J. Reynoso, C. Diaz Q., and H. Applegate, appeared in 1989. This publication included a wealth of original data and analyses over several years for carbon monoxide (CO), ozone, and total suspended particulates (TSP). El Paso was out of federal compliance during this time while no data existed for Ciudad Juárez. Carbon monoxide, in particular, had been found to have dramatically high values for hourly maxima—nearly 200ppm at some times at the inspection stations. This ultimately led to the re-design of a clean air supply system for inspection booths on international bridges.

Other issues addressed by Gray et al. (1989) were the subjects of various symposia, proposals for international accords, and impacts of the new treaty, the La Paz Agreement, which was signed in 1983 by Mexican President Miguel de la Madrid and United States President Ronald Reagan. The La Paz Agreement and future annexes, which also have the standing of the treaty in United States law, specified that the EPA and the Mexican Secretaría de Desarrollo Urbano y Ecología (SEDUE) were the designated federal agencies, and that local officials were to be included. This agreement permitted the EPA to spend money for air pollution studies or abatement programs that would take place in border areas—which were perceived to be of lower priority, at the time, for the Mexican government than the markedly more serious air quality problems in Mexico City. In the 1990s, the La Paz Agreement expedited the process for acquiring air pollution data by the various responsible Mexican agencies in the PdNA. Today, CO, O_3, oxides of nitrogen (NO_X), and particles less than 10 microns in diameter (PM_{10}) are routinely measured on both sides of the border.

Institutions Involved with Air Quality

The 1990s in the PdNA were characterized both by more research and by a much higher level of citizen and nongovernment agency participation in air quality issues. For several years, the Paso del Norte Air Quality Task Force has been quite active as a forum for debate and presentation of issues on both sides of the border. It typically alternated meeting sites between El Paso, Ciudad Juárez, and less frequently, Sunland Park, New Mexico. Typically, representatives of all local, state, and federal agencies with a vested interest on both sides of the border attended. The academic research community has been well represented by local non-governmental organizations such as the Clean Cities Coalition and by international non-governmental organizations such as Environmental Defense.

The Task Force advocated the formation of an International Joint Advisory Committee for the improvement of air quality in the Airbasin that covers Ciudad Juárez, Chihuahua; El Paso, Texas; and Doña Ana County, New Mexico. The International Joint Advisory Committee now meets regularly to address air issues in the basin. This committee has not existed long enough to estimate its effectiveness. The meeting notifications and minutes distribution are managed through the Texas Commission on Environmental Quality (TCEQ) Region 6 office in El Paso (Valenzuela 1999).

Another Task Force issue was lobbying for commuter lanes to speed up bridge crossing. Various "fast identification" methods for pre-registered drivers and the commuter lane have been developed, according to a report to the Joint Air Quality Advisory Committee. Yet another issue is the export of United States automobiles that fail United States emissions tests to Ciudad Juárez. This results in a conflict between economic incentive to export them and efforts to reduce mobile source emissions. Another issue is whether United States oxygenated fuels are exported to Ciudad Juárez and what replacements exist in the United States if the oxygenator MTBE (methyl-tertiary-butyl-ether) is banned. Grassroots political action and citizen participation in *ad hoc* groups concerned about air quality have been important in raising public awareness in the PdNA.

Air quality research in the 1990s first focused on the component of the usually measured respirable fine particles that are less than 2.5 μm in aerodynamic diameter, or $PM_{2.5}$. The TCEQ project, *El Paso-Juárez 1990 PM-10 Receptor Modeling Feasibility Study* (Dattner 1994) obtained $PM_{2.5}$ and the total PM_{10} using dichotomous samplers. The values, up to 100 $\mu g/m^3$ in parts of the PdNA, are comparable to the $PM_{2.5}$ maxima coming out of the U.S. EPA-sponsored pilot study in 1998.

With more health effects data showing excess mortality from urban air pollution in other western metropolitan areas now available (Schartz 1996), the 30% to 75% of the PM_{10} that turned out to be in the respirable "fine" fraction reported by Dattner is of greater concern than before. In Dattner's report, he noted that established dogma at that time (1994 and some years before) argued that the fine fraction penetrates into the lower respiratory that tract, the process creating the fine particles differs from those creating the rest of PM_{10}, and that the fine mass is frequently more toxic than coarse mass. These statements remain unchallenged. The other research studies of the 1990s will be discussed in a separate section, but the first reports in that decade point out the anticipated health effects of the findings.

A variety of public and private groups and organizations are now involved in air quality in the PdNA. Some companies and utilities have participated in ways that have both present and future value through their environmental divisions. Two organizations with facilities on the Rio Grande have made their engineers available to display the most sophisticated modern air pollution control equipment to the students in area academic institutions. One such company is ASARCO, Inc. Their facilities (Figure 1) essentially eliminated the hundreds of tons per day of sulfur oxides flowing from their smoke stack with "ConTop" smelting reactors, installed around 1993. The former waste product was then marketed as sulfuric acid. This facility is presently idled as a consequence of low copper prices and thus, for the first time in 100 years, is contributing no air contamination to the PdNA. El Paso Electric Company has two plants in the PdNA that burn clean natural gas but must have sophisticated temperature feedback control to prevent the NO_x emissions from exceeding regulatory limits. This utility has a pro-active environmental education program and successfully interacts with academic institutions in the area. The various public institutions involved in air quality in the PdNA are listed in Table 1.

Table 1. Institutions Involved in Air Quality in the PdNA

Local Government	Air Group, El Paso City-County Health Department Dirección de Desarrollo Urbano y Ecología del Gobierno del Municipio de Juárez
State Governments	Dirección General de Desarrollo Urbano y Ecología del Gobierno del Estado de Chihuahua New Mexico Environment Department Texas Commission on Environmental Quality Western Governors Association
Federal Government	Instituto Nacional de Ecología of México Secretaría de Medio Ambiente y Recursos Naturales U.S. Environmental Protection Agency U.S. Centers for Disease Control and Prevention
International; U.S.-Mexico	Joint Advisory Committee for the Improvement of Air Quality in the Ciudad Juárez, Chihuahua; El Paso, Texas;Doña Ana County, New Mexico Airbasin
Academic Institutions	Arizona State University New Mexico Institute of Technology New Mexico State University University of Texas at El Paso University of Utah San Diego State University Universidad Autónoma de Ciudad Juárez Southwest Center for Environmental Research & Policy
Non-Governmental Organizations	Border Health Research Center of the Paso del Norte Health Foundation Environmental Defense Clean Cities Coalition Physicians for Social Responsibility Paso del Norte Air Task Force

Geography and Demographics

The physical situation of El Paso and Ciudad Juárez is shown in Figure 2, which also shows typical winter morning inversion height at a few hundred feet. On this day in December 1997, the sharply defined pall of dust and co-existing urban pollutants is most visible between downtown El Paso (tall buildings) and the foot of the Sierra de Juárez Mountains. Downtown El Paso is within three blocks of the international border; consequently, most of the area under heavy visible pollution on this day is in Ciudad Juárez. Additional details of topography are provided at www.ozonemap.org (Gray 1999).

On this day in December 1997, the sharply defined pall of dust and co-existing urban pollutants is most visible between downtown El Paso (tall buildings) and the foot of the Sierra de Juárez Mountains. Downtown El Paso is within three blocks of the international border; consequently, most of the area under heavy visible pollution on this day is in Ciudad Juárez. Additional details of topography are provided at www.ozonemap.org (Gray 1999).

Figure 2. South-Westerly View Taken from the End of the Franklin Mountains (Scenic Drive) above El Paso

Reference Materials

A project by the ATR Institute of the University of New Mexico (Cockerill 1998) catalogued reference material for transportation-related issues along the border. It included most studies of any description performed in El Paso through 1997. This reference source was catalogued by the authors, funding agency, and performing institution. More recent El Paso studies since the ATR publication were compiled but are not included. However, they are referenced in subsequent sections herein.

Direct access to ozone data in the PdNA (Gray 1999) is provided by the Center for Environmental Resource Management (CERM) at the UTEP website www.ozonemap.org. This site is linked to related web pages for other projects at CERM/UTEP.

Geography, Meteorology, Demographics, and Air Quality

Local Topography

The PdNA is part of the basin-range geography of the southwestern United States and northern Mexico. It includes three cities: El Paso, Texas; Ciudad Juárez, Chihuahua; and Sunland Park, New Mexico. El Paso is bisected by the narrow north-south trending Franklin Mountains in El Paso and the southwest trending Sierra de Juárez Mountains south of the Rio Grande (Figures 1 and 2).

Local Climate Conditions

The climate and the meteorology have a profound influence on the air quality situation. The annual rainfall varies from 5 inches to 12 inches. The dry top layers of soil contain fine particles that are entrained by wind currents. The health effects of the mix of urban and crustal material—which, contrary to some expectations is well within the respirable size range, is unknown.

Non-Uniform Ambient Air Quality

The PdNA is classified as "nonattainment" for particulate matter, carbon monoxide, and ozone. As noted earlier, the most obvious evidence of air quality degradation in Paso del Norte is the frequent, well-defined haze hanging over the region during the morning hours (Figure 2). Parts of El Paso County fail to meet the United States National Ambient Air Quality Standards (NAAQS) for PM_{10}, carbon monoxide (CO), and O_3. Sunland Park, New Mexico, exceeds the NAAQS for ozone and PM_{10}. Ciudad Juárez air pollution levels exceed the Mexican ambient air quality standards for PM_{10} ($150 \mu g/m^3$ for a 24-hour average and $50 \mu g/m^3$ for an annual average), ozone (0.11ppmv for a one-hour average), and CO (11ppmv for an eight-hour average). The Mexican longer-term averaged standards are comparable or more stringent than those of the United States.

The current population in the combined community of El Paso, Ciudad Juárez, and Sunland Park exceeds 2 million, about one-third of those residents live in El Paso. It is anticipated that the El Paso population will grow by 18,000 people to 20,000 people per year and the Ciudad Juárez population will grow at about 40,000 people per year. According to the El Paso Metropolitan Planning Organization, approximately 200,000 vehicles are registered in El Paso and 350,000 vehicles in Ciudad Juárez. The average number of vehicles crossing the border each day is approximately 40,000.

Ambient Air Monitoring and Emissions Inventories

State of Texas and El Paso City-County

TCEQ, El Paso City-County, Ciudad Juárez municipal government, and the New Mexico Environment Department (NMED) operate air monitoring stations in the PdNA. Most of these stations also have PM_{10}, CO, and NO_x monitoring. Non-methane hydrocarbons are monitored at the Chamizal site in El Paso. The total number of monitoring stations, exclusive of the new $PM_{2.5}$ EPA program, is 13 in the United States and six in Ciudad Juárez, Chihuahua.

There are eight $PM_{2.5}$ monitoring stations running or being made operational in the Texas portion of the PdNA and two run by the NMED, totaling 10 in the PdNA in the United States. The expectation is that the fine fraction of PM_{10} may be more important for heath risk assessment. The first report of $PM_{2.5}$ sampling in Texas, including one sampler downtown at the Tilman Health Center, appeared in December 1998 (Tropp 1998). The proposed regulation is that the 24-hour average $PM_{2.5}$ should not exceed $65 \mu g/m^3$ for a three-year average of annual 98^{th} percentiles at any population-oriented monitoring site. The El Paso preliminary results show maxima above this level.

Emissions inventories and models have been much more intensely examined in the 1990s than ever before. TCEQ periodically produces the El Paso Industrial Emissions Inventory. The most recent monitoring data is available on the TCEQ website at www.tceq.tx.us. This information and the hydrocarbon source apportionment portion of the 1996 Paso del Norte Ozone Study (Fujita 1998) was combined with the development of a gridded emission inventory for the entire PdNA (Haste 1998).

Health and Air Pollution Levels

Risk assessment of exposure to inhalable fine particles in the Paso del Norte Airshed has received little attention. Adverse health effects are commonly anticipated after exposure to inhalable fine particles produced by urban air pollutant sources, sandstorms, or combinations of the two (Hefflin 1994; U.S. EPA 1995; Pope 1996).

In other western areas, the urban particle fraction alone has been shown to increase the mortality rate (Pope 1999). The only study of the adverse effects of inhalable fine particles in the PdNA has appeared recently. Hart et al. (1999) modeled pediatric emergency room admissions in 1994-1995 for respiratory illness as a function of ambient levels of PM_{10} and ozone. In the PdNA, an increase in asthma-related emergency room visits was found to be associated with a decrease in dew point temperature on the same day and an increase in PM_{10} two days before.

Future Issues of Policy and Research

The health issues addressed in the previous section depend on socio-economic factors as well as scientific work. In the development of *Characterization of Ambient Particulate Matter in the Paso del Norte Region* (Li 1999) for the Southwest Center for Environmental Research and Policy (SCERP), the investigators noted:

> In order to understand the factors controlling particulate concen trations in the Paso del Norte Airbasin, one needs to take into consideration an international, tri-state setting with different environmental laws, regulations, standards, enforcement, and monitoring operations in the various jurisdictions at the federal, state, county, and city level; frequent and lengthy periods of intense traffic congestion at the international border crossings; atmospheric and topographic conditions which foster the devel opment of inversions, regularly trapping pollutants and facilitating the build-up of ozone precsors, CO, PM, and other potentially hazardous air pollutants; rapid industrial and population growth that has outpaced the supporting infrastructure; and several zones of high population density which lead to traffic congestion with in El Paso and Ciudad Juárez.

References

American Association for the Advancement of Science. 1965. *Air Conservation Committee Report*. Washington, D.C.:

Cockerill, K., and J. Espinosa. 1998. *Border Air Quality Research Matrix*. Albuquerque, New Mexico: ATR Institute, University of New Mexico.

Fujita, E. 1998. *Hydrocarbon Source Apportionment for the 1996 Paso del Norte Ozone Study*. Reno: Energy and Environment Engineering Center, Desert Research Institute.

Gray, R. W., J. Reynoso, C. Diaz Q., and H. Applegate. 1989. *Vehicular Traffic and Air Pollution in El Paso-Ciudad Juárez*. El

Paso, Texas: Texas Western Press.

Gray, R. W. 1999. www.ozonemap.org. El Paso: Center for Environmental Resource Management, University of Texas at El Paso.

Hart, R., J. VanDerslice, B. Vera, C. Gotway-Crawford, S. Kieszak, R. Philen, and M. McGeehin. 1999. *Ambient Air Quality and Acute Pediatric Respiratory Illness in the Paso del Norte Airshed.* Atlanta: National Center for Environmental Health, Center for Disease Control.

Haste, T. L., N. Kumar, L. R. Chinkin, P. T. Roberts, M. Saeger, and S. Mulligan. 1998. *Compilation and Evaluation of a Gridded Emission Inventory for the Paso del Norte Area. Sonoma Technology, Inc. Report No. STI-998110–1828-FR.* U.S. EPA Region 6.

Hefflin, B. J., B. Jalaludin, E. McClure, N. Coob, C. A. Johnson, L. Jecha, and R.A. Etzel. 1994. "Surveillance for Dust Storms and Respiratory Diseases in Washington State, 1991." *Archives of Environmental Health* 49:170–174.

Li, W., R. Currey, R., V. Valenzuela, et al. 1999. *Characterization of Ambient Particulate Matter in the Paso del Norte Region.* St. Louis: Air and Waste Management Association Proceedings.

Parks, N. J.; C. D. Turner, S. L. Dattner, J. Saenz, V. Valenzuela, J. A. VanDerslice, O. E. Chavez, E. Tarin, N. Castro, R. Orquiz, and R. W. Gray. 1998. *Trans-Border Visibility Analysis: Quantitative Analysis of Dynamic, Multi-Site Video Images of the Paso del Norte Airshed.* Southwest Center for Environmental Research and Policy, Project No. AQ96-PP96I-13. San Diego: SCERP.

Pope, C. A. 1996. "Particulate pollution and health: A Review of the Utah Valley Experience." *Journal of Exposure Analysis and Environmental Epidemiology* 6:23–34.

Pope, C. A., R. W. Hill, and G. M. Villegas. 1999. "Particulate Air Pollution and Daily Mortality on Utah's Wasatch Front." *Environmental Health Perspectives* 107(7): 567–573.

Roberts, P., et al. 1996. *Operating Plan for Ozone Modeling Data Collection in El Paso-Ciudad Juárez-Sunland Park.* Draft Final Report under U.S. EPA Contract 68-D3–0030.

Schwartz, J., G. Norris, T. Larson, L. Sheppard, C. Claiborne, and J. Keonig. 1999. "Episodes of High Coarse Particle

Concentrations Are Not Associated with Increased Mortality." *Environmental Health Perspectives* 107(5): 339–342.

Tropp, R. J.,S. D. Kohl, J. C. Chow, and C. A. Frazier. 1998. *Final Report for the Texas $PM_{2.5}$ Sampling and Analysis Study*. Desert Research Institute, Document No. 6570–685–7770.1F (15 December).

Valenzuela, V. 1999. *Joint Air Quality Commission Meeting Notifications and Proceedings*. El Paso: Texas Commission on Environmental Quality, Region 6.

IV

Correlation of Wind Flow and Visibility at Big Bend National Park

R. Okrasinski and J. Greenlee

ABSTRACT

Deterioration of visibility at Big Bend National Park by man-made pollutants is of great concern. Contaminants that most effectively reduce visibility can persist in the atmosphere for several days and may have been transported from sources that are hundreds of miles away. To help identify the sources and source-areas of these pollutants, several years of atmospheric data were analyzed to characterize the flow of air into the park and to relate different flow patterns to park visibility. Five-day back trajectories from Big Bend were computed every six hours between 1991 and 1994, using the Atmospheric Transport and Dispersion model developed by the National Oceanic and Atmospheric Administration (NOAA), and routine upper-air data collected by the weather services of the United States and Mexico. These trajectories represent estimates of paths air followed in the previous five days before entering the park. The airflow into the park was spatially characterized for different times of the year by computing the relative number of trajectory positions in sectors of a 600km radius circle surrounding Big Bend. Flow over different sectors was then correlated with visibility measured at the park to identify likely contaminant source areas.

The data suggested that the worst Big Bend visibility is caused by

pollutants emitted in Eastern Texas between Brownsville and Waco. These areas of Texas are heavily industrialized and emit a significant quantity of pollutants. This is also true for areas to the east and northeast of the 600km analysis area, and it is possible that contaminants emitted there may be transported into the Brownsville-to-Waco region on their way to the park.

Correlación del Flujo de Aire y Visibilidad en el Parque Nacional Big Bend

R. Okrasinski y J. Greenlee

Resumen

El deterioro de la visibilidad en el Parque Nacional Big Bend por contaminantes producidos por el hombre es un asunto de preocupación enorme. Los contaminantes que más efectivamente reducen la visibilidad pueden permanecer en la atmósfera durante varios días y haber sido transportados de fuentes ubicadas a cientos de millas a distancia. Para ayudar a identificar las fuentes y áreas de emisión de estos contaminantes, se analizaron varios años de datos atmosféricos para caracterizar el flujo del aire hacia al parque y relacionar diferentes patrones de flujo con la visibilidad en el parque. Trayectorias de cinco días en Big Bend fueron registradas cada seis horas entre 1991 y 1994 utilizando el Modelo de Transporte Atmosférico y Dispersión desarrollado por la Administración Nacional Oceánica y Atmosférica (NOAA, por sus siglas en inglés), y los datos rutinarios de aire superior obtenidos por los servicios del clima de los Estados Unidos y México. Estas trayectorias representan estimaciones de la dirección que siguió el aire en los cinco días anteriores a su ingreso al Parque. El flujo de aire entrante al Parque fue caracterizado espacialmente para diferentes temporadas del año

computando el número relativo de posiciones en las trayectorias para sectores en círculo con radio de 600km rodeando Big Bend. El flujo sobre diferentes sectores fue entonces correlacionado con la visibilidad medida en el parque para identificar las posibles áreas de emisión de contaminación.

Los datos sugieren que la peor visibilidad en Big Bend es causada por contaminantes emitidos en la parte Este de Texas entre Brownsville y Waco. Estas áreas de Texas están altamente industrializadas y emiten una cantidad significativa de contaminantes. Esto también es cierto para áreas hacia el este y noreste del área de análisis de 600km, y es posible que contaminantes emitidos ahí sean transportados hacia la región Brownsville-a-Waco en su ruta hacia el Parque.

INTRODUCTION

The degradation of air quality in the Big Bend region of Texas and Mexico from man-made pollutants is a major concern. There are numerous parks and reserves in the area. In Texas, these include the Big Bend National Park, the Big Bend Ranch Natural Area, and Black Gap State Refuge. In Mexico, there is the Maderas del Carmen protected area in Chihuahua and the Cañon de Santa Elena Reserve in Coahuila. Big Bend National Park is a Class I protected area under the Clean Air Act. The most conspicuous problem is the deterioration in visibility that obscures scenic features and ultimately decreases the number of visitors to the area. This deterioration of visibility could have a detrimental economic impact on the regional tourism industry. Deposition of acidic atmospheric contaminants may also have significant unfavorable effects on the plants and animals in the region. Poor air quality is also of concern to McDonald Observatory, one of the largest observatories in the world, which is located just north of Big Bend National Park. In addition to reducing visibility, some pollutants also damage the coating on the telescopes' mirrors, necessitating expensive repairs.

Visibility is most effectively decreased by suspended fine particles whose diameter is close to the visible light wavelengths (0.4 microns to 0.7 microns). Particles of this size can persist in the atmosphere for several days and are often transported hundreds of miles. As a consequence, pollutant sources that are considerable distances from the park can still have a significant effect on visibility. Most of these particles are created by chemical reactions in which gases emitted by industrial processes are converted to particulate matter. Considerable quantities of these gases are emitted by industrial facilities in northern Mexico and Eastern Texas.

To develop effective strategies to improve the air quality at Big Bend, researchers must develop an understanding of the relative significance of the various pollution sources within the region and how much the air quality would improve or degrade as a result of changes in those emissions. To further this understanding, four years of atmospheric data collected between 1991 and 1994 were analyzed to determine the characteristics of the air flow into Big Bend for different seasons and how flow over different areas is related to visibility measured at the park.

Visibility at Big Bend

Visibility at Big Bend National Park is monitored hourly by a transmissometer as part of the Interagency Monitoring of Protected Visual Environments (IMPROVE) measurement program, a cooperative effort between the United States Environmental Protection Agency (EPA) and several federal land management and state air agencies. The transmissometer, situated approximately three miles southeast of Panther Junction at an elevation of 1,067 meters above sea level, transmits light several kilometers to a receiver. A comparison of the transmitted and received light intensities determines the path-averaged light extinction due to atmospheric scattering and absorption from which the visibility can then be derived. Because the main purpose of the measurements is to determine the amount of light loss due to atmospheric gases and haze or fog, the data are flagged and not used. Data are also flagged if there are equipment failures, obstructions, or distortions of the light beam. A complete description of the instrumentation and the data reduction techniques can be found in Sisler (1993).

Ten-minute averaged transmission data are used to compute the atmospheric extinction coefficient and visibility for every hour of each day. The extinction coefficient is given by $b_{ext} = -\ln (I/I_0)/r$, where I and I_0 are the amount of light reaching the receiver and the amount being transmitted, respectively, and r is the distance between the source and receiver.

Visibility is often expressed as the standard visual range, which is the distance where the light loss is 98%. It is calculated from the extinction coefficient as follows: visual range = $3.91/b_{ext}$.

Another visibility unit, the deciview (dV), has been developed in recent years (Pitchford and Malm 1993). This is similar to the decibel used in sound intensity measurements and is defined as $dV = 10 \ln (b^{ext} /.01)$, where the extinction coefficient is in km^{-1}. The index increases with decreasing visibility. Equal changes in the index are equally perceptible to the human eye.

IMPROVE transmissometer data collected between 1991 and 1994 were statistically analyzed to show the seasonal and diurnal characteristics of Big Bend visibility. Only the data not flagged for fog, precipitation, or measurement problems (about 60%) were used. Except in August 1994 when data were available for only three days, most days in the four-year period were represented.

The seasonal characteristics of Big Bend visibility are shown in Figure 1, where the median, 25^{th} percentile, and 75^{th} percentile visibility expressed as visual range and deciview for each month are plotted versus the time of the year. Visibility was highest during winter and lowest in summer. The highest monthly median visual range was 113km in January and the lowest was 71km in August. The diurnal variations in average visibility during different times of the year are shown in Figure 2. Visibility was best in the late afternoon and poorest in early morning. This is due to the fact that many aerosols, particularly sulfates, are hygroscopic. This means that atmospheric water vapor tends to condense when the relative humidity is high but is significantly below 100%. For sulfates, the threshold is about 70%. The addition of the condensed water significantly increases the light scattering properties of the particles. The visibility in humid air, therefore, may be considerably less than the visibility in dry air with the same pollutant concentration. On most days, the relative humidity is highest near dawn when the lowest temperatures usually occur.

Figure 1. Median (solid line), 25th Percentile, and 75th Percentile (dashed lines) Visibility Expressed as Visual Range and Deciviews for Each Month at Big Bend National Park

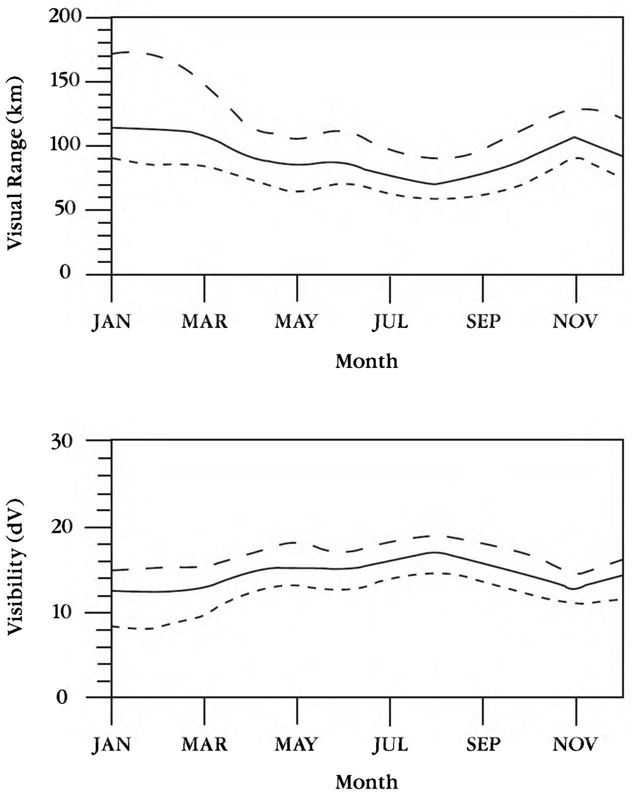

Figure 2. Mean Visibility in Deciviews (solid line) and Visual Range (dashed line) Versus Time-of-Day at Big Bend National Park

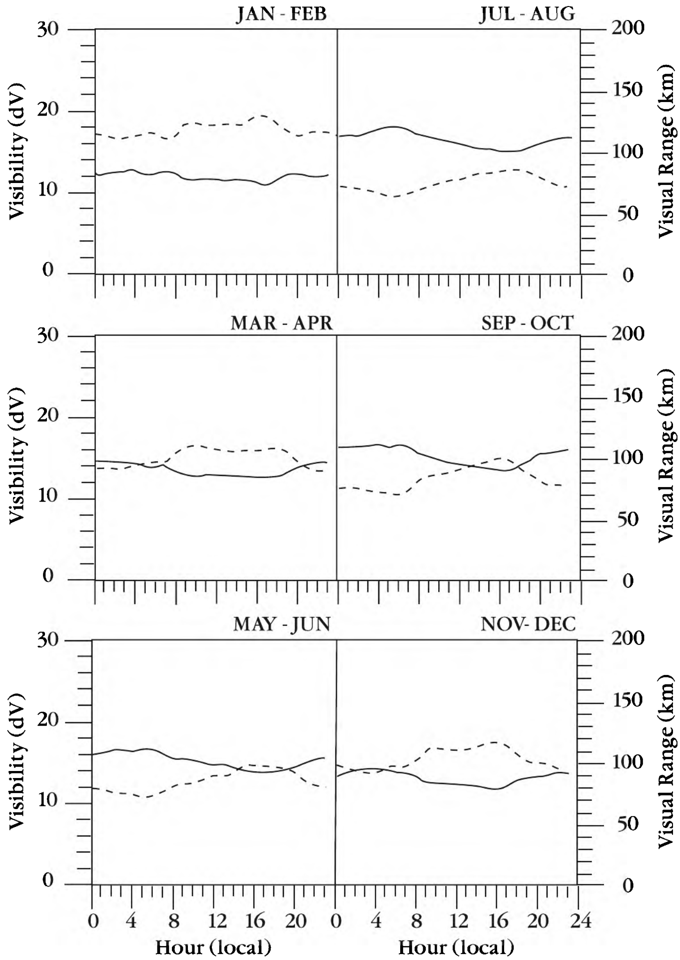

WIND FLOWS INTO BIG BEND

Upper-air data collected between 1991 and 1994 at eight weather stations surrounding Big Bend National Park were used to compute five-day back trajectories from the park. These are estimates of the paths air entering Big Bend followed during the previous five days. Pollutants transported into the park from distant sources would most likely have originated under these paths.

The back trajectories were calculated by the Atmospheric Transport and Diffusion (ATAD) model (Heffter 1980). This is a one-layer Lagrangian model that has been used by several investigators to study long-range transport into other national parks (Green and Gebhart 1997; Pitchford and Pitchford 1985; White et al. 1994). The upper-air data required by ATAD are routinely collected by radiosondes that are released daily by the weather services of the United States and Mexico. In the original computer program, these data are read from specially formatted tapes created at the National Climatic Data Center (NCDC). NCDC stopped providing these data after 1992, however. The program was, therefore, modified to read the data from a series of specified ASCII files, each containing one month of upper air data from one station.

The ATAD trajectories are computed in 40 three-hour segments starting at 0000, 0600, 1200, and 1800, and going backward in time five days. Each segment is calculated from weather station measurements collected within a specified distance from its starting position. The first distance attempted is 250 nautical miles. If there are data from at least two stations within this distance or data from one station within half this distance, the segment is computed. Otherwise, the distance is increased to 600 nautical miles, and the search is performed again. If this condition is still not satisfied, the segment is not calculated.

Each selected weather station is assigned a transport layer with a base 150m above the average terrain elevation and a top determined from the vertical temperature structure. The transported pollutants are confined below the top of the transport layers by temperature inversions. Layer depths are generally higher in the summer when there is greater atmospheric instability. The maximum layer depth is 3,000m. The average winds within these layers are used to compute the trajectory segments.

The influence of each station is weighted according to its proximity and azimuth orientation with respect to the trajectory segment being computed. If there are no data for a station at the time of a segment, but there are data six hours earlier and six hour later, the mean of the layer-averaged winds at the two observation times are used. For example, if a 1200-1500 segment is being computed and there are 0600 and 1800 data for a station and no data at 0600, the mean of the layer-averaged 1200 and 1800 winds are used in the trajectory computation.

The principal ATAD outputs are the latitude and longitude of each three-hour trajectory segment endpoint and the transport layer depth for each endpoint. The latter is a weighted average of the transport layer depths at the weather stations used to compute the trajectory segment.

The names and elevations of the upper-air stations used to calculate the Big Bend trajectories and their distances and azimuth angles from Big Bend National Park are tabulated in Table 1.

Table 1. Radiosonde Stations Used in the Analysis

Station	Elevation (m)	Distance (km)	Azimuth (degrees)
Brownsville, Texas	7	688	123.3
Corpus Christi, Texas	14	584	106.9
Chihuahua, Mexico	1,428	289	256.6
Del Rio, Texas	313	220	88
El Paso, Texas	1,199	412	312.4
Midland, Texas	873	307	17.5
Monterrey, Mexico	450	484	142.0
Stephenville, Texas	399	571	55.4

All stations operated during the entire four-year period except Stephenville, Texas, which stopped operations on July 11, 1994. Data were usually collected twice daily, at 0600 and 1800, by the United States stations. There were more than two soundings on some days. Data were available at 0600 and 1800 for more than 98% of the days in 1991, 1992, and 1994. In 1993, however, there were more missing data. The percentage of 1993 data available, expressed as the number of radiosonde observations divided by twice the number of days in the year, was approximately 74% at Del Rio, Texas, 63% at Stephenville, Texas, and between 93% and 96% at the other stations in the state.

Less data was available from the two Mexican stations. Most of the time there was only one flight each day (at 1800), and there were more missing days. The number of measurement heights was also smaller. Chihuahua had data for 85%, 93%, 63%, and 72% of the days during 1991, 1992, 1993, and 1994, respectively, and Monterrey had data for 60% to 70% of the days for those years.

Using the above information, back trajectories from Big Bend National Park were computed four times daily between 1991 and 1994. To characterize their spatial distribution, a 600km circle surrounding the park was divided into eight 45-degree sectors according to compass direction, and the percentage of the trajectory endpoints that were in each sector was calculated. Averages of the transport layer depths at the endpoints within each sector were also computed. A map of the Big Bend area showing the locations of the upper-air weather stations and the surrounding 600km circle is shown in Figure 3.

Figure 3. Map of Big Bend Region Showing Radiosonde Stations and 600km Radius Study Area

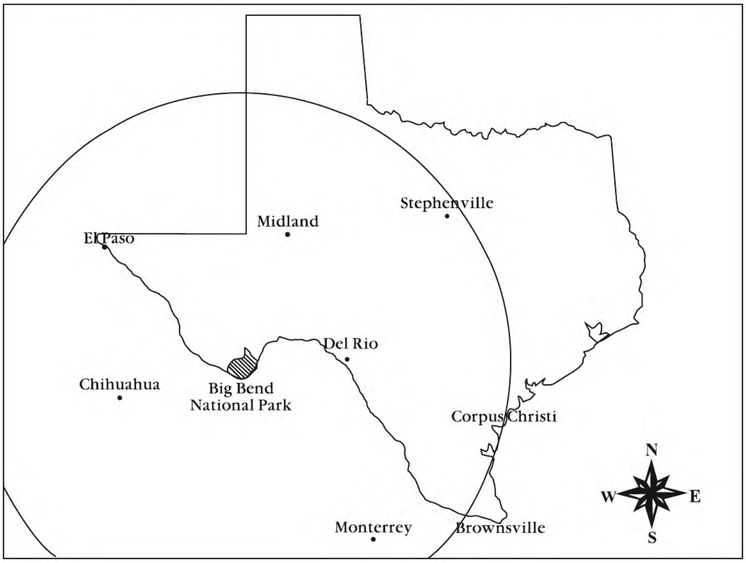

The trajectory endpoint frequencies and average transport layer depths in each sector are plotted in Figure 4 for six two-month periods. Nearly all the summer flow was from the south and southeast.

Eighty-seven percent of the July and August trajectory positions were within these two sectors and another 8% were in the eastern sector. Only 5% were in the others. In winter, there was a much more even distribution of the trajectory positions. Flow from the northeast and east was somewhat less common than flow from other directions. The trajectory distributions in the spring and fall were intermediate between summer and winter, with approximately half of the flow from the southeast and south and half from other directions.

As expected, the transport layer depths were higher in the summer. Except from July to August when nearly all the trajectories were in the east and south sectors, the layer depths were greatest when the flow was from the west, northwest, and north and smallest when the flow was from the east and southeast.

Figure 4. Trajectory Frequency (bars) and Average Transport Layer Depth (circles) Versus Direction from Big Bend National Park from 1991-94

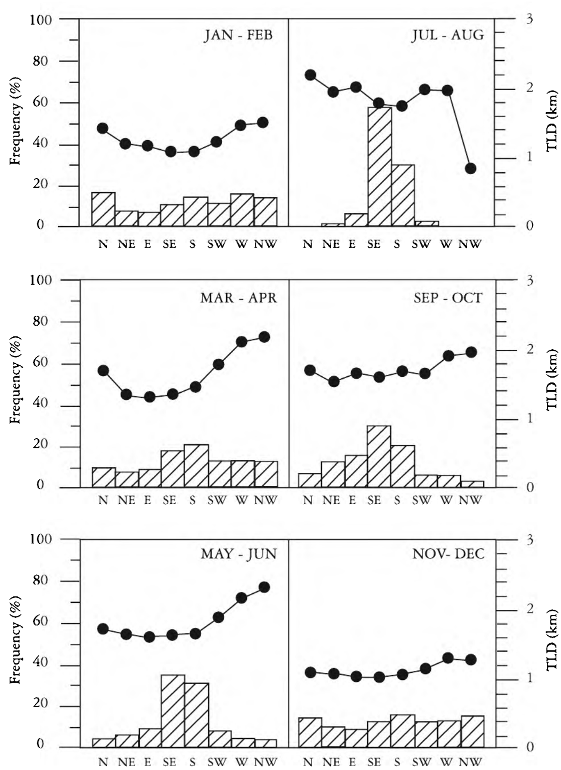

Wind Flow and Visibility

To correlate wind flow with Big Bend visibility, the trajectory endpoint frequencies were recomputed using only those trajectories where an unflagged transmissometer measurement was available at the start of the trajectory. A total of 3,669 back trajectories (63%), satisfied this condition. An average visual range was then computed for each of the eight 45-degree sectors defined in the previous section. This was done by assigning each trajectory endpoint with the visual range measured at the beginning of that trajectory and then averaging those visual ranges in each sector. For example, if a sector contained 100 trajectory endpoints, the 100 visual ranges assigned to those endpoints would be averaged to obtain an average visual range for that sector. Sectors that are sources of large amounts of light-reducing pollutants are expected to have lower visual ranges associated with them than surrounding areas where there are fewer pollutants. This analysis, therefore, helps determine the relative importance of different source areas to the reduction of Big Bend visibility.

The results are plotted in Figure 5 for six different two-month periods. The bars show the frequency distribution of the trajectory endpoint azimuths, and the lines show the average visual range associated with each flow direction. The frequency distributions do not appear to be significantly different than the distributions shown in Figure 4 for all trajectories. Trajectories with endpoints in the northwest and north sensors had the highest average visual ranges, and those with endpoints in the northeast, east, southeast, and south sectors had the lowest. The highest visual ranges (139km to 140km) were associated with north and northwest flow during January and February. The lowest visual ranges (66km to 69km) were associated with northeast and east flow in July and August.

Figure 5. Trajectory Frequency (bars) and Average Visual Range (circles) Versus Direction from Big Bend National Park from 1991-94

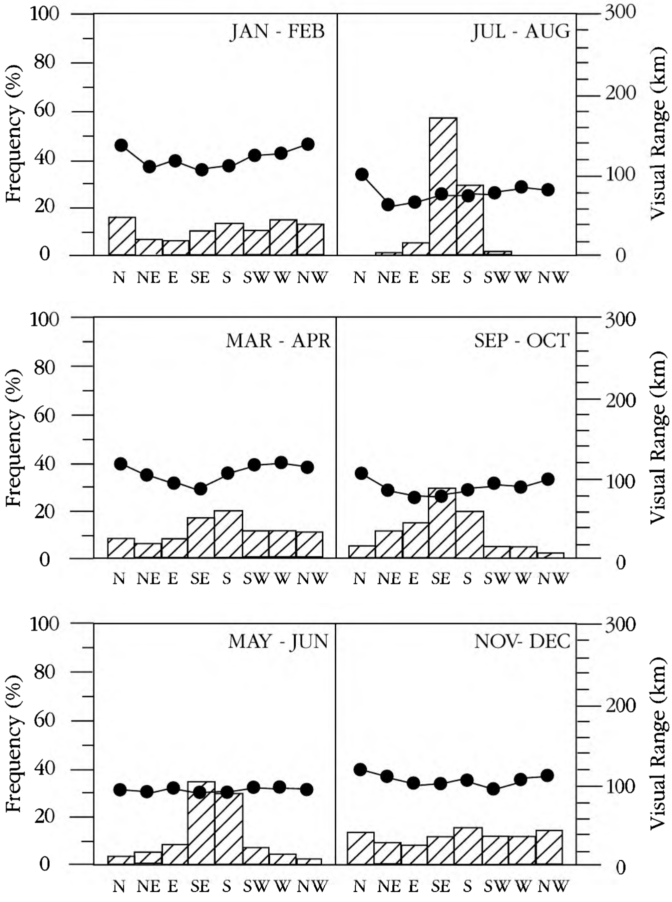

This analysis was repeated using only the highest and lowest 20% of the assigned visual ranges. The results are plotted in Figures 6 and 7 and show the same relationship between flow direction and park visibility. When only the highest visual ranges were considered, flow directions associated with higher visibility in the previous analysis increased in frequency, and flow directions associated with lower visibility decreased in frequency. The opposite occurred when only the lowest visual ranges were analyzed.

Figure 6. Trajectory Frequency (bars) and Average Visual Range (circles) Versus Direction from Big Bend National Park from 1991-94 Using Highest 20% of the Visual Ranges

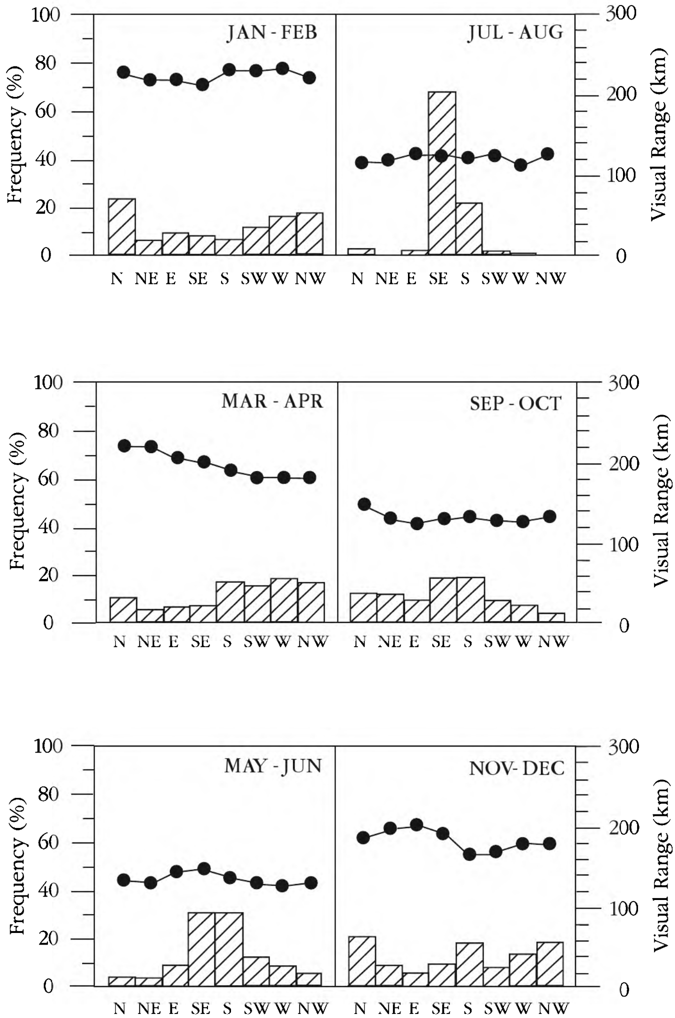

Figure 7. Trajectory Frequency (bars) and Average Visual Range (circles) Versus Direction from Big Bend National Park from 1991-94 Using Lowest 20% of the Visual Ranges

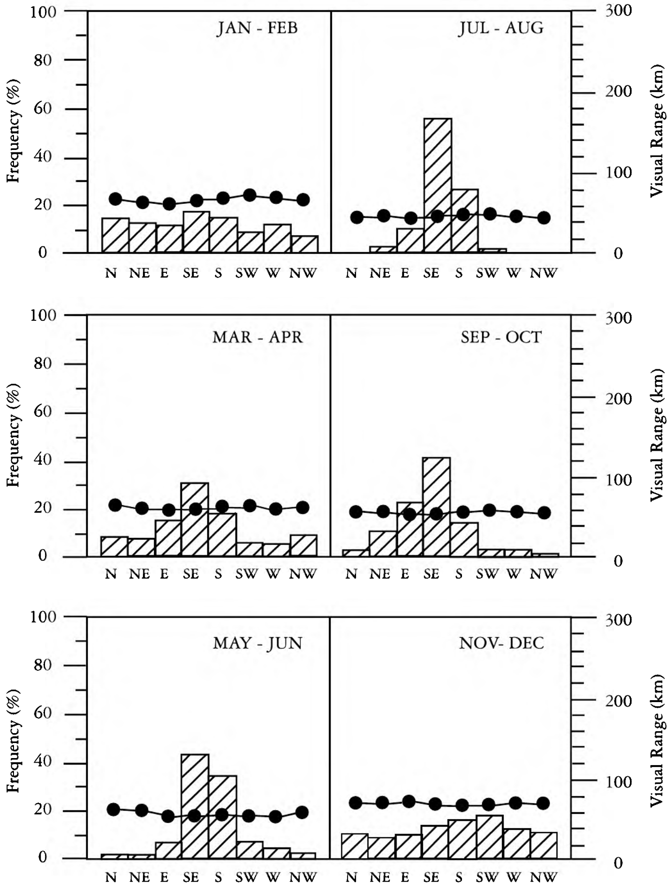

The Carbón I and II plants east of Eagle Pass, Texas, are often suspected to be the most significant sources of visibility-reducing contaminants in the Big Bend due to their proximity and emission volume. To investigate the relative importance of this and other areas to Big Bend air quality the above statistics were also computed for smaller areas defined by 16 compass points and 100km range increments. The results are shown in Tables 2 through 7 for six two-month periods.

The narrow distribution of the summer flow is revealed in Table 6. About one-half of the July and August trajectory endpoints were in the south-southeast sector, another quarter were in the southeast sector, 10% were in the south sector, and 8% were in the east-south-east sector. Less than 9% were in the others.

Table 2. Trajectory Frequency and Average Visual Range Versus Direction and Distance from Big Bend National Park from January and February, 1991–94

Trajectory Azimuth Frequency (%)

Direction	Range (km)						
	0-100	100-200	200-300	300-400	400-500	500-600	0-600
N	9.5	7.4	6.9	8.4	9.8	10.1	8.6
NNE	5.3	3.5	4.5	6.9	6.3	9.0	5.9
NE	4.3	3.4	3.5	4.2	3.9	2.4	3.6
ENE	4.0	3.0	3.0	3.4	3.7	2.3	3.2
E	3.5	3.6	4.1	4	3.7	2.4	3.6
ESE	3.7	3.3	4.4	6.1	3.2	4.1	4.2
SE	4.4	4.1	5.7	6.9	5.9	6.1	5.6
SSE	8.6	8.1	8.5	8.1	6.9	4.6	7.5
S	8.6	6.8	9.0	7.9	7.5	7.9	7.9
SSW	8.0	8.4	6.4	4.0	3.4	2.9	5.4
SW	5.8	6.6	6.6	4.9	4.7	4.2	5.5
WSW	7.8	8.4	7.1	6.3	7.7	5.1	7.1
W	6.9	7.5	6.5	7.1	10.0	10.2	8.0
WNW	5.9	7.9	7.4	7.5	9.8	13.2	8.6
NW	6.0	7.8	5.7	4.8	5.1	7.2	6.1
NNW	7.8	10.1	10.7	9.4	8.4	8.2	9.2

Visual Range (km)

Direction	Range (km)						
	0-100	100-200	200-300	300-400	400-500	500-600	0-600
N	152	143	137	144	138	152	144
NNE	121	108	119	106	134	121	119
NE	131	112	124	106	94	83	109
ENE	127	125	142	119	93	76	115
E	124	137	143	122	103	85	122
ESE	137	120	130	112	89	84	112
SE	133	115	116	108	99	95	109
SSE	124	111	108	101	101	98	107
S	114	116	112	109	123	103	113
SSW	117	116	123	119	119	117	119
SW	128	124	119	133	111	126	123
WSW	137	132	147	135	132	154	138
W	135	132	136	121	128	137	131
WNW	136	120	124	122	115	121	122
NW	159	143	135	150	148	143	145
NNW	140	142	142	145	142	148	143

Table 3. Trajectory Frequency and Average Visual Range Versus Direction and Distance from Big Bend National Park from March and April, 1991–94

Trajectory Azimuth Frequency (%)

Direction	Range (km)						
	0-100	100-200	200-300	300-400	400-500	500-600	0-600
N	5.1	6.1	3.7	3.9	4.2	5.3	4.7
NNE	4.6	4.0	2.3	2.6	4.0	3.6	3.5
NE	4.0	3.2	4	3.8	2.8	2.5	3.4
ENE	3.3	3.1	3.7	2.5	3	3.1	3.1
E	2.9	4.6	5.2	4.5	3.6	3.3	4.0
ESE	4.8	4.9	5.4	7.5	7.8	10.1	6.9
SE	6.1	6.7	7.7	10.2	9.8	10.9	8.7
SSE	8.7	10.2	11	12.8	10.4	9.5	10.5
S	11.9	11.3	13.2	10.6	9.1	9.2	10.9
SSW	10.4	8.3	6.8	7.6	6.7	6.7	7.6
SW	7.0	7.6	6.7	5.0	5.0	4.3	5.9
WSW	7.4	6.6	7.2	6.6	6.7	6.4	6.8
W	4.3	5.4	5	5.8	8.1	7.8	6.2
WNW	7.1	6.3	5.6	7.8	7.8	7.2	7.0
NW	6.5	6.1	6.5	4.8	5.9	5.2	5.8
NNW	5.8	5.7	6.0	4.0	5.1	4.8	5.2

Visual Range (km)

Direction	Range (km)						
	0-100	100-200	200-300	300-400	400-500	500-600	0-600
N	137	135	112	112	110	103	119
NNE	120	97	108	102	121	113	111
NE	107	102	99	119	89	85	101
ENE	114	116	120	114	78	81	104
E	102	102	112	90	85	77	96
ESE	107	107	125	88	75	78	92
SE	101	100	93	78	78	81	86
SSE	99	97	93	92	95	94	94
S	110	106	103	105	125	106	109
SSW	122	120	126	113	114	115	118
SW	118	119	118	113	114	114	116
WSW	116	120	109	114	115	117	115
W	142	136	126	120	114	118	124
WNW	132	119	121	118	119	124	122
NW	117	132	115	112	105	109	115
NNW	129	139	123	108	106	99	118

Table 4. Trajectory Frequency and Average Visual Range Versus Direction and Distance from Big Bend National Park from May and June, 1991–94

Trajectory Azimuth Frequency (%)

Direction	Range (km)						
	0-100	100-200	200-300	300-400	400-500	500-600	0-600
N	2.2	2.1	1.1	1.2	2.8	1.6	1.8
NNE	2.5	2.5	2.5	3.0	3.2	3.0	2.8
NE	2.7	2.4	2.4	3.3	3.0	3.0	2.8
ENE	3.1	3.6	4.3	3.5	2.6	2.1	3.2
E	4.7	4.8	3.3	4.0	3.4	4.7	4.1
ESE	6.0	4.9	5.7	8.0	10.9	7.6	7.3
SE	13.7	14.1	15.9	19.4	21.8	23.9	18.4
SSE	22.2	25.4	28.9	26.2	24.1	25.9	25.6
S	17.6	15.9	17	14.4	13.4	12.2	15
SSW	8.5	7.8	5.1	3.9	4.0	3.7	5.4
SW	4.9	4.9	3.9	3.8	2.3	2.9	3.7
WSW	3.0	3.9	3.4	3.5	1.8	1.8	2.9
W	2.8	2.2	1.5	1.3	2.1	2.3	2.0
WNW	2.0	2.4	1.7	2.1	1.6	1.6	1.9
NW	2.0	1.7	1.8	1.6	1.4	1.4	1.6
NNW	2.0	1.4	1.4	0.9	1.6	2.2	1.6

Visual Range (km)

Direction	Range (km)						
	0-100	100-200	200-300	300-400	400-500	500-600	0-600
N	91	95	87	88	93	95	92
NNE	94	86	88	89	93	96	91
NE	93	90	97	88	88	86	90
ENE	97	97	99	100	87	89	96
E	89	91	93	100	102	87	93
ESE	91	102	94	96	92	95	94
SE	94	89	92	92	89	88	90
SSE	90	89	88	92	90	91	90
S	88	85	88	91	90	87	88
SSW	87	96	95	97	94	86	92
SW	104	93	95	91	101	101	97
WSW	94	99	96	103	95	102	98
W	93	102	105	105	106	97	101
WNW	87	93	82	94	97	83	90
NW	93	97	94	96	102	105	98
NNW	89	92	96	82	94	94	92

Table 5. Trajectory Frequency and Average Visual Range Versus Direction and Distance from Big Bend National Park from July and August, 1991–94

Trajectory Azimuth Frequency (%)

Direction	Range (km)						
	0-100	100-200	200-300	300-400	400-500	500-600	0-600
N	0.8	0.9	0.2	0	0.1	0.7	0.4
NNE	0.8	0.5	0.2	0.4	0.3	0.1	0.4
NE	1.1	1.2	0.8	0.4	0.2	0.5	0.7
ENE	3.9	1.7	1.0	0.8	0.9	1.0	1.5
E	6.1	3.5	2.8	1.8	1.6	1.2	2.8
ESE	10.9	9.0	5.0	6.6	6.5	7.9	7.6
SE	22.6	24.8	25.5	27.2	29.0	28.1	26.2
SSE	35.8	41.6	49.2	52.3	51.3	51.6	47.0
S	12.5	11.6	11.6	8.8	8.7	7.1	10.1
SSW	2.6	2.1	1.2	0.6	0.1	0.6	1.2
SW	1.5	1.4	1.5	0.8	0.8	1.0	1.2
WSW	0.5	1.2	0.8	0.2	0.3	0.1	0.5
W	0.4	0.5	0.1	0.1	0	0	0.2
WNW	0.3	0	0	0	0	0	0
NW	0.3	0	0	0	0	0	0
NNW	0.1	0.1	0	0	0	0	0

Visual Range (km)

Direction	Range (km)						
	0-100	100-200	200-300	300-400	400-500	500-600	0-600
N	96	95	79	0	115	115	100
NNE	95	114	115	115	115	115	109
NE	71	67	71	70	63	59	68
ENE	73	67	55	44	39	41	60
E	75	74	65	53	57	51	67
ESE	82	78	64	65	65	59	70
SE	86	87	83	82	78	82	83
SSE	78	77	78	78	78	77	78
S	73	78	78	80	80	77	77
SSW	83	82	79	99	140	88	85
SW	91	97	85	78	65	71	83
WSW	99	81	66	74	83	102	80
W	85	73	102	102	0	0	83
WNW	86	0	0	0	0	0	86
NW	86	0	0	0	0	0	86
NNW	126	45	0	0	0	0	86

Table 6. Trajectory Frequency and Average Visual Range Versus Direction and Distance from Big Bend National Park from September and October, 1991-94

Trajectory Azimuth Frequency (%)

Direction	Range (km)						
	0-100	100-200	200-300	300-400	400-500	500-600	0-600
N	2.9	4.7	3.1	2.1	3.0	2.7	3.1
NNE	3.7	4.8	4.7	5.4	6.0	5.7	5.1
NE	6.8	5.7	5.2	5.4	8.4	7.1	6.4
ENE	6.3	6.8	6.3	5.9	8.4	7.0	6.8
E	7.4	8.0	6.3	8.7	8.2	8.0	7.8
ESE	7.3	6.8	9.2	10.5	9.9	13.0	9.4
SE	9.3	11.7	17.2	20.3	20.0	23.2	17.1
SSE	14.3	16.8	19.1	16.5	14.1	12.7	15.7
S	11.3	10.8	12.2	10.9	7.9	7.7	10.1
SSW	8.1	7.8	3.8	3.1	1.6	1.7	4.3
SW	4.7	3.5	2.6	2.1	2.8	2.2	2.9
WSW	4.9	3.9	2.7	2.6	3.1	2.9	3.3
W	5.0	2.7	2.1	2.7	2.9	2.4	2.9
WNW	2.8	1.8	1.1	0.8	2.1	2.3	1.8
NW	2.8	2.0	1.9	1.3	0.8	0.6	1.5
NNW	2.4	2.4	2.7	1.5	0.9	1.0	1.8

Visual Range (km)

Direction	Range (km)						
	0-100	100-200	200-300	300-400	400-500	500-600	0-600
N	79	94	114	129	119	109	106
NNE	86	95	107	100	103	111	101
NE	85	86	89	86	88	90	87
ENE	84	81	85	84	83	80	83
E	85	76	83	81	78	69	79
ESE	80	83	80	80	70	67	76
SE	80	84	81	82	77	80	80
SSE	87	87	87	82	83	84	85
S	87	87	86	86	88	91	87
SSW	93	91	86	83	93	101	91
SW	92	96	98	94	97	102	96
WSW	101	87	90	88	92	98	93
W	93	90	95	93	88	106	93
WNW	87	92	95	101	103	106	97
NW	91	104	98	104	131	107	102
NNW	93	102	102	119	122	104	104

Table 7. Trajectory Frequency and Average Visual Range Versus Direction and Distance from Big Bend National Park from November and December, 1991-94

Trajectory Azimuth Frequency (%)

Direction	Range (km)						
	0-100	100-200	200-300	300-400	400-500	500-600	0-600
N	6.2	6.6	6.4	7.1	5.7	6.6	6.5
NNE	5.4	5.8	6.1	6.8	8.0	9.1	6.9
NE	4.3	5.9	4.4	4.6	4.2	3.7	4.5
ENE	4.2	4.3	2.9	2.7	2.7	2.9	3.2
E	4.4	4.4	4.0	4.3	5.9	1.6	4.1
ESE	4.6	4.4	5.2	7.2	6.1	3.5	5.3
SE	6.1	4.9	5.4	6.6	6.6	7.2	6.1
SSE	8.7	8.8	11.5	6.5	5.2	5.5	7.7
S	12.1	9.9	9.2	7.2	7.5	6.5	8.6
SSW	7.7	7.7	6.4	6.0	5.1	5.3	6.3
SW	5.8	5.0	4.8	5.4	7.0	7.3	5.9
WSW	6.2	5.5	5.9	6.3	7.3	8.5	6.6
W	5.2	5.3	6.4	5.5	6.0	6.5	5.8
WNW	4.8	6.6	6.8	6.5	5.4	9.3	6.6
NW	6.2	5.9	6.2	9.2	8.2	8.5	7.5
NNW	8.1	8.9	8.2	8.1	9.2	8.1	8.5

Visual Range (km)

Direction	Range (km)						
	0-100	100-200	200-300	300-400	400-500	500-600	0-600
N	110	108	115	118	132	116	117
NNE	109	108	113	118	118	110	113
NE	98	110	112	116	120	97	110
ENE	104	112	108	112	105	118	110
E	127	94	95	112	96	107	103
ESE	96	97	102	98	101	96	99
SE	108	102	112	105	92	88	100
SSE	122	116	114	107	104	99	111
S	104	106	102	103	106	107	105
SSW	106	107	99	94	89	96	99
SW	102	95	95	91	93	80	92
WSW	100	119	112	103	101	95	104
W	113	104	115	105	109	104	108
WNW	103	112	111	105	112	99	107
NW	113	105	117	114	112	119	114
NNW	109	112	116	127	142	119	122

In summer, the lowest visual ranges were associated with the east-southeast sector, located between 500km and 600km from Big Bend. During the rest of the year, the lowest visibility was associated with areas that are between 500km and 600km northeast to southeast of the park. This corresponds to the part of Texas from the far south-east to Waco.

The Carbón I and II plants are in the east-southeast sector that is between 200km and 300km from the park. The average associated visibility for this sector was somewhat higher than the visual ranges associated with eastern Texas. Compared to the other 15 sectors in the 200km to 300km range, the average visual range for this area was the lowest in September and October and the second lowest in July and August. For the four other periods, its ranking ranged from 4th to 14th lowest.

Conclusions

Analysis of the spatial distribution from 1991 to 1994 back trajectories from Big Bend National Park showed significant seasonal differences in the airflow. More than 90% of the July and August trajectory positions were between east-southeast and south of the park. About one-half were to the south-southeast and another quarter were to the southeast. The flow directions were much more evenly distributed in January and February. Flow from between the west and the north was somewhat more common than the other directions, and flow from between the northeast and east-southeast was somewhat less common. The flow characteristics for other two-month periods were intermediate between these two regimes.

In general, visibility was best when the flow was from the north and northwest and poorest when it was from between northeast and south. When radial distances were considered, trajectory positions in the northeast, east-northeast, east, east-southeast, and southeast sectors between 500km and 600km from Big Bend were associated with the poorest visual ranges. This suggests that the worst Big Bend visibility is caused by pollutants emitted in Eastern Texas between Brownsville and Waco. These areas of Texas are heavily industrialized and emit a significant quantity of pollutants. This is also true for areas to the east and northeast of the 600km analysis area, and it is possible that contaminants emitted there may be transported into the Brownsville-to-Waco region on their way to the park.

ACKNOWLEDGEMENTS

The authors would like to acknowledge the significant contributions of Kristi Gebhart of the National Park Service who provided the ATAD trajectory model and James Sisler of the Cooperative Institute for Research at Colorado State University who provided the Big Bend transmissometer data.

REFERENCES

Green M. C. and K. A. Gebhart. 1997. "Clean Air Corridors: A Geographic and Meteorologic Characterization." *Journal of the Air & Waste Management Association* 47(3): 403–410.

Heffter J. L. 1980. *Air Resources Laboratories Atmospheric Transport and Dispersion Model* (ARL-ATAD). Technical Memorandum ERL ARL-81. Rockville, Maryland: National Oceanic and Atmospheric Association.

Pitchford M. and A. Pitchford. 1985. "Analysis of Regional Visibility in the Southwest Using Principal Component and Back Trajectory Techniques." *Atmospheric Environment* 19(8): 1301–1316.

Pitchford M. L. and W. C. Malm. 1994. "Development and Applications of a Standard Visual Index." *Atmospheric Environment* 28(5): 1049–1054.

Sisler J. F., D. Huffman, and D. A. Latimer. 1993. *Spatial And Temporal Patterns and the Chemical Composition of the Haze in the United States: An Analysis of Data from the IMPROVE Network,* 1988–91. Fort Collins, Colorado: Interagency Monitoring of Protected Visual Environments (IMPROVE).

White W. H., E. S. Macias, J. D. Kahl, P. J. Samson, J. V. Molenar, and W. C. Malm. 1994. "On the Potential of Regional-Scale Emissions Zoning as an Air Quality Management Tool for the Grand Canyon." *Atmospheric Environment* 28(5): 1035–1045.

V

Characterization and Dynamics of Air Pollutants in the Lower Rio Grande Valley

G. M. Mejia-Velázquez, S. Sheya, J. Dworzanski, M. Rodriguez-Gallegos, D. D. Tejeda-Honstein, J. M. Cardona-Carrizalez, and H. L. C. Meuzelaar

ABSTRACT

The Lower Rio Grande Valley (LRGV) has become a region of increasing interest because of its rapid economic development, increased international border crossing traffic, and extensive agricultural activities. Over the past few years, air pollution problems in the region have substantially increased. However, very few air quality studies have been performed in the area. This paper provides a characterization of air pollutant dynamics and a model in the LRGV, which include the comprehensive interactions of criteria pollutants, VOC's/SVOC's (volatile organic compounds/semi-volatile organic compounds) and fine particulate matter (PM_{fine}). The analysis involved researchers on both sides of the U.S.-Mexican border. A highly mobile monitoring station equipped with a broad array of physical and chemical samplers and sensors was used in December 1995 and March 1998. PM_{10}/ $PM_{2.5}$ and oxides of nitrogen (NO_x) (the latter only in the March 1998 study) concentrations were measured in Reynosa, Río Bravo, and Matamoros, Tamaulipas; Hidalgo,

Coahuila; Brownsville, Texas; and along the freeway between Brownsville and McAllen, Texas. The photochemical model predicted peak ozone concentrations that reached, and on some days exceeded, air quality standards. The concurrent $PM_{10}/PM_{2.5}$ study involved both physical (size distributed counting) and time-resolved (two-hour) organic chemical (VOC/SVOC-type PM_{fine} adsorbates) characterization methods. Recently completed multivariate data analysis results from a December 1995 study at one of the sites (Hidalgo International Bridge) are presented to illustrate the capabilities of the time-resolved PM_{fine} characterization approach. The results of this work show that the LRGV region does not yet appear to have grave air pollution problems, with the possible exception of transient episodes of extremely high PM concentrations. However, with the increase in cross-border traffic over the next few years, air quality is likely to deteriorate.

Dinámica y Caracterización de Contaminantes del Aire en el Valle Bajo del Río Grande

G. M. Mejia-Velázquez, S. Sheya, J. Dworzanski, M. Rodriguez-Gallegos, D. D. Tejeda-Honstein, J. M. Cardona-Carrizalez, y H. L. C. Meuzelaar

RESUMEN

El Valle Bajo del Río Grande (VBRG) se ha convertido en una región de interés creciente debido a su rápido desarrollo económico, el incremento del cruce fronterizo internacional, y sus actividades agriculturales extensivas. En el transcurso de los últimos años, los problemas de contaminación del aire se han incrementado substancialmente en la región. Sin embargo, muy pocos estudios de calidad del aire han sido realizados en el área. Este capítulo proporciona una caracterización de la dinámica de contaminantes del aire y un modelo en el VBRG, el cuál incluye interacciones comprensibles de contaminantes criterio, COV/COSV (compuestos orgánicos volátiles/compuestos orgánicos semi-volátiles) y partículas finas de materia (PM_{fina}). En el análisis participaron investigadores de ambos lados de la frontera E.U.-México. Una estación de monitoreo de alta movilidad equipada con una amplia gama de muestreadores físicos y químicos y sensores fue usada en diciembre de 1995 y marzo de 1998. Concentraciones de $PM_{10}/PM_{2.5}$ y óxidos de nitrógeno (NO_x) (el último solo para el estudio de 1998) fueron medidas en Reynosa, Río Bravo, y Matamoros, Tamaulipas; Hidalgo, Coahuila; Brownsville, Texas; y a lo largo de la autopista entre Brownsville y McAllen, Texas. El modelo fotoquímico predijo concentraciones máximas de ozono que alcanzaron, y en algunos días excedieron, estándares de calidad del aire. El estudio simultáneo de $PM_{10}/PM_{2.5}$ involucró ambos tipos de caracterización, el físico (conteo por distribución de tamaño) y químico orgánico de solución por tiempo (dos-horas) (PM_{fina} absorbida de tipo COV/COSV). Los análisis multivariados de los datos completados recientemente de un estudio para diciembre de 1995 en uno de los sitios (Puente Internacional Hidalgo), son presentados para ilustrar las capacidades de la solución en tiempo para el enfoque PM_{fina}. Los resultados de este trabajo muestran que la región VBRG aún no parece tener problemas graves de contaminación del aire, con la excepción posible de episodios transitorios con concentraciones de PM sumamente altas. Sin embargo, con el aumento en el tránsito fronterizo durante los próximos años, la calidad del aire probablemente vaya a deteriorarse.

INTRODUCTION

Air quality throughout the Lower Rio Grande Valley (LRGV) is being threatened by rapid urbanization, extensive industrial and agricultural development, and significant increases in vehicular cross-border traffic (Gilbreath 1992). Yet, until recently, relatively few air quality studies of the LRGV area have been published, and emission inventory data for the LRGV area are far from complete. In 1997, results of the multi-media Lower Rio Grande Valley

Environmental Scoping Study (LRGVESS) (Mukerjee 1997) began providing systematic data on air pollution sources, transboundary transport mechanisms, and exposure risks. Also, preliminary emission inventory data reported by Mejia and Rodriguez (1997) enabled the Instituto Tecnológico y de Estudios de Superiores de Monterrey (ITESM) team to perform a first assessment of photochemical pollution mechanisms (Mejia and Meuzelaar 1997).

In 1995, the University of Utah and ITESM started a collaborative effort, sponsored by the Southwest Center for Environmental Research and Policy (SCERP), aimed at physical, chemical, and biological characterization of fine particulate matter (PM_{fine} also known as $PM_{2.5}$) in the LRGV (Mejia and Meuzelaar 1997). In December 1995, 48- to 72-hour-long scoping studies were carried out at four selected sites (Hidalgo International Bridge, Santa Ana Wildlife Refuge, Brownsville International Bridge, and Matamoros Industrial Park). Typically, PM_{fine} levels and size distributions were measured around-the-clock and microgram-sized samples were collected on quartz fiber filters at two-hour intervals for subsequent laboratory analysis by means of specialized GC/MS techniques. Simultaneously, PM_{fine} samples were taken for microbiological analysis, meteorological parameters were recorded, and a limited number of VOC samples were collected and analyzed on site using the University of Utah's mobile analytical laboratory with field-portable GC/MS equipment.

Although detailed multivariate analysis of the extensive data sets obtained continued into 1998, preliminary evaluation of the voluminous data revealed modest overall PM_{fine}- and VOC-type air pollutant levels when compared with earlier field tests in Nogales, Arizona (Dworzanski et al. 1993), with the exception of one severe nocturnal PM_{fine} episode at the Hidalgo site and unexpectedly high levels of airborne fecal bacteria at the Brownsville site. The application of a diagnostic meteorological model for the LRGV at the Hidalgo site provided plausible explanations for the observed severe PM_{fine} episode, which apparently followed the passage of a cold front accompanied by low inversion layer and urban dust trapped above Reynosa slow drifting into the Hidalgo International Bridge area. The specific origin of the high levels of airborne fecal bacteria at the Brownsville International Bridge is still unknown, but they probably originate from the Rio Grande.

Based on the preliminary VOC and PM_{fine} findings of the scoping studies, a follow-up field study was performed that focused on detailed physical (including size distribution) and organic chemical characterization of PM_{fine} at selected receptor sites on both sides of the border. In addition, an attempt was made to model simultaneously and monitor criteria pollutants such as NO_x, ozone (O_3), and sulfur dioxide (SO_2) in order to understand the origin and dynamics of both primary and secondary PM_{fine} in the LRGV section of the U.S.-Mexican border. Consequently, in March 1998, a second five-day field study was undertaken on both sides of the U.S.-Mexican border between the twin cities of Brownsville-Matamoros and McAllen-Reynosa. During this study, PM_{10}, $PM_{2.5}$, and NO_x concentrations were measured in Reynosa, Río Bravo, and Matamoros, Tamaulipas; Hidalgo, Coahuila; Brownsville, Texas; and along the freeway between Brownsville and McAllen, Texas. A diagnostic meteorological model was applied to the region to simulate wind patterns during the sampling period.

This work consisted of two parts: (1) development of a comprehensive criteria pollutant model for selected LRGV areas involving the integrated use of emission, dispersion, and photochemical submodels that attempted validation by field monitoring data obtained in March 1998, and (2) development of a novel time-resolved $PM_{10}/PM_{2.5}$ characterization approach. This approach combined fast, sensitive physical and chemical receptor monitoring techniques. The work used principal component analysis techniques to detect and identify the dominant emission sources for the selected sites and time windows. It focused on the Hidalgo International Bridge data obtained in December 1995.

METHODOLOGY

Data Collection

On-site monitoring and sample collection were performed with the University of Utah's mobile laboratory, which is equipped with a Medium Vol (50 l/s) PM_{10} sampling tower with a QFF (quartz fiber filter) sample collector, a 400 Ah battery bank with 2000 W battery charger/inverter, a four kW propane-driven generator, a Peltier-cooled refrigerator for sample storage, and a broad range of air pollutant measurement and sampling devices as described below.

Physical measurements included particle size distribution determinations obtained from a six-channel CLIMET aerosol counter, and meteorological measurements (temperature, pressure, humidity, wind speed, and direction) using a Davis model III weather station. Planned on-site chemical analyses involved NO_x and O_3 measurements, as well as VOC/SVOC speciation using a novel GC/MS technique with miniaturized, fast GC and Curie-point desorption modules. Off-site chemical analyses of QFFs obtained at two-hour intervals were performed at the University of Utah Center for Micro Analysis with a standard HP GC/MSD equipped with a special Curie-point desorption/pyrolysis inlet. Detailed descriptions of these techniques have been given elsewhere (Mejia and Meuzelaar 1997; Dworzanski et al. 1993). Multivariate analysis of physical and chemical measurement data involved the use of principal component analysis (PCA) techniques in combination with graphical rotation methods (Dworzanski et al. 1993).

Several problems were encountered during the 72-hour measurement period (March 11–14, 1998), namely: (1) frequent rain showers that reduced pollutant levels and necessitated longer collection periods while turning monitoring sites into mud pools; (2) electrical failure of the ozone analyzer; and (3) intermittent leaks in the VOC/SVOC desorption inlet. As a result, the number of monitoring sites, originally anticipated to be as high as 20, had to be reduced to six.

Modeling of Photochemical Pollutants

Modeling techniques used by the ITESM group included the application of a diagnostic meteorological model, the use of GIS to generate an emission database, and the application of a photochemical model. The meteorological model was used to reconstruct wind fields in the LRGV during the periods studied. Data from United States and Mexican monitoring stations and airports in the region were used as input to the model. The GIS was used to create a database of meteorological, emission, and predicted concentration. The database made it easier to create input data files for the photochemical model and to display wind, emission, and concentration data in a map of the LRGV for better understanding of the results.

The CIT Photochemical Model (McRae, et al. 1982) was applied to study the dynamics of pollutants in the region. Input data files included emissions, wind fields, incoming solar and UV radiation, and land use. Outputs of the model are maps of pollutant concentrations in the region and time series for different pollutants. In this paper, the predicted SO_2 and O_3 concentrations when a cold front passed through the region on December 6, 1995, are discussed. Predicted NOx concentrations are compared with data collected during the monitoring study in March 1998.

Emissions in Mexico were estimated using the Mobile5 Juárez model developed for Ciudad Juárez by the United States Environmental Protection Agency (U.S. EPA) (Tejeda and Mejia 1998; Kishan et al. 1996). Other emissions in the area were estimated in a previous study based on fuel consumption and emission factors (Mejia and Rodriguez 1997). Stationary source emissions in Texas were obtained from the Texas Commission on Environmental Quality (TCEQ). Mobile source emissions were not available but were estimated using a regression analysis of population and emissions of other counties in Texas made in a previous study of the border area (Mendoza 1996). Wind fields were reconstructed with a diagnostic meteorology model developed to interact with the CIT model. Data obtained with the monitoring station and from the airports were used for this purpose. Land use data of the LRGV were obtained from Instituto Nacional de Estadística, Geográfica, e Informática (INEGI) and from the United States Geological Survey in digitized form. Solar radiation measurements were not available and, therefore, data were estimated from the geographical coordinates and calculated incoming solar radiation (Seinfeld 1986).

Results

Wind Patterns in the LRGV

Transport of air pollutants in the LRGV is dominated by air flowing in from the Gulf of Mexico (from east to west), although at night, quiet periods are common and sometimes the wind blows from the land to the sea ("land breeze"). In winter, cold fronts coming from the north transport pollutants from west to east at ground level, while the warm air from the Gulf of Mexico flows in the opposite direction in the upper part of the atmosphere. This effect may cause periods with high concentrations of particles and other air pollutants in some areas of the LRGV, especially when occurring in combination with low mixing heights.

Meteorology data from the Matamoros and Reynosa airports and United States monitoring stations in the LRGV were used in the meteorology model to estimate wind field vectors in the region for December 1995 and March 1998. The data analyzed showed dominant winds coming from the Gulf of Mexico, the east, and the southeast for the two periods. In particular, on December 6, 1995, a cold front coming from the northwest collided with the warm air coming from the southeast. The leading edge of the cold front slid below the warm front but over the lowest elevations, trapping urban dust (mostly from unpaved roads) under a low inversion ceiling and also causing precipitation of air pollutants emitted upwind in the warm air. This explained the high levels of PM_{10} measured in Hidalgo at the same time and day during the 1998 monitoring trip, as discussed in the following sections.

PM_{10} Physical Size Distribution

Table 1 shows the average particle size distribution for the different sites and monitoring periods covered during the field trip in March 1998. The data from five of the six channels of the CLIMET are shown in the first column, and covered the range from 0.3 microns to 10 microns. Three of these ranges covered $PM_{2.5}$. The sixth channel covered the number of particles larger than 10 microns, but it is not shown in this table. The average number of particles per every $2ft^3$ sampled are shown in the second column, N(dp). The flow rate of the CLIMET was $1ft^3/min$. The volume of particles in each range (Vi) was calculated assuming that particles were spherical (Seinfeld 1986). The total volume (Vt) is the sum of the Vi, hence, Vi/Vt represents the volume fraction of each range of particles.

Table 1. Average Particle Size Distribution at the Monitoring Sites in the Lower Rio Grande Valley

Hidalgo, Texas. March 11, 1998. Sampling period: 10:30 to 18:30 hrs.				
dp (microns)	N (dp)	Vi (thousand of microns^{2})	Vi/Vt	ΣVi/Vt
0.3-0.5	801026	26.84	0.0482	0.0482
0.5-1.0	124480	27.5	0.0494	0.1550
1.0-2.5	20935	58.75	0.1056	0.2033
2.5-5.0	7061	194.95	0.3504	0.5536
5.0-10.0	1124	248.35	0.4464	1.0000
Total	954626	556.39	1.0000	
Matamoros, Tamps. March 12, 1998. Sampling period: 0:00 to 4:30 hrs.				
dp (microns)	N (dp)	Vi (thousand of microns^{2})	Vi/Vt	ΣVi/Vt
0.3-0.5	889181	29.8	0.0374	0.0374
0.5-1.0	130958	28.93	0.0363	0.0738
1.0-2.5	28517	80.02	0.1005	0.1743
2.5-5.0	13737	379.31	0.4766	0.6509
5.0-10.0	1258	277.88	0.3491	1.0000
Total	1063652	795.94	1.0000	
Reynosa, Tamps. March 13, 1998. Sampling period: 0:00 to 2:00 hrs.				
dp (microns)	N (dp)	Vi (thousand of microns^{2})	Vi/Vt	ΣVi/Vt
0.3-0.5	1377389	46.16	0.0233	0.0233
0.5-1.0	469544	103.72	0.0523	0.0756
1.0-2.5	62086	174.22	0.0879	0.1635
2.5-5.0	36804	1016.22	0.5126	0.6761
5.0-10.0	2908	642.25	0.3239	1.0000
Total	1948730	1982.57	1.0000	
Reynosa, Tamps. March 13, 1998. Sampling period: 6:00 to 12:00 hrs.				
dp (microns)	N (dp)	Vi (thousand of microns^{2})	Vi/Vt	ΣVi/Vt
0.3-0.5	653962	21.91	0.3075	0.3075
0.5-1.0	47599	10.51	0.1475	0.4550
1.0-2.5	2420	6.79	0.0953	0.5503
2.5-5.0	520	14.35	0.2013	0.7516
5.0-10.0	80	17.7	0.2484	1.0000
Total	704580	71.27	1.0000	
Río Bravo, Tamps. March 13, 1998. Sampling period: 16:00 to 18:30 hrs.				
dp (microns)	N (dp)	Vi (thousand of microns^{2})	Vi/Vt	ΣVi/Vt
0.3-0.5	1538943	51.57	0.0722	0.0722
0.5-1.0	629158	138.98	0.1946	0.2668
1.0-2.5	37294	104.65	0.1465	0.4133
2.5-5.0	5736	158.38	0.2217	0.635
5.0-10.0	1180	260.71	0.365	1.0000
Total	2212311	714.29	1.0000	
Brownsville, Texas. March 14, 1998. Sampling period: 9:00 to 13:00 hrs.				
dp (microns)	N (dp)	Vi (thousand of microns^{2})	Vi/Vt	ΣVi/Vt
0.3-0.5	1026347	34.39	0.0175	0.0175
0.5-1.0	225479	49.81	0.0253	0.0428
1.0-2.5	81753	229.41	0.1165	0.1593
2.5-5.0	30711	847.97	0.4306	0.5899
5.0-10.0	3655	807.47	0.4101	1.0000
Total	1367945	1969.05	1.0000	
Hidalgo, Texas. March 14, 1998. Sampling period: 15:00 to 17:00 hrs.				
dp (microns)	N (dp)	Vi (thousand of microns^{2})	Vi/Vt	ΣVi/Vt
0.3-0.5	1236071	41.42	0.0229	0.0229
0.5-1.0	229274	50.65	0.0281	0.0510
1.0-2.5	72259	202.77	0.1123	0.1634
2.5-5.0	32180	888.55	0.4923	0.6557
5.0-10.0	2813	621.47	0.3443	1.0000
Total	1572598	1804.87	1.0000	

In general, Table 1 shows that although small particles are large in number, big particles are more important in volume and, consequently, in mass. On the other hand, $PM_{2.5}$ represents the fraction of PM_{10} most hazardous to health. During the monitoring trip, $PM_{2.5}$ were found to represent approximately 16% to 20% of PM_{10} in Hidalgo and Brownsville. Similar values were found in Matamoros. In the case of Reynosa and Río Bravo, $PM_{2.5}$ was found to account for 55% and 41.3% of PM_{10}, respectively. These values were found during monitoring periods that corresponded to high traffic at the sites—0600–1200 in Reynosa and 1600–1830 hours in Río Bravo. These two cities are located downwind, have many unpaved streets, and receive most of the pollutants emitted from the highway between Matamoros and Reynosa. In Reynosa, during a monitoring period from 0000 to 0200 it was found that $PM_{2.5}$ accounted for 16.3% of PM_{10}. This value was obtained at night after a rainy period and at a monitoring site with very low traffic. From these results, $PM_{2.5}$ was observed to be an important fraction of PM_{10} in locations downwind of the LRGV. However, to obtain more reliable results and conclusions, more data collected during different seasons of the year are necessary, as are measurements of mass concentration of PM_{10} to obtain concentrations of $PM_{2.5}$, which can then be used to evaluate the population's health exposure to particles.

Multivariate Data Analysis and Integration

Preliminary findings from the 1998 field tests showed:

- PM_{10}/ $PM_{2.5}$ and VOC levels well below the maximum levels allowed by all applicable United States and Mexican air quality standards at all monitoring sites
- Repeated NO_x levels in excess of 100ppb at the Hidalgo International Bridge and along the freeway near the city of Harlingen, Texas

Organic PM_{fine} characterization data are still being integrated and processed. However, multivariate analysis of the 1995 scoping study data for the Brownsville and Hidalgo International Bridge sites has been completed and some results for the latter site, also included in our 1998 field study, are discussed.

Table 2 shows the variables included in the final principal component analysis of the Hidalgo PM_{fine} scoping study involving 24 samples obtained at two-hour intervals. Note that this includes organic chemical compounds and meteorological parameters, as well as PM_{10} and $PM_{2.5}$ density estimates. After varimax rotation, only five principal components were needed to explain nearly 80% of the total variance in the data set. The loadings for these five (varimax-rotated) factors are listed in Table 2 and reveal a relatively well-behaved clustering of the variables along the different principal component axes. Fortunately, a reasonable chemical and physical interpretation of the first four factors appears to be relatively straightforward and is in agreement with the dominant trends observed by Mukerjee et al. in their varimax-rotated principal component analysis of inorganic PM_{Fine} characterization data for the LRGV region (1999).

Figure 1 shows the power of the time-resolved PM_{fine} analysis approach in that it provides the opportunity to help tie observed receptor sample patterns to possible emission sources on the basis of known circadian human activity cycles and events (e.g. traffic peaks, waste burning) or observed meteorological patterns and events. (Note characteristic morning and afternoon rush hour peaks "in automotive emissions" component and major "urban dust" event in the late evening of the second day.)

Table 2. Factor Loadings After Varimax Rotation in Hidalgo, 1995 Study

Parameters	Factor 1	Factor 2	Factor 3	Factor 4	Factor 5
4-hour daytime intercal	-0.376	-0.055	0.217	-0.320	0.216
Ambient temperature	-0.099	**-0.942**	0.045	0.100	-0.136
Ambient pressure	0.209	0.205	-0.071	0.218	-0.121
Wind speed	0.371	0.030	-0.131	0.107	**-0.710**
N/S wind vector	-0.362	-0.177	-0.083	-0.066	0.050
E/W wind vector	-0.081	-0.193	-0.081	0.168	<u>**-0.910**</u>
PM10 concentration	-0.299	0.102	0.125	<u>**-0.949**</u>	0.087
PM2.5 concentration	-0.210	0.121	0.118	<u>**-0.955**</u>	0.061
D PM (PM10-PM2.5)	-0.397	-0.130	0.178	-0.672	0.361
m/z 83-85 alkanes/alkenes (f)	-0.500	-0.011	-0.017	<u>**-0.846**</u>	-0.009
m/z 99 tributylphosphate (f)	-0.196	<u>**-0.910**</u>	0.088	-0.039	0.084
m/z 129 quinoline	-0.165	0.073	-0.348	0.065	**0.731**
m/z 149 DEP (f)	0.163	0.092	<u>**-0.945**</u>	0.092	0.121
m/z 149 DBP (f)	0.027	<u>**-0.920**</u>	-0.071	0.161	-0.194
m/z 149 DPP (f)	-0.075	<u>**-0.964**</u>	0.124	0.108	0.007
m/z 149 DOP (f)	0.013	-0.145	0.058	0.069	-0.087
m/z 151 4-acetyl-2-methoxyphenol (f)	-0.099	<u>**-0.930**</u>	0.124	0.088	0.009
m/z 153 4-acetyl-2,5-dimethoxyphenol (f)	0.338	0.205	-0.542	0.332	-0.179
m/z 165 4-vinyl-2,6-dimethoxyphenol (f)	0.145	0.088	<u>**-0.922**</u>	0.188	-0.204
m/z 191 17a(H),21b(H)-hopanes (f)	<u>**-0.917**</u>	-0.136	0.085	-0.243	-0.009
m/z 191a hopane [C29H50] (f)	<u>**-0.916**</u>	-0.037	0.073	-0.335	-0.005
m/z 191b hopane [C30H52] (f)	<u>**-0.892**</u>	-0.216	0.092	-0.159	-0.013
m/z 202 PNAHs [C16H10]	<u>**-0.930**</u>	-0.053	0.150	-0.210	0.114
m/z 202a fluoranthene	**0.830**	-0.018	0.046	-0.456	0.145
m/z 202b pyrene	**-0.931**	-0.076	0.218	0.001	0.080
m/z 219 retene (f)	0.131	0.060	<u>**-0.957**</u>	0.083	0.079
m/z 239 methyl dehydroabietate (f)	-0.092	0.139	0.112	<u>**-0.972**</u>	0.036
m/z 306 tetraphenylene	-0.128	0.136	0.088	<u>**-0.975**</u>	-0.012

(f) fragment ion, DEP = diethyl phthalate, DBP = dibutyl phthalate, DPP = dipentyl phthalate, DOP = dioetyl phthalate. Bolded figures are those above 0.6, underlined figures are above 0.8.

Figure 1. Standardized Principal Component Scores (varimax-rotated) Corresponding to the Loadings of Ambient Temperature, Pressure, Wind Speed and Direction over Two Days

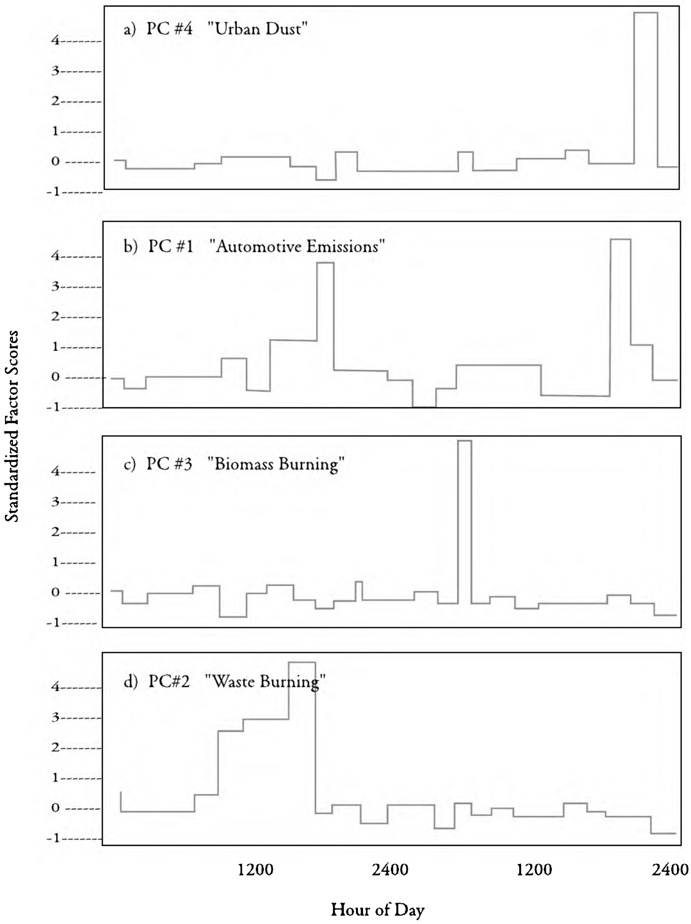

The factor scores in the abscissa of Figure 1 are standardized, thereby permitting a rough estimate of the statistical significance of the various events. Assuming multivariate normal distributions, both the (inferred) "urban dust" event in Figure 1a, which followed the arrival of the cold front on day two, and the "biomass burning" (primarily hardwood-markers dominated) event in Figure 1c can be classified as being well in the four-sigma range. The high amplitude of both events may create the mistaken impression that the corresponding chemical markers were only detected during these events. In fact, even when leaving out these extreme episodes, the nature of the underlying parameter associations does not change much at all. In addition, the first principal component ("automotive emissions," Figure 1b) shows regular, traffic-peak-related fluctuations dominated by the afternoon rush hours when most of the traffic was passing on the same (downwind) side of the bridge on which the mobile lab was stationed. The proposed "urban dust" factor is speculative at this point since the peaks at m/z 239 (abietic acid, aprominent filler in car tires) and at m/z 306 (tetraphenylene, perhaps an oily-road tire stabilizer) have not yet been positively identified in local source profiles and the "waste burning" events are inferred from the prominent contributions of alkylphthalate-type plasticizers. However, the "automotive emissions" and "biomass burning" events are firmly rooted in the pioneering GC/MS studies of well defined source samples described by Rogge et al. (1991). Also, the inferred, broad "waste burning" event in Figure 1d was primarily characterized by the presence of several different types of plasticizers, plus a fire retardant. Finally, the very similar "urban dust," "automotive emissions," "biomass burning," and "waste burning" factor loading and score behavior was observed in the Brownsville International Bridge site data obtained during the same 1995 scoping study, as well as in two earlier December time window studies at the U.S.-Mexican border (Nogales, Arizona in 1991 and Mexicali, California in 1993). This suggests a marked degree of similarity in major PM_{Fine} sources along the border and further supporting the chemical and physical significance of the numerically extracted principal component patterns.

Sulfur Dioxide and Ozone Dynamics

Emission sources in the LRGV include mobile sources in Mexico and the United States, small stationary sources in Cameron and Hidalgo counties in the United States, a Pemex refinery in Reynosa, and a power plant in Río Bravo. Several uncertainties exist in the estimated emissions used to create the data files for the CIT photochemical model. These uncertainties include aspects such as a lack of data to estimate mobile source emissions from both the United States and Mexico. Furthermore, an official emission inventory of stationary sources in Mexico is not yet available; biogenic emissions from vegetation are not known and were estimated from land use; distribution of mobile emissions in highways is not well known; emissions from diesel trucks were estimated; and diurnal variations in emissions of mobile sources were not considered. These uncertainties represent research areas from which results are needed to improve the data necessary to obtain more reliable results. Nevertheless, the results represent general trends of transport of air pollutants and potential areas affected by high levels of pollution.

The region of study, the domain, and computational mesh covered with the photochemical model covered a surface of 180km X 180km, with cells of 5km X 5km (i.e., 1,296 cells). Five layers were defined in the vertical dimension, which makes a total of 6,480 cells. A GIS database was loaded with the necessary emission and land use data files to create the input files to run the CIT Photochemical Model. The files were created using a procedure developed within the GIS for automatic transfer data to each cell. This procedure was generated with a computer, minimizing processing time and numerical errors when data were assigned to each cell.

The results of the model give average hourly concentration data for the different pollutants in each cell in the three spatial dimensions. Understanding results given as lists of numbers is very difficult and usually visualization techniques are used to facilitate this procedure. In this paper, the predicted SO_2 and O_3 concentrations in the different monitoring sites during December 6, 1995, are analyzed. Figure 2 shows plots of SO_2 concentrations for seven sites in the domain: Reynosa (REY), McAllen (MCA), Hidalgo Bridge (PHO), Santa Ana Park (ANA), Matamoros (MAT), Brownsville (BRW), and Brownsville Bridge (PBO).

Figure 2. SO_2 Concentrations Predicted by the Photochemical Model on December 6, 1995, for Seven Sites in the Domain

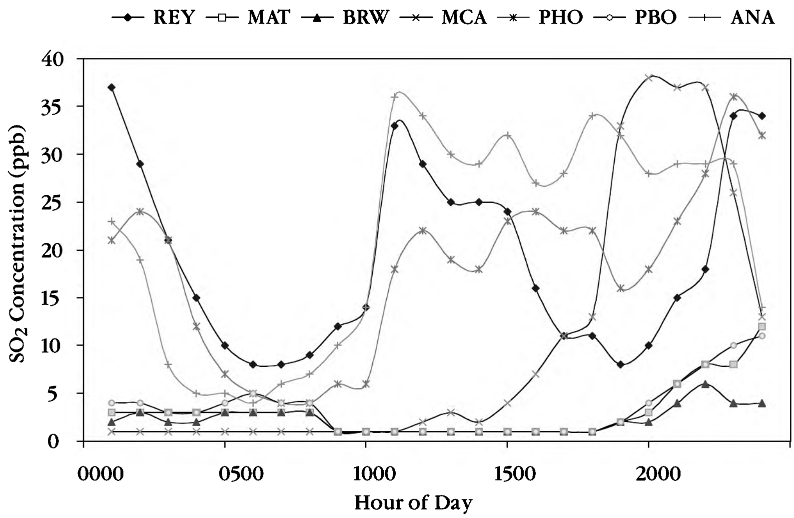

The data displayed in this figure show higher concentrations of SO_2 in the area of Reynosa-McAllen. This is expected since air is blowing from the sea and SO_2 emissions of the Emilio Portes-Gil power plant and the Pemex refinery in Reynosa are transported west of the source. The figure also shows the effect of dispersion predicting different concentrations in REY, MCA, PHO, and ANA, which are located downwind. It is important to note that the higher concentrations predicted by the model are close to 40ppb, which is well below the Mexican air quality standard for SO_2 of 130ppb. The effect of the cold front passing that day is reflected in Figure 2. The model also predicts low concentrations of SO_2 in the area of Matamoros-Brownsville. This, too, is expected since air is blowing from east to west and emission sources are located west of these cities. When the cold front arrived in the region, the wind changed direction and the air blew from west to east, bring SO_2 emissions to the area of Matamoros-Brownsville and thus decreasing SO_2 concentrations in the area of Reynosa-McAllen. As mentioned above, if sulfur content in fuel is lower than the values assumed, lower SO_2 concentrations are expected in the area. Fluctuations in SO_2 concentrations are most often caused by changes in atmospheric stability during the day and the night. During the day, dispersion increases in the atmosphere and SO_2 concentration increases at ground level in McAllen, Reynosa, and Río Bravo. At night the atmosphere becomes stable and, in the same locations, the ground level concentrations decrease.

Emissions of mobile and industry sources have a significant direct impact on carbon monoxide (CO), hydrocarbon (HC), and NO_X concentrations, which indirectly react to produce O_3. Concentrations of this pollutant for the same seven sites are shown in Figure 3.

Figure 3. Ozone Concentrations Predicted by the Photochemical Model on December 6, 1995, for Seven Sites in the Domain

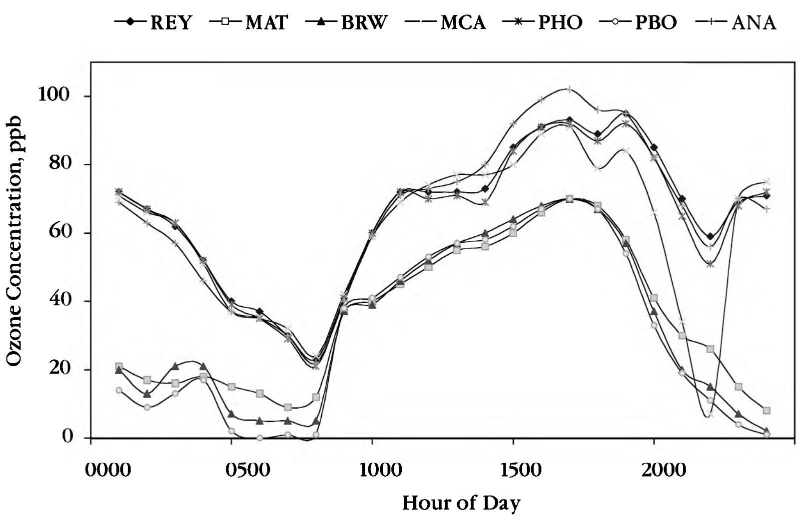

This figure shows the same levels of predicted ozone concentrations in nearby sites. This is due to mobile source pollutants emitted mainly in the cities and highways along the domain. Higher concentrations of O_3 in sites located downwind in McAllen-Reynosa, as is the case for SO_2 concentrations, were found. As expected, the figure shows the cycle in ozone formation during the day. Ozone is formed by photolysis of nitrogen dioxide (NO_2) and, consequently, its concentration increases during the morning, peaks early in the afternoon, and decreases at night. High levels of ozone may be encountered at night if it is not dispersed in the atmosphere or if it is not consumed by nitric oxide (NO) when the concentration or emission of this pollutant are low at night. The model predicts peak ozone concentration of approximately 90ppb to 100ppb, which is close to the Mexican and United States air quality standards for ozone of 110ppb and 120ppb respectively.

One of the pollutants of higher concern in the LRGV is SO_2. With the application of the photochemical model, it is possible to study the daily variations and impacted areas of the different pollutants. Maps of predicted concentrations of SO_2 are shown in Figures 4 through 7 for the study of December 6, 1995. These figures show the daily variations in concentrations and expected areas impacted by emissions of this pollutant. Figure 4 shows a map of SO_2 concentrations at 0300.

Figure 4. Map of SO_2 Concentrations in the LRGV at 0300, December 6, 1995

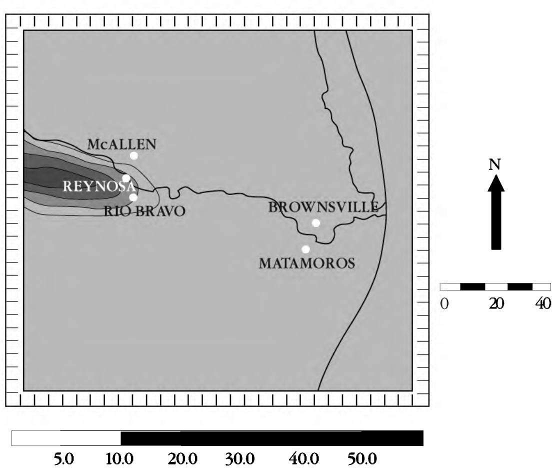

Although several sources of this pollutant exist in the area (Mejia and Rodriguez 1997) and were considered in the application of the model, this figure shows that the impact on air quality results mostly from the power plant located in Río Bravo. This plant's emissions were calculated assuming that fuel oil with 3.5% of sulfur and natural gas with 0.5% of sulfur were consumed. Today, this plant has been using fuel oil and natural gas with lower sulfur content. Therefore, SO_2 emissions are expected to be lower than those used in the model. Nevertheless, even with high SO_2 emissions, values of concentrations of this pollutant are below 40ppb west of the urban areas of Reynosa and McAllen, and this value is well below the Mexican air quality standard of 130ppb for 24-hour average. At 0900 hours, the conditions of the atmosphere become unstable, and the mixing is favored by buoyancy forces. At this hour, Figure 5 shows that concentrations close to Reynosa increase to values between 50ppb and 60ppb, which are still below the air quality standard.

Figure 5. Map of SO_2 Concentrations in the LRGV at 0900, Hours, December 6, 1995

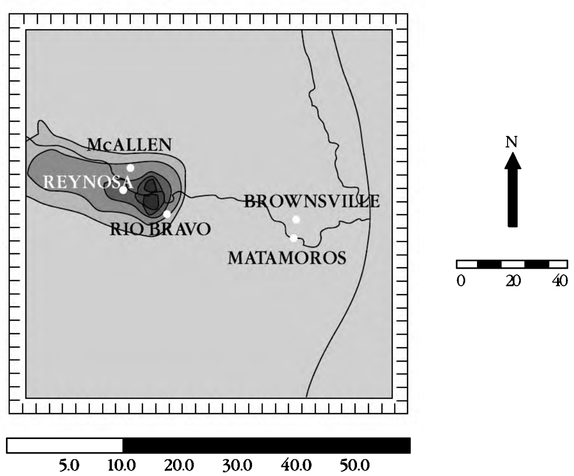

With higher temperatures, the land reaches its peak temperature during the day, and, for example, at 1500 hours the atmosphere becomes unstable and the higher values of SO_2 concentration are located between Río Bravo and Reynosa. However, the values are only in the range of 40ppb to 60ppb as shown in Figure 6.

Figure 6. Map of SO_2 Concentrations in the LRGV at 1500 Hours, December 6, 1995

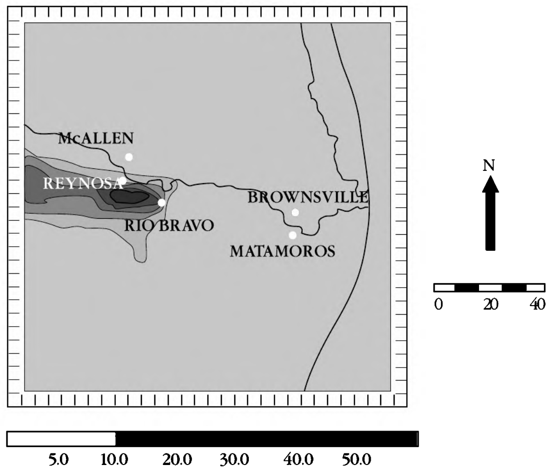

In the evening, the atmosphere becomes stable and the dispersion of pollutants decreases. In this case, Figure 7 shows the higher concentrations of SO_2 at 2100 hours are now found downwind in the urban areas of Reynosa and McAllen.

Figure 7. Map of SO_2 Concentrations in the LRGV at 2100, December 6, 1995

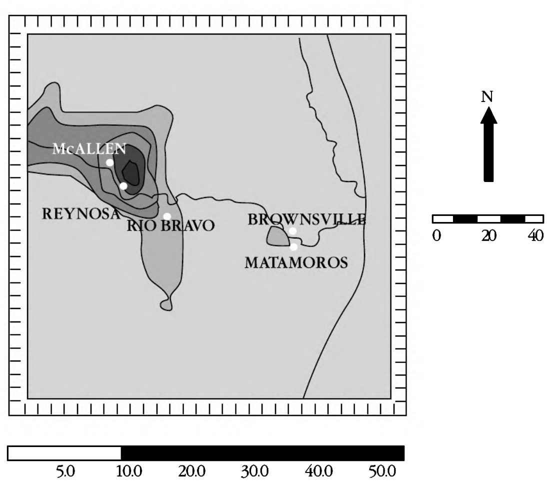

As before, the predicted higher values are around 50ppb and occur in McAllen. Figures 4 to 7 also show that, because of transport and dispersion of gases and particles in the atmosphere, higher concentrations of pollutants may be found in rural areas rather than in urban areas. An important limitation is that these results obtained with the model were not validated since actual air pollutant concentration data did not exist for the December 1995 study.

In the study of March 1998, NO_X concentrations were measured at the different sites. The results of the predicted values with the photochemical model and the actual concentrations measured are shown in Figure 8.

Figure 8. NO_X Concentrations Predicted with the Photochemical Model and Actual Measurements in the LRGV in March 1998

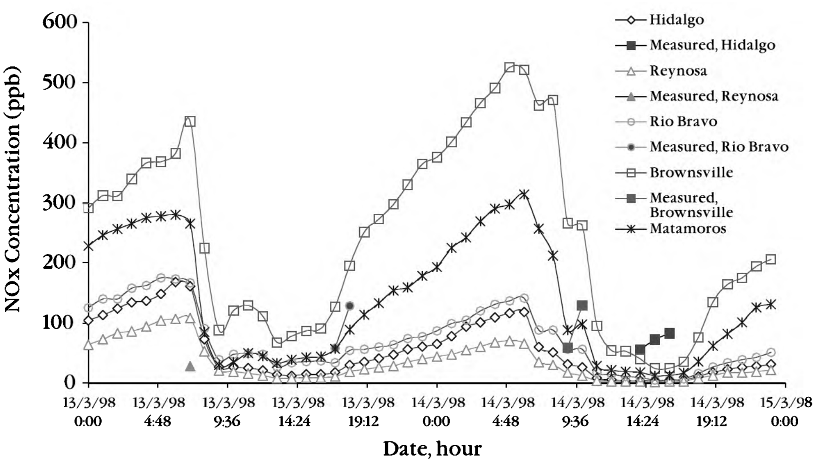

In this figure, the model predicts concentrations of NO_X in Brownsville and Matamoros that exceed the one-hour air quality standard of 210ppb, while measured concentrations of NO_X and values predicted for other cities are below this standard. Reasonable correspondence was observed between predicted and measured NO_X concentration profiles or trends at some sites. The discrepancies between measured and modeled NO_X values at other sites are thought to be due to the highly unusual weather conditions, the lack of sufficient data points to fully calibrate the models, and the lack of complete emission inventories (particularly the fact that United States emission data are summed per county and not specified by highway).

Conclusions

The results of this study show that the LRGV has, in general, relatively low levels of PM_{10}. Depending on meteorological conditions, these levels may increase to high concentrations during some periods of the day. Size distribution results show that $PM_{2.5}$ seems to be an important component of PM_{10}. It is important to obtain data for longer periods and different seasons in the year to achieve more reliable results for the size composition of PM_{10}. To obtain better calculated values of ozone, SO_2, and other pollutants it is necessary to have better emission estimates of stationary and mobile sources as well as their diurnal and spatial variation.

The predicted concentrations of SO_2 do not exceed the air quality standard in the LRGV, including the impact of the power plant located in Río Bravo. Moreover, this plant's emissions were estimated consuming fuel oil and natural gas with high sulfur content and, since today it is using combined cycles with natural gas that has a lower sulfur content, it is expected that its impact will be below the predicted values of SO_2 concentrations.

It is necessary to obtain actual concentrations of air pollutants to validate their predicted concentrations with the photochemical model. Usually air quality data are collected in urban areas. However, transport of pollutants to rural areas may cause higher concentrations there. Technical and logistic achievements were trouble-free crossing (twice) of the U.S.-Mexican border with a fully equipped mobile laboratory and successful (nearly around-the-clock) operation of a mobile laboratory on both sides of the U.S.-Mexican border with a binational team of investigators while covering six sites over a 200-mile distance within a 72-hour period.

Acknowledgments

The research reported here was supported by the Southwest Center for Environmental Research and Policy (SCERP). The research team thanks the personnel of Secretaría de Desarrollo Social de Tamaulipas for their valuable support during the monitoring trip. The information supplied by the Texas Commission on Environmental Quality, Subsecretaría de Ecología de Nuevo León and Secretaría de Comunicaciones y Transportes is gratefully acknowledged.

References

Dworzanski, J. P.; H. L. C. Meuzelaar, W. Maswadeh, X. Nie, P. A. Cole, and N. S. Arnold. 1993. "Development of Field Portable Mass Spectrometric Techniques for Particulate Organic Matter in PM-10." Proceedings of the 1993 International Symposium on Field Screening Methods for Hazardous Wastes and Toxic Chemicals, Las Vegas, Nevada.

Gilbreath, J. 1992. *Planning for the Border's Future: The U.S.-Mexican Integrated Border Environmental Plan*. U.S.-Mexican Occasional Paper No. 1. Austin, Texas: U.S.-Mexican Policy Studies Program, Lyndon B. Johnson School of Public Affairs, The University of Texas at Austin.

Kishan, S.; R. Meredith, and C. Weyn. 1998. *Development of Mobile Emissions Factor Model for Ciudad Juárez, Chihuahua.* Austin, Texas: Air Quality Planning Division Texas Commission on Environmental Quality.

McRae, G. J.; W. R. Goodin, and J. H. Seinfeld. 1982. "Development of a Second-Generation Mathematical Model for Urban Air Pollution – I. Model Formulation." *Atmospheric Environment* 16 (4): 679–696.

Mendoza, A. 1996. "Aplicación Preliminar del Modelo Fotoquímico de Calidad del Aire CIT a la Zona de la Frontera Mexico-Estados Unidos." Masters Thesis, Instituto Tecnológico y de Estudios Superiores de Monterrey, Monterrey, Nuevo León, Mexico.

Mejia, G. M. and H. L. Meuzelaar. 1997. "Characterization and Dynamics of Air Pollutants in the Southeastern Mexico-U.S.

Border Area." Final Report, Southwest Center for Environmental Research and Policy (SCERP) Project No. AQ95–10. San Diego: SCERP.

Mejia, G. M. and M. Rodriguez. 1997. "Characteristics and Estimated Air Pollutant Emissions of the Industry and Vehicles in the Matamoros-Reynosa Border Region." *Environment International* 23 (5): 733–744.

Mukerjee, S; W. Ellenson, R. Lewis, K. Stevens, M. Somerville, D. Shadwick, and R. Willis. 1997. "An Environmental Scoping Study in the Lower Rio Grande Valley of Texas (parts I, II, and III)." *Environment International* 23: 611–628 and 643–674.

Mukerjee, S.; D. S. Shadwick, K. E. Dean, and L. Y. Carmichael. 1999. "Assessing Transboundary Issues in the Lower Rio Grande Valley." 92nd Annual Air & Waste Management Association Meeting, St. Louis, Missouri.

Rogge, W. F.; L. M. Hildemann, M. A. Mazurek, G. R. Cass, and B. R. T. Simoneit. 1998. "Sources of Fine Organic Aerosol, 1–9." *Environmental Science & Technology* 24: 1112-1125.

Seinfeld, J. 1986. *Atmospheric Chemistry and Physics of Air Pollution*. New York: John Wiley and Sons.

Tejeda, D. and G. Mejia. 1998. "Impact of NAFTA on Mobile Source Emissions Along the Dallas-Saltillo Corridor." Proceedings of the International Symposium on Environmental Engineering and Earth Sciences, 26-30 October, Cholula, Puebla, Mexico.

Index